國立臺灣大學工學院化學工程學系

博士論文

Department of Chemical Engineering

College of Engineering

National Taiwan University

Doctoral Dissertation

球形膠體粒子在同心球形孔隙中之磁流力運動

Magnetohydrodynamic Motions of a Colloidal Sphere in a
Concentric Spherical Cavity

謝子賢

Tzu-Hsien Hsieh

指導教授：葛煥彰 教授

Advisor: Huan-Jang Keh, Professor

中華民國一百零二年六月

June, 2013

誌 謝

　　最先感謝的就是我的指導老師葛煥彰教授，葛教授在膠體領域的專業讓我在博士論文研究中得到非常大的幫助，讓我從碩士班以來一路都很享受做研究的樂趣，並在博士班時鑽研過去較少研究的領域。也很感謝葛教授讓我可以自由發揮並提供寶貴的建議，讓我在讀博士的四年間對膠體領域的理解能力提高許多。同時也感謝口試委員張建成教授、曹恆光教授、魏憲鴻教授、王大銘教授與廖英志教授對論文提供寶貴的建議，幫助我補足過去思考不周之處，由衷感謝各位委員的辛勞。

　　實驗室的各個夥伴也是我要感謝的對象，先正學長、義偉學長都提供我相當寶貴的工作經驗，讓我對業界有更多了解。育晨同學、秉元學弟兩位更是我研究時請益的對象，也特別感謝雅茹學妹協助我處理一些學校的申請文件，瑋君學弟、弘憲學弟、冠宇學弟也是討論研究的好夥伴。在北上新竹工作及往返台北讀書的一年半間，特別感謝新竹勝利堂的牧者與弟兄姐妹的關心，讓我在忙碌生活之餘有很好的充電機會。

　　最重要的家人，是我在求學過程中的後盾，很感謝父母讓我沒有後顧之憂可以專心做研究並順利完成學業。在讀博士學位期間，我也順利完成終身大事，很感謝千儀一路陪伴，並為我生下寶貝女兒品熹豐富我的人生，這過程中的酸甜苦辣只有妳最了解。

　　最後，要感謝我的神，因為信仰讓我在困難時沒放棄可以繼續前進。

For ever since the world he was created, people have seen the earth and sky.　Through everything God made, they can clearly see his invisible qualities-his eternal power and divine nature. So they have no excuse for not knowing God. (Romans 1:20)
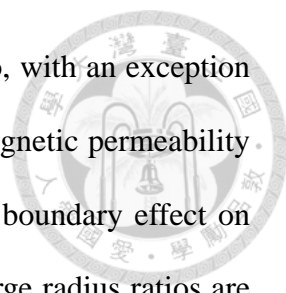

2013.6.21

謝子賢

Abstract

The quasi-steady motions of a spherical colloidal particle inside a concentric spherical cavity filled with a conducting fluid induced by the magnetohydrodynamic (MHD) effect are analyzed at low Reynolds number.   Through the use of a generalized reciprocal theorem to the Stokes equations modified with the Lorentz force density resulting from the interaction of an applied magnetic field with the existing electric current and the consideration of the Maxwell stress to the force exerted on the particle, the translational and angular velocities of the particle under various conditions are obtained in closed forms valid for an arbitrary value of the particle-to-cavity radius ratio. The boundary effects on the motions of the particle caused by the MHD force are generally equivalent to (yet different from) that in sedimentation.

In Chapter 2, an analytical study is presented for the MHD effects on a translating and rotating charged sphere in an arbitrary unbounded electrolyte solution prescribed with a general flow field and a uniform magnetic field.   The electric double layer surrounding the charged particle may have an arbitrary thickness relative to the particle radius.   Through the use of a simple perturbation method, the Stokes equations modified with an electric force term, including the Lorentz force contribution, are dealt with using a generalized reciprocal theorem.   Using the equilibrium double-layer potential distribution from solving the linearized Poisson-Boltzmann equation, we obtain closed-form formulas for the translational and angular velocities of the spherical particle induced by the MHD effects to the leading order.   It is found that the MHD effects on the particle movement associated with the translation and rotation of the particle and the ambient fluid are monotonically increasing functions of κa, where κ

is the Debye screening parameter and a is the particle radius. Any pure rotational Stokes flow of the electrolyte solution in the presence of the magnetic field exerts no MHD effect on the particle directly in the case of a very thick double layer ($\kappa a \to 0$). The MHD effect caused by the pure straining flow of the electrolyte solution can drive the particle to rotate, but it makes no contribution to the translation of the particle.

In Chapter 3, the MHD effects on the translation and rotation of a charged sphere situated at the center of a charged spherical cavity filled with an arbitrary electrolyte solution when a constant magnetic field is imposed are analyzed. The electric double layers adjacent to the solid surfaces may have an arbitrary thickness relative to the particle and cavity radii. Through the same method of analysis in Chapter 2, we obtain explicit formulas for the translational and angular velocities of the colloidal sphere produced by the MHD effects valid for all values of the particle-to-cavity size ratio. The boundary effect on the MHD motion of the spherical particle is a qualitatively and quantitatively sensible function of the parameters a/b and κa, where b is the radius of the cavity. In general, the proximity of the cavity wall reduces the MHD migration but intensifies the MHD rotation of the particle.

In Chapter 4, the electromagnetophoretic (EMP) motion of a spherical colloidal particle positioned at the center of a spherical cavity filled with a conducting fluid is analyzed. Under uniformly applied electric and magnetic fields, the electric current and magnetic flux density distributions are solved for the particle and fluid phases of arbitrary electric conductivities and magnetic permeabilities. Applying a generalized reciprocal theorem to the Stokes equations modified with the resulted Lorentz force density, we obtain a closed-form formula for the migration velocity of the particle valid for an arbitrary value of the particle-to-cavity radius ratio. The particle velocity in

general decreases monotonically with an increase in this radius ratio, with an exception for the case of a particle with high electric conductivity and low magnetic permeability relative to the suspending fluid. The asymptotic behaviors of the boundary effect on the EMP force and mobility of the confined particle at small and large radius ratios are discussed.

In Chapter 5, an analytical study is presented for the magnetic-field-induced motion of a colloidal sphere with spontaneous electrochemical reactions on its surface situated at the center of a spherical cavity filled with an electrolyte solution. The zeta potential associated with the particle surface may have an arbitrary distribution, whereas the electric double layers adjoining the particle and cavity surfaces are taken to be thin relative to the particle size and the spacing between the solid surfaces. The electric current and magnetic flux density distributions are solved for the particle and fluid phases of arbitrary electric conductivities and magnetic permeabilities. Applying a generalized reciprocal theorem to the Stokes equations with the resulted Lorentz force term, we obtain explicit formulas for the translational and angular velocities of the colloidal sphere valid for all values of the particle-to-cavity size ratio. The dipole and quadrupole moments of the zeta potential distribution over the particle surface cause the particle translation and rotation, respectively. The induced velocities of the particle are unexpectedly significant, and their dependence on the characteristics of the particle-fluid system is physically different from that for EMP particles or phoretic swimmers. The particle velocities decrease monotonically with an increase in the particle-to-cavity size ratio. The boundary effect on the movement of the particle with interfacial self-electrochemical reactions induced by the MHD force is much stronger than that in phoretic swimming.
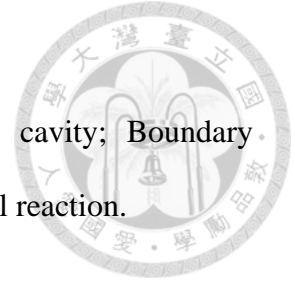
摘要

本論文探討在擬穩態與低雷諾數的情況下,一球形膠體粒子在一充滿導電流體之球形孔隙中心受磁流力效應作用所進行的各種運動。勞倫茲力 (Lorentz force) 為磁場與電流交互作用下所產生的作用力,將廣義互等定理 (generalized reciprocal theorem) 應用於含有勞倫茲力的 Stokes 方程式並考慮粒子表面上的馬克斯威爾應力 (Maxwell stress),可求得粒子在任意粒子/球孔半徑比值之移動與轉動速度。一般來說,粒子受到磁流力作用進行運動之邊界效應,與粒子受到重力進行沉降之邊界效應大小相當,但也存在明顯差異。

在第二章中,吾人探討球形帶電膠體粒子於一任意無邊界電解質溶液中並施以任意流場與均勻磁場,因磁流力效應所產生之移動與轉動,帶電粒子周圍的電雙層厚度可為任意值。透過微擾法與廣義互等定理可處理含有靜電力與勞倫茲力效應的 Stokes 方程式,並利用求解線性 Poisson-Boltzmann 方程式所得之平衡時電雙層電位分佈,可求得球形粒子在一階微擾展開下因磁流力效應所產生的移動與轉動速度。此移動與轉動速率與無因次電動力半徑 κa 為一單調遞增函數之關係,其中 κ 為德拜 (Debye) 屏蔽參數,a 為粒子半徑。在電雙層很厚($\kappa a \to 0$)的情況下,電解質在純轉動的 Stokes 流場下不具磁流力效應。此外,電解質溶液在純形變流動情況下的磁流力效應可使粒子轉動,但不會造成粒子移動。

在第三章中,吾人探討球形帶電膠體粒子於充滿任意電解質溶液之帶電球孔中心並施以均勻磁場下,因磁流力效應所產生之移動與轉動,帶電粒子周圍及球孔表面的電雙層厚度相較粒子與球孔半徑可為任意值。透過與第二章相同的分析方法,亦可求得球形粒子在任意粒子/球孔半徑比(a/b) 及任意 κa 值下因磁流力
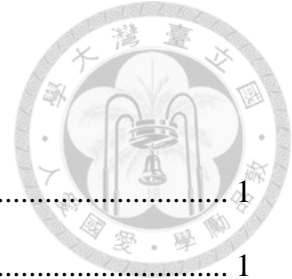
效應所產生的移動與轉動速度，其中 b 為球孔半徑。一般來說，邊界接近時會使磁流效應之移動速率減慢，但會加強轉動速率。

第四章探討一球形膠體粒子在充滿導電流體球孔中心之電磁泳運動。在施加均勻電場與磁場的情況下，可求得電流密度與磁通密度在任意電導度與磁透度下之解析解。將廣義互等定理應用於含有勞倫茲力的 Stokes 方程式並計算相對重要的馬克斯威爾應力在粒子上之作用，可求得粒子在任意 a/b 值下的移動速度。除了粒子相對於流體具有高導電性與低磁透性的情況下，粒子速率一般隨 a/b 值遞增而遞減。本章亦分別探討邊界效應在低與高 a/b 值的情況下，電磁作用力與粒子可動度的漸近現象。

在第五章中，吾人探討具表面自發電化學反應之球形膠體粒子，在充滿電解質溶液之球孔中心因磁場誘導所產生之運動。粒子表面之電位可為任意分佈，但電雙層厚度遠小於粒子半徑或粒子與球孔間距。求得電流與磁通密度分佈在任意電導度與磁透度下之解析解後，將廣義互等定理應用於含有勞倫茲力的 Stokes 方程式，可求得粒子在任意 a/b 值下的移動與轉動速度。粒子的移動與轉動分別與表面電位分佈的偶極 (dipole) 與四極 (quadrupole) 有關。此磁場誘發之運動相當重要，且在物理上之意義不同於現有之電磁泳動及其他泳動效應。粒子運動速率亦隨 a/b 值增加而遞減。具表面自發電化學反應之粒子，因磁流力誘導所產生運動之邊界效應較其他泳動現象為強。
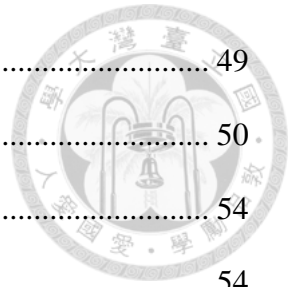
關鍵字: 磁流體力學、球形膠體粒子、球形孔隙、邊界效應、電動力學、電磁泳、自發電化學反應

Table of Contents

List of Figures

X

Chapter 1

Introduction

1.1 Background of colloidal magnetohydrodynamics

The flow of an electrically conducting, Newtonian fluid caused by its interaction with an electromagnetic force is known as the magnetohydrodynamic (MHD) effect (Jackson 1976; Hubbard and Wolynes 1981; Davidson 2001; Grant et al. 2002; Qian and Bau 2005; Luca 2009) which is described by the modified Navier-Stokes equations and Maxwell's equations. This flow results from the Lorentz force exerted on the fluid as an electric current and a non-collinear magnetic field are prescribed in it. In the absence of applied electric fields, the Lorentz force exerted on an electrolyte solution may be expressed as a force density $\rho \mathbf{v} \times \mathbf{B}$ acting on a differential volume of the solution, where ρ is the space charge density, $\mathbf{v}$ is the fluid velocity, and $\mathbf{B}$ is the applied magnetic field. This driving force, pointing toward the direction normal to both $\mathbf{v}$ and $\mathbf{B}$ and playing as an additional term in the Navier-Stokes equations, produces the MHD flow of the fluid.

Most colloidal particles bear charges on their surfaces as a consequence of dissociation of functional groups or crystal lattice defects when immersed in an electrolyte solution. The counterions in the solution are attracted by the surface charge of the particle so that their concentration becomes higher in the vicinity of the particle surface than the bulk value. On the other hand, the coions are repelled from the particle surface. Hence, a region of mobile ions that is not electrically neutral forms surrounding the particle. The combination of this region and the fixed charge on the

particle surface is well known as an electric double layer with the space charge density ρ. When an external electric field is applied, the interaction between the particle's surface charge and this field drives the particle to migrate at an electrophoretic velocity in one direction, while the movement of the counterions in the double layer induces an ambient fluid flow in the opposite direction. Electrophoresis has long been used as an effective technique for separation and identification of biologically active compounds in the biochemical and clinical fields (O'Brien and White 1978; Ohshima et al. 1983; Huang and Keh 2005; Chang and Keh 2008; Cheng et al. 2008). The movement of a charged particle caused by the MHD effect, in which both parts of the electric double layer experience the Lorentz force, is relevant to electrophoresis, but the difference between them is evident.

On the other hand, an electrically conducting, Newtonian fluid in the presence of an electric current density $\mathbf{J}$ and a magnetic flux density $\mathbf{B}$ will undergo a MHD flow in the direction perpendicular to both fields. This fluid flow is driven by the resulted Lorentz force density $\mathbf{J} \times \mathbf{B}$, which also plays as an additional term in the Navier-Stokes equation (Jackson 1976; Grant et al. 2002; Qin and Bau 2012). In an enclosed fluid, the MHD force is compensated by an established pressure gradient, analogous to the hydrostatic pressure gradient in gravitational field, and the fluid will be at rest.

When a colloidal particle is freely suspended in a fluid subjected to the Lorentz force, the force acts on both the fluid and the particle. If the force exerted on the particle is different from that on the fluid, then relative migration, known as electromagnetophoresis (EMP), of the particle occurs in the direction of or against $\mathbf{J} \times \mathbf{B}$, depending on their relative electromagnetic properties. The mechanism of

EMP was first reported by Kolin (Kolin 1953; Leenov and Kolin 1954) who carried out an analysis for a spherical particle of radius a in an unbounded fluid of viscosity η with arbitrary particle-to-fluid electric conductivity ratio σ^* and obtained a simple formula for the particle velocity $\mathbf{U}$ which can be expressed as
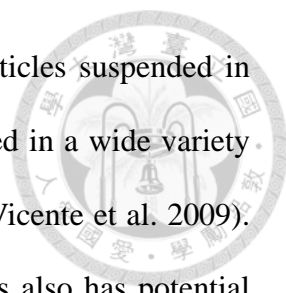
$$\mathbf{U} = \frac{4a^2}{9\eta}(\frac{\sigma^*-1}{\sigma^*+2})\mathbf{J}\times\mathbf{B}. \tag{1.1}$$

This analysis has since been extended to a particle of non-spherical geometries (Moffatt and Sellier 2002; Sellier 2003, 2007; Yariv and Miloh 2007). The EMP force and torque exerted on a fixed particle of arbitrary shape as well as the translational and angular velocities of a freely suspended, non-spherical particle are also found to be bilinear in $\mathbf{J}$ and $\mathbf{B}$.

In practical applications of the EMP effect, colloidal particles are not isolated and will move in the proximity of solid boundaries (Watarai et al. 2004; Iiguni and Watarai 2005). Therefore, it is of interest to examine the boundary effects on the EMP migration of a particle. Recently, the EMP motions of a spherical particle in the vicinity of a plane wall were investigated using spherical bipolar coordinates (Sellier 2005, 2006) and a method of reflections (Yariv and Miloh 2009). Asymptotic expansions in λ, the ratio of the particle radius to the distance of the particle center from the wall, generated by the reflection method indicate that the leading-order wall-induced corrections (retardation effects) to the EMP force and migration velocity of the particle appear at $O(\lambda^3)$ and $O(\lambda)$, respectively.

1.2 Applications of colloidal magnetohydrodynamics
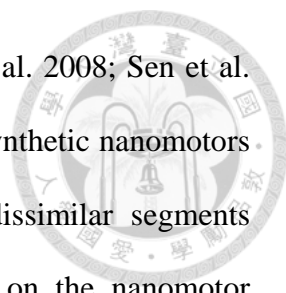
Magnetohydrodynamics is often used to describe the plasma physics, and recently

it has applications in the field of colloidal science. Colloidal particles suspended in electrolyte solutions prescribed with a magnetic field have been used in a wide variety of applications (Sekhar et al. 2005; De Las Cuevas et al. 2008; de Vicente et al. 2009). The addition of magnetic fields or MHD flows to colloidal systems also has potential applications in the manipulation and self-assembly of charged nanoparticles, which are usually not isolated and will move in the vicinity of solid boundaries (Kalsin et al. 2006; Shevchenko et al. 2006; Bishop and Grzybowski 2007; Tretiakov et al. 2009).

The effect of EMP is of considerable importance in numerous practical applications, such as the separation of biological particles (DNA fragments, proteins, cells, yeasts, etc.) due to the differences in their sizes and electric conductivities (Kolin and Kado 1958; Mills 1968; Ozawa et al. 2011), aggregation and disaggregation of colloidal suspensions (Tombácz et al. 1991; Busch et al. 1996; Stuyven et al. 2009), removal of small nonmetallic inclusions or impurities from molten metals (Xu et al. 2007; Haverkort and Peeters 2010), measurement of the particle-wall interaction force (Iiguni and Watarai 2003; 2010), determination of glycation on diabetic erythrocytes (Nozaki et al. 2004), and operation of multicolor display devices (Chung and Liang 2009).

On the other hand, manipulation of autocatalytic micro/nanomotors or other colloidal particles is an important application of colloidal particles (Yang et al. 2003; Burdick et al. 2008; Chaturvedi et al. 2010). Autonomously propelled micro/nanomotors or swimmers (e.g., by the usual auto-electrophoresis or auto-diffusiophoresis mechanism) can perform various nanoscale tasks ranging from drug delivery to cargo transport in microfluidic devices without the need for externally supplied energy have been designed and fabricated (Dreyfus et al. 2005; Kline et al.

2005; Kline et al. 2006; Golestanian et al. 2007; Laocharoensuk et al. 2008; Sen et al. 2009; Gibbs et al. 2010; Moran et al. 2010; Wei and Jan 2010).   Synthetic nanomotors often take the form of Janus nanoparticles consisting of two dissimilar segments suspended in a liquid fuel with asymmetric reactions occurring on the nanomotor surface, and a typical example is a self-propelled bimetallic nanomotor that swims due to the spontaneous decomposition (electrochemical reduction and oxidation) of hydrogen peroxide fuel to oxygen and water in aqueous solutions.   These electrochemically grown nanomotors have also been engineered to perform controlled motion under applied magnetic fields.   But, there are few theoretical investigations on the motion of autonomously propelled nanomotors induced by externally applied magnetic fields available in the literature and we will extend this research.

1.3 Purpose of the thesis

In this thesis, we analyze the quasi-steady motions of a spherical colloidal particle inside a concentric spherical cavity filled with a conducting fluid induced by the MHD effect at low Reynolds number.   Through the use of a generalized reciprocal theorem to the modified Stokes equations and consideration of the Maxwell stress to the force exerted on the particle, the translational and angular velocities of the particle under various conditions will be obtained.

In Chapter 2, we examine the translation and rotation of a charged spherical particle in an arbitrary electrolyte solution with a prescribed general velocity field subjected to an external magnetic field in the absence of applied electric fields.   The thickness of the double layer surrounding the charged particle is arbitrary relative to the particle radius.   The purpose is to determine the motion of the particle induced by the

MHD force. Closed-form formulas for the induced translational and angular velocities of the particle are obtained in Eqs. (2.14) and (2.15).

In Chapter 3, we investigate the general motion of a charged colloidal sphere in a concentric spherical cavity filled with an electrolyte solution subject to a prescribed magnetic field in the absence of external electric fields. The thickness of the electric double layers adjacent to the solid surfaces is arbitrary relative to the particle and cavity radii. Explicit formulas for the translational and angular velocities of the confined spherical particle induced by the MHD effect are obtained in Eqs. (3.20) and (3.21).

In Chapter 4, the EMP motion of a colloidal sphere in a concentric spherical cavity filled with a conducting fluid subject to uniformly prescribed electric and magnetic fields is analyzed with the consideration of the total force (including the Maxwell stress) exerted on the particle, where the particle and fluid may have arbitrary values in electric conductivity and magnetic permeability. Although the concentric cavity is an idealized abstraction of some real systems, the result of boundary effect on the electrophoretic velocity of a charged sphere obtained in this geometry (Zydney 1995) agrees with that for a circular cylindrical pore (Keh and Chiou 1996). The geometric symmetry in this model system allows closed-form formulas for the EMP force and migration velocity of the confined particle to be obtained in Eqs. (4.15) and (4.18), respectively.

In Chapter 5, the magnetic-field-induced motion of a spherical particle with self-electrochemical reactions on its surface situated at the center of a spherical cavity filled with an ionic fluid is examined analytically, where the particle and fluid may have arbitrary values in electric conductivity and magnetic permeability. The translational and angular velocities of the particle caused by the MHD force are determined explicitly in Eq. (5.20) for the general case of an arbitrary distribution of the zeta potential at the

particle surface, where only the dipole and quadrupole moments of this potential distribution are involved. In Section 5.4.1, some examples are given to show how different types of variation in the zeta potential distribution might affect the movement of a particle. The spherical geometry of the cavity does not limit the validity of these expressions for a real-world application and this model might be adaptable to other geometries, such as that in a recent experimental study of the magnetically guided motion of electrocatalytic nanorod motors within microchannel networks (Burdick et al. 2008).

Chapter 2

Magnetohydrodynamic effects on a charged sphere with arbitrary double-layer thickness

In this chapter, we consider the steady motion of a translating and rotating colloidal sphere of radius a and zeta potential ζ_p in an unbounded electrolyte solution with a general linear velocity field in the presence of a uniformly applied magnetic field as shown in Figure 2.1.   The thickness of the electric double layer adjacent to the particle surface is arbitrary relative to the particle radius.   Gravitational effects are ignored.   Our objective is to determine the additional particle motion induced by the existence of the constant magnetic field.

To evaluate the translational and angular velocities of the particle induced by the MHD effect, it is necessary to first solve for the equilibrium electric potential and velocity fields in the fluid phase.

2.1 Equilibrium electric potential distribution

When the Debye-Hückel approximation applicable for the case of low electric potentials is used, the equilibrium double-layer potential distribution ψ in the absence of the imposed velocity field and magnetic field is governed by the linearized Poisson-Boltzmann equation,

$$\nabla^2 \psi = \kappa^2 \psi , \tag{2.1}$$

where κ is the Debye screening parameter.   The boundary conditions for ψ at the particle surface and infinity are simply that

$$\psi = \zeta_{\text{p}} \quad \text{at} \quad r = a \tag{2.2a}$$

$$\psi = 0 \quad \text{as} \quad r \to \infty, \tag{2.2b}$$

where r is the radial coordinate from the particle center. The solution of Eqs. (2.1) and (2.2) is (Henry 1931)

$$\psi = \frac{a}{r} e^{-\kappa(r-a)} \zeta_{\text{p}}. \tag{2.3}$$

2.2 Fluid velocity distribution

With knowledge of the equilibrium electric potential distribution in the electrolyte solution outside the particle, we can now proceed to find the fluid velocity field. The fluid motion in the presence of a magnetic flux density $\mathbf{B}_\infty$ is governed by the Stokes equations modified with an electric force (including the Lorentz force) term,

$$\eta \nabla^2 \mathbf{v} = \nabla p - \rho (\mathbf{v} \times \mathbf{B}_\infty - \nabla \psi), \tag{2.4a}$$

$$\nabla \cdot \mathbf{v} = 0. \tag{2.4b}$$

In these equations, $\mathbf{v}$ and p are the fluid velocity and dynamic pressure distributions, respectively, η is the fluid viscosity, ρ is the total space charge density related to the net local electric field $\mathbf{v} \times \mathbf{B}_\infty - \nabla \psi$ by Poisson's equation as (Tai 1964)

$$\rho = \varepsilon \nabla \cdot (\mathbf{v} \times \mathbf{B}_\infty - \nabla \psi), \tag{2.5}$$

where ε is the dielectric permittivity of the fluid, and the expression for ψ has already been given in Eq. (2.3). Here, the linear superposition of the equilibrium electric field $-\nabla \psi$ and the Lorentz field $\mathbf{v} \times \mathbf{B}_\infty$ is valid since the latter is practically weak relative to the former. Note that the induced charge density that arises from the magnetic flux density imposed on the moving fluid is included in Eq. (2.5).

Equation (2.4a) shows that a magnetic field can drive an electrolyte solution to move

only if there exists an electric current density perpendicular to it. In this study we consider the current flow produced by the general case of a charged sphere translating with velocity $\mathbf{U}_p$ and rotating with angular velocity $\mathbf{\Omega}_p$ in a Stokes flow which can be uniform, rotational, or straining at infinity. The velocity and pressure fields in Eq. (2.4) can be expressed by the following simple perturbation expansions:

$$\mathbf{v} = \mathbf{v}_0 + \alpha\mathbf{v}_M + O(\alpha^2), \tag{2.6a}$$

$$p = p_0 + \alpha p_M + O(\alpha^2), \tag{2.6b}$$

where $\alpha = \varepsilon\zeta_p|\mathbf{B}_\infty|/\eta$ is a small dimensionless parameter, the subscript 0 represents the prescribed Stokes flow in the absence of the magnetic field, and $\mathbf{v}_M$ and p_M denote respectively the fluid velocity and pressure distributions caused by the magnetic flux density $\mathbf{B}_\infty$ orthogonal to the flow direction.

The governing equations of the zeroth-order flow field without the MHD effect ($\alpha = 0$) are

$$\eta\nabla^2\mathbf{v}_0 = \nabla p_0, \tag{2.7a}$$

$$\nabla \cdot \mathbf{v}_0 = 0. \tag{2.7b}$$

The boundary conditions for this flow field with a prescribed general linear Stokes flow can be expressed as

$$\mathbf{v}_0 = \mathbf{U}_p + \mathbf{\Omega}_p \times \mathbf{r} \qquad \text{at} \quad r = a, \tag{2.8a}$$

$$\mathbf{v}_0 = \mathbf{U}_\infty + \mathbf{\Omega}_\infty \times \mathbf{r} + \mathbf{E}_\infty \cdot \mathbf{r} \qquad \text{as} \quad r \to \infty, \tag{2.8b}$$

where $\mathbf{U}_\infty$ and $\mathbf{\Omega}_\infty$ are constant translational and angular velocity vectors, respectively, $\mathbf{E}_\infty$ is a constant rate-of-strain dyadic, and $\mathbf{r}$ is the position vector from the particle center. Evidently, the three terms on the right-hand side of Eq. (2.8b) represent the uniform, pure

rotational, and pure straining undisturbed flows, respectively. The translational velocity $\mathbf{U}_p$ and angular velocity $\mathbf{\Omega}_p$ of the particle may result from the prescribed flow field given by Eq. (2.8b) or from some external force and torque acting on the particle. The solution of Eqs. (2.7) and (2.8) is (Keh and Chen 1996)

$$\mathbf{v}_0 = \mathbf{U}_\infty + \mathbf{\Omega}_\infty \times \mathbf{r} + (\frac{3a}{4r} + \frac{a^3}{4r^3})(\mathbf{U}_p - \mathbf{U}_\infty) + \frac{3}{4}(\frac{a}{r^3} - \frac{a^3}{r^5})(\mathbf{U}_p - \mathbf{U}_\infty) \cdot \mathbf{rr}$$

$$+ \frac{a^3}{r^3}(\mathbf{\Omega}_p - \mathbf{\Omega}_\infty) \times \mathbf{r} + (1 - \frac{a^5}{r^5})\mathbf{E}_\infty \cdot \mathbf{r} - \frac{5}{2}(\frac{a^3}{r^5} - \frac{a^5}{r^7})\mathbf{E}_\infty : \mathbf{rrr}. \qquad (2.9)$$

Substituting Eq. (2.5) and the expansions given by Eq. (2.6) into Eq. (2.4) and collecting the first-order terms of the small perturbation parameter α, we obtain

$$\alpha(\eta\nabla^2\mathbf{v}_M - \nabla p_M) = -\varepsilon\mathbf{D}(\nabla \cdot \mathbf{D}), \qquad (2.10a)$$

$$\nabla \cdot \mathbf{v}_M = 0, \qquad (2.10b)$$

where $\mathbf{D} = \mathbf{v}_0 \times \mathbf{B}_\infty - \nabla\psi$ is the net electric field involving the zeroth-order velocity field $\mathbf{v}_0$. The boundary conditions for the fluid velocity $\mathbf{v}_M$ are

$$\alpha\mathbf{v}_M = \mathbf{U}_M + \mathbf{\Omega}_M \times \mathbf{r} \qquad \text{at} \quad r = a, \qquad (2.11a)$$

$$\mathbf{v}_M = \mathbf{0} \qquad \text{as} \quad r \to \infty. \qquad (2.11b)$$

Here, $\mathbf{U}_M$ and $\mathbf{\Omega}_M$ are the translational and angular velocities, respectively, of the particle of the leading order in α resulting from the MHD effect to be determined.

2.3 Induced particle velocities

The induced translational and angular velocities of the particle in Eq. (2.11a) can be obtained by the use of the reciprocal theorem of Lorentz (Happel and Brenner 1983). Following Tuebner's approach with a generalized reciprocal theorem (Teubner 1982; Yoon 1991; Kim and Yoon 2002; 2003), as presented in Appendix A, we can express the force and

torque balance equations as

$$6\pi\eta a\mathbf{U}_M = \iint_{r=a}\boldsymbol{\sigma}^E\cdot\frac{\mathbf{r}}{r}\,\mathrm{d}S + \varepsilon\iiint_{r>a}\overline{\mathbf{v}}_0^{-T}\cdot\mathbf{D}(\nabla\cdot\mathbf{D})\,\mathrm{d}V,\qquad(2.12a)$$

$$8\pi\eta a^3\boldsymbol{\Omega}_M = \iint_{r=a}\mathbf{r}\times(\boldsymbol{\sigma}^E\cdot\frac{\mathbf{r}}{r})\,\mathrm{d}S + \varepsilon\iiint_{r>a}\overline{\mathbf{v}}_0^{-R}\cdot\mathbf{D}(\nabla\cdot\mathbf{D})\,\mathrm{d}V,\qquad(2.12b)$$

where

$$\overline{\mathbf{v}}_0^{-T} = (\frac{3a}{4r}+\frac{a^3}{4r^3})\mathbf{I} + \frac{3}{4}(\frac{a}{r}-\frac{a^3}{r^3})\frac{\mathbf{rr}}{r^2},\qquad(2.13a)$$

$$\overline{\mathbf{v}}_0^{-R} = -\frac{a^3}{r^3}\boldsymbol{\varepsilon}\cdot\mathbf{r},\qquad(2.13b)$$

$$\boldsymbol{\sigma}^E = \varepsilon(\mathbf{DD}-\frac{1}{2}|\mathbf{D}|^2\mathbf{I}),\qquad(2.13c)$$

$\mathbf{I}$ is the unit dyadic, and $\boldsymbol{\varepsilon}$ is the alternating unit triadic. In Eqs. (2.12) and (2.13), the dyadics $\overline{\mathbf{v}}_0^{-T}$ (dimensionless) and $\overline{\mathbf{v}}_0^{-R}$ (with the dimension of length) represent the normalized Stokes flow fields around an uncharged sphere translating and rotating, respectively, in an unbounded fluid for the generalized reciprocal theorem, and $\boldsymbol{\sigma}^E$ is the electric Maxwell stress tensor.

After the substitution of Eqs. (2.3), (2.9), and (2.13) into Eq. (2.12) and some mathematical manipulations, we obtain

$$\mathbf{U}_M = \frac{\varepsilon\zeta_p}{\eta}[M_0(\kappa a)\mathbf{U}_p - M_\infty(\kappa a)\mathbf{U}_\infty]\times\mathbf{B}_\infty,\qquad(2.14a)$$

$$\boldsymbol{\Omega}_M = \frac{\varepsilon\zeta_p}{\eta}\{[N_0(\kappa a)\boldsymbol{\Omega}_p - N_\infty(\kappa a)\boldsymbol{\Omega}_\infty]\times\mathbf{B}_\infty - N_\infty(\kappa a)\mathbf{E}_\infty\cdot\mathbf{B}_\infty\},\qquad(2.14b)$$

where

$$M_0(t) = \int_1^\infty\frac{e^{t(1-\gamma)}}{24\gamma^5}[4(1+t\gamma)(3\gamma^2-1)-t^2(15\gamma^4+2\gamma^2-1)]\,\mathrm{d}\gamma,\qquad(2.15a)$$

13

$$M_\infty(t) = M_0(t) - \frac{2}{3},$$

(2.15b)

$$N_0(t) = N_\infty(t) + \frac{1}{6},$$

(2.15c)

$$N_\infty(t) = \frac{t}{6} - t^2 \int_1^\infty \frac{e^{t(1-\gamma)}}{6\gamma^3} \, d\gamma .$$

(2.15d)
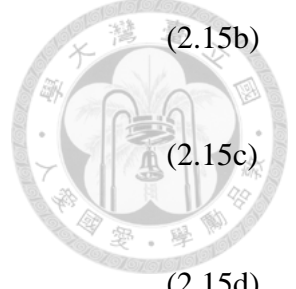
Equation (2.14a) illustrates that the induced translational velocity of the particle depends on the prescribed translational velocities of the particle and unbounded fluid, and it is in the direction perpendicular to both the relevant prescribed velocities and the applied magnetic field. Equation (2.14b) indicates that the induced angular velocity of the particle depends on the prescribed angular velocities of the particle and unbounded fluid, and it is also in the direction normal to both the relevant prescribed angular velocities and the imposed magnetic field. Note that, for any given value of κa, the dimensionless mobility parameter M_0 is greater than M_∞ and N_0 is greater than N_∞ by fixed values 2/3 and 1/6, respectively. Thus, the MHD effect on a charged particle induced by the prescribed translation and rotation of the particle is more significant than that induced by a translational and rotational fluid flow.

Equation (2.14) shows that the rate-of-strain dyadic of the unbounded fluid flow is able to drive the particle to rotate (also with the mobility parameter N_∞), whereas it makes no contribution to the translation of the particle. This outcome can be understood by a careful examination of the cross product of the velocity field of a pure straining or extensional flow and an applied magnetic field, which indicates that the resulting Lorentz effect is force-free but can exert a couple on the particle.

2.4 Results and discussion

In this section, we first consider the expressions for the dimensionless mobility

parameters M_0, M_∞, N_0, and N_∞ in Eq. (2.15) for the two limiting cases of the parameter κa. Results of the general case for the MHD effect on the particle motion will then be discussed.

In the limit of a very thin electric double layer ($\kappa a \to \infty$), Eq. (2.15) results in $M_0 = 1$, $M_\infty = 1/3$, $N_0 = 2/3$, and $N_\infty = 1/2$, and thus Eq. (2.14) reduces to

$$\mathbf{U}_{\mathrm{M}} = \frac{\varepsilon \zeta_{\mathrm{p}}}{3\eta}(3\mathbf{U}_{\mathrm{p}} - \mathbf{U}_\infty) \times \mathbf{B}_\infty, \tag{2.16a}$$

$$\mathbf{\Omega}_{\mathrm{M}} = \frac{\varepsilon \zeta_{\mathrm{p}}}{6\eta}[(4\mathbf{\Omega}_{\mathrm{p}} - 3\mathbf{\Omega}_\infty) \times \mathbf{B}_\infty - 3\mathbf{E}_\infty \cdot \mathbf{B}_\infty]. \tag{2.16b}$$

In the limit of a very thick double layer ($\kappa a \to 0$), Eq. (2.15) leads to $M_0 = 11/24$, $M_\infty = -5/24$, $N_0 = 1/6$, and $N_\infty = 0$, and then Eq. (2.14) becomes

$$\mathbf{U}_{\mathrm{M}} = \frac{\varepsilon \zeta_{\mathrm{p}}}{24\eta}(11\mathbf{U}_{\mathrm{p}} + 5\mathbf{U}_\infty) \times \mathbf{B}_\infty, \tag{2.17a}$$

$$\mathbf{\Omega}_{\mathrm{M}} = \frac{\varepsilon \zeta_{\mathrm{p}}}{6\eta}\mathbf{\Omega}_{\mathrm{p}} \times \mathbf{B}_\infty. \tag{2.17b}$$

From Eqs. (2.16) and (2.17), we can find that a uniform Stokes flow in the uniform magnetic field will induce an MHD translational velocity of the particle in the direction opposite to (or same as) that induced by the prescribed translation of the particle in the case of a very thin (or thick) electric double layer. A pure rotational flow and a pure straining flow in the uniform magnetic field exert no MHD effect on the particle movement directly in the case of a very thick double layer, but can produce the MHD rotation of the particle in the case of a thin double layer. Also, the MHD effect on a translating and rotating particle is more significant in the case of a thin double layer than in the case of a thick double layer. This outcome is predictable knowing that the space charge density in a narrow region of diffuse ions near the particle surface is much larger for the case of thin double layer than for the case

15

of thick double layer.

The numerical values of the dimensionless mobility parameters M_0, M_∞, N_0, and N_∞, as defined by Eq. (2.14) and calculated from formulas in Eq. (2.15), are plotted versus the parameter κa in Figure 2.2 and Figure 2.3. The integrations in these formulas are performed numerically using a personal computer. Except for M_∞, which can be a negative or positive value, all the other three mobility parameters are always positive. Thus, according to Eq. (2.14b), the prescribed rotation of the particle will always induce its MHD angular velocity in the direction opposite to that induced by the prescribed angular velocity of the fluid. The mobility parameters M_0 and M_∞ are monotonically increasing functions of κa respectively from 11/24 and -5/24 at $\kappa a = 0$ to 1 and 1/3 as $\kappa a \rightarrow \infty$, and the mobility parameters N_0 and N_∞ are also monotonically increasing functions of κa respectively from 1/6 and 0 at $\kappa a = 0$ to 2/3 and 1/2 as $\kappa a \rightarrow \infty$.

It is interesting to observe the special case that both the spherical particle and the suspending fluid move with the same translational and angular velocities (which occurs if the particle is freely suspended in the linear fluid flow without externally applied force and torque) and the fluid flow has no rate of strain in the magnetic field. Substituting $\mathbf{U}_\infty = \mathbf{U}_\mathrm{p}$, $\mathbf{\Omega}_\infty = \mathbf{\Omega}_\mathrm{p}$, and $\mathbf{E}_\infty = \mathbf{0}$ into Eq. (2.14), we obtain

$$\mathbf{U}_\mathrm{M} = \frac{2\varepsilon\zeta_\mathrm{p}}{3\eta}\mathbf{U}_\mathrm{p} \times \mathbf{B}_\infty, \tag{2.18a}$$

$$\mathbf{\Omega}_\mathrm{M} = \frac{\varepsilon\zeta_\mathrm{p}}{6\eta}\mathbf{\Omega}_\mathrm{p} \times \mathbf{B}_\infty. \tag{2.18b}$$

Namely, the MHD effect on the particle motion in this special case is independent of the double-layer thickness. For a very thick double layer ($\kappa a \rightarrow 0$), Eq. (2.18) can also be obtained in a simple, alternative way by balancing the hydrodynamic drag force and torque

with the Lorentz force and moment, respectively, on the particle, for which the total surface

charge can be related to the zeta potential as $4\pi a \varepsilon \zeta_\mathrm{p}$.
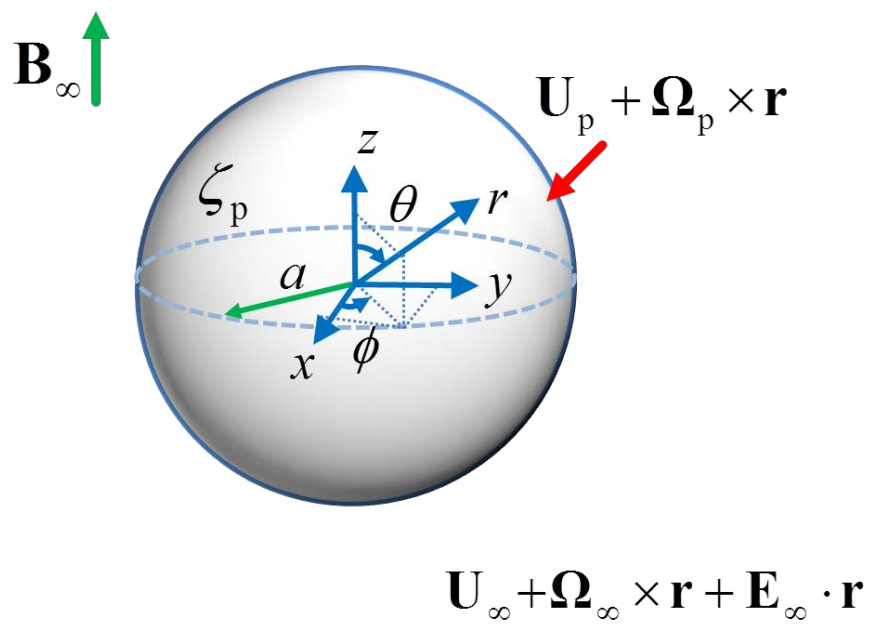
Figure 2.1   Geometric sketch for the MHD effect on the motion of a charged spherical particle in an unbounded electrolyte solution under applied Stokes flow and magnetic induction fields.
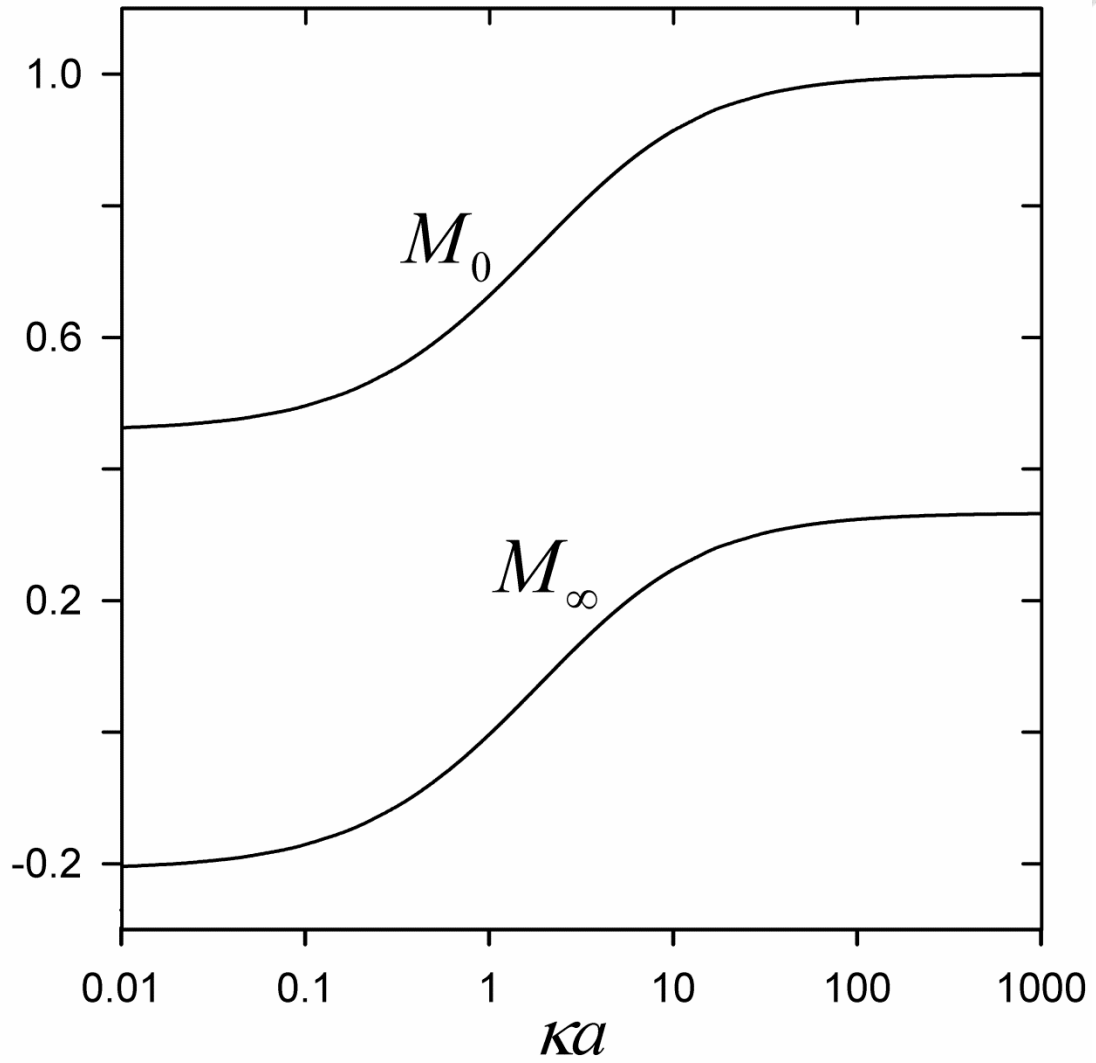
Figure 2.2　　Plots of the dimensionless mobility parameters M_0 and M_∞ as defined by

Eq. (2.14a) and calculated from Eqs. (2.15a) and (2.15b) versus the parameter κa.
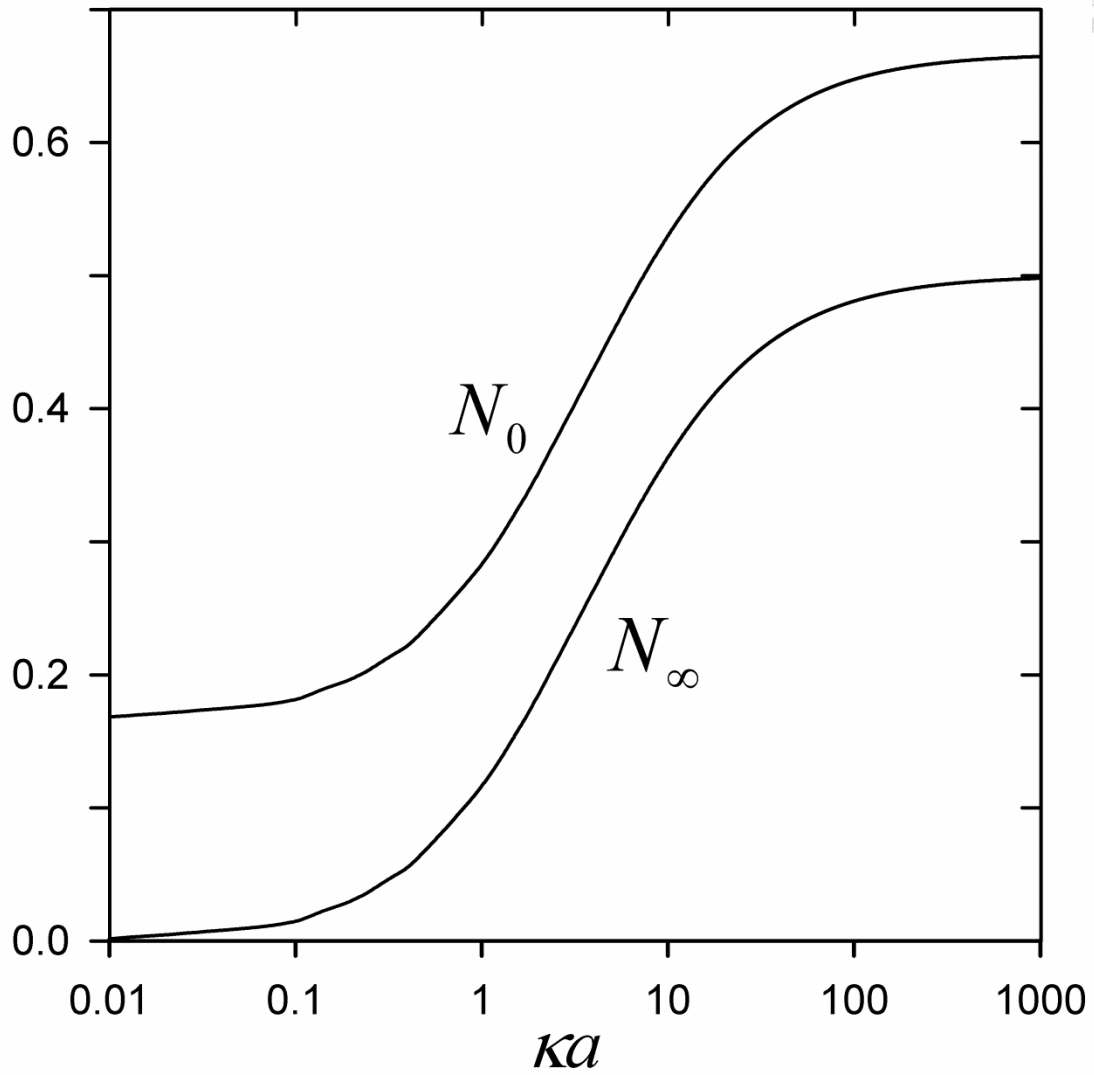
Figure 2.3   Plots of the dimensionless mobility parameters N_0 and N_∞ as defined by Eq.

(2.14b) and calculated from Eqs. (2.15c) and (2.15d) versus the parameter κa.

Chapter 3

Magnetohydrodynamic effects on a charged sphere in a charged spherical cavity with arbitrary double-layer thickness

In this chapter, we consider the quasisteady translation and rotation of a neutrally buoyant colloidal sphere of radius a and zeta potential ζ_p in a concentric, translating and rotating spherical cavity of radius b and zeta potential ζ_w filled with an electrolyte solution in the existence of a constant magnetic field as shown in Figure 3.1. The thickness of the electric double layers adjacent to the particle surface and cavity wall is arbitrary compared with the particle and cavity radii. Our purpose is to evaluate the boundary effect on the additional particle motion induced by the application of the uniform magnetic field.

To determine the translational and angular velocities of the confined particle caused by the MHD effect, we first need to ascertain the equilibrium electric potential and velocity distributions in the fluid phase.

3.1 Equilibrium electric potential distribution

With the use of the Debye-Hückel approximation applicable for the case of low electric potentials, the equilibrium double-layer potential distribution ψ in the absence of the applied velocity field and magnetic field is governed by the linearized Poisson-Boltzmann equation, same as Eq. (2.1),

$$\nabla^2 \psi = \kappa^2 \psi ,\tag{3.1}$$

where κ is the reciprocal of the Debye screening length. The boundary conditions for ψ

at the particle and cavity surfaces are

$$\psi = \zeta_p \quad \text{at} \quad r = a,$$ (3.2a)

$$\psi = \zeta_w \quad \text{at} \quad r = b,$$ (3.2b)

where r is the radial coordinate from the particle/cavity center. The solution of Eqs. (3.1) and (3.2) is

$$\psi = \frac{\zeta_w \sinh[t\lambda(\gamma-1)] + \zeta_p \lambda \sinh[t(1-\lambda\gamma)]}{\lambda\gamma\sinh[t(1-\lambda)]},$$ (3.3)

where

$$\gamma = r/a, \quad \lambda = a/b, \quad t = \kappa b.$$ (3.4a,b,c)

3.2 Fluid velocity distribution

Having obtained the solution for the equilibrium electric potential distribution in the fluid phase, we can now proceed to deal with the velocity field. Because the Reynolds number is small, the fluid motion in the presence of a magnetic flux density $\mathbf{B}_\infty$ is governed by the Stokes equations modified with an electric force (including the Lorentz force) term,

$$\eta\nabla^2\mathbf{v} = \nabla p - \rho(\mathbf{v}\times\mathbf{B}_\infty - \nabla\psi),$$ (3.5a)

$$\nabla\cdot\mathbf{v} = 0.$$ (3.5b)

In the above equations, $\mathbf{v}$ and p are the fluid velocity and dynamic pressure distributions, respectively, η is the fluid viscosity, ρ is the total space charge density related to the net local electric field $\mathbf{v}\times\mathbf{B}_\infty - \nabla\psi$ by Poisson's equation as

$$\rho = \varepsilon\nabla\cdot(\mathbf{v}\times\mathbf{B}_\infty - \nabla\psi),$$ (3.6)

where ε is the permittivity of the dielectric fluid, and the expression for ψ has already been given in Eq. (3.3). Here, the linear superposition of the equilibrium electric field
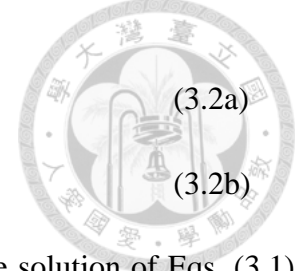
$-\nabla\psi$ and the Lorentz field $\mathbf{v}\times\mathbf{B}_\infty$ is valid since the latter is practically weak relative to the former. Note that the induced charge density that arises from the magnetic field prescribed in the moving fluid is included in Eq. (3.6).

Equation (3.5a) indicates that a magnetic field can drive an electrolyte solution to move only if there exists an electric current density perpendicular to it. We now consider the current flow caused by the case of a charged sphere translating with velocity $\mathbf{U}_p$ and rotating with angular velocity $\mathbf{\Omega}_p$ in a concentric spherical cavity whose wall translates with velocity $\mathbf{U}_w$ and rotates with angular velocity $\mathbf{\Omega}_w$. The velocity and pressure fields in Eq. (3.5) can be expressed by the perturbation expansions

$$\mathbf{v} = \mathbf{v}_0 + \alpha\mathbf{v}_M + O(\alpha^2), \tag{3.7a}$$

$$p = p_0 + \alpha p_M + O(\alpha^2), \tag{3.7b}$$

where $\alpha = \varepsilon\zeta_p|\mathbf{B}_\infty|/\eta$ is a small dimensionless parameter, the subscript 0 denotes the fluid flow in the absence of the magnetic field, and $\mathbf{v}_M$ and p_M represent the fluid velocity and pressure distributions, respectively, produced by the magnetic field $\mathbf{B}_\infty$. Equations (3.5)-(3.7) are the same as Eqs. (2.4)-(2.6).

The Stokes equations for the zeroth-order flow field without the MHD effect ($\alpha = 0$) are

$$\eta\nabla^2\mathbf{v}_0 = \nabla p_0, \tag{3.8a}$$

$$\nabla \cdot \mathbf{v}_0 = 0, \tag{3.8b}$$

and the relevant boundary conditions are

$$\mathbf{v}_0 = \mathbf{U}_p + \mathbf{\Omega}_p \times \mathbf{r} \quad \text{at} \quad r = a, \tag{3.9a}$$

$$\mathbf{v}_0 = \mathbf{U}_w + \mathbf{\Omega}_w \times \mathbf{r} \quad \text{at} \quad r = b, \tag{3.9b}$$

where $\mathbf{r}$ is the position vector from the particle/cavity center. The translational velocity

$\mathbf{U}_{\text{p}}$ and angular velocity $\mathbf{\Omega}_{\text{p}}$ of the particle may result from the translational and angular velocities of the confining cavity wall given by Eq. (3.9b) and from some external force and torque acting on the particle. We obtain the solution of Eqs. (3.8) and (3.9) as

$$\mathbf{v}_0 = \frac{1}{\Gamma_{\text{T}}}[a_1\mathbf{U}_{\text{p}} + a_2\mathbf{U}_{\text{w}} + 3a_3(\mathbf{U}_{\text{p}} - \mathbf{U}_{\text{w}}) \cdot \frac{\mathbf{rr}}{r^2}] + \frac{1}{\Gamma_{\text{R}}}(a_4\mathbf{\Omega}_{\text{p}} + a_5\mathbf{\Omega}_{\text{w}}) \times \mathbf{r}, \tag{3.10}$$

where

$$a_1 = 1 - \lambda^3 + 6\lambda^3\gamma^5(1 - \lambda^2) + 3\gamma^2(1 - \lambda^5) - \lambda\gamma^3(9 - 5\lambda^2 - 4\lambda^5), \tag{3.11a}$$

$$a_2 = -1 + \lambda^3 + \gamma^2[4\gamma - 3 - \lambda^3\gamma(6\gamma^2 - 5) + 3\lambda^5(2\gamma^3 - 3\gamma + 1)], \tag{3.11b}$$

$$a_3 = (1 - \lambda^3)(\gamma^2 - 1) - \lambda^3\gamma^2(1 - \lambda^2)(\gamma^3 - 1), \tag{3.11c}$$

$$a_4 = 1 - \lambda^3\gamma^3, \tag{3.11d}$$

$$a_5 = \gamma^3 - 1; \tag{3.11e}$$

$$\Gamma_{\text{T}} = \gamma^3(1 - \lambda)^4(4 + 7\lambda + 4\lambda^2), \tag{3.12a}$$

$$\Gamma_{\text{R}} = \gamma^3(1 - \lambda^3). \tag{3.12b}$$

Substituting Eqs. (3.6) and (3.7) into Eq. (3.5) and collecting the first-order terms of the small perturbation parameter α, we obtain

$$\alpha(\eta\nabla^2\mathbf{v}_{\text{M}} - \nabla p_{\text{M}}) = -\varepsilon\mathbf{D}(\nabla \cdot \mathbf{D}), \tag{3.13a}$$

$$\nabla \cdot \mathbf{v}_{\text{M}} = 0, \tag{3.13b}$$

where

$$\mathbf{D} = \mathbf{v}_0 \times \mathbf{B}_\infty - \nabla\psi,$$

(3.14)

which is the net electric field involving the zeroth-order velocity field $\mathbf{v}_0$. The boundary conditions for the fluid velocity $\mathbf{v}_{\text{M}}$ can be expressed as

$$\alpha\mathbf{v}_{\text{M}} = (\mathbf{U}_{\text{M}} + \mathbf{\Omega}_{\text{M}} \times \mathbf{r}) \qquad \text{at} \quad r = a, \tag{3.15a}$$

24

$$\mathbf{v}_\mathrm{M} = \mathbf{0} \qquad \text{at} \quad r = b, \qquad (3.15b)$$

where $\mathbf{U}_\mathrm{M}$ and $\mathbf{\Omega}_\mathrm{M}$ are the translational and angular velocities, respectively, of the confined particle of the leading order in α produced by the MHD effect to be determined.
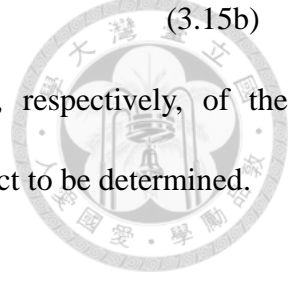
3.3 Induced particle velocities

The translational and angular velocities of the particle appearing in Eq. (3.15a) induced by the MHD effect can be obtained by the use of the reciprocal theorem of Lorentz (Happel and Brenner 1983). Following Tuebner's approach with a generalized reciprocal theorem (Teubner 1982; Yoon 1991; Kim and Yoon 2002; Keh and Hsieh 2008), we can express the force and torque balance equations as

$$6\pi\eta a f_\mathrm{T} \mathbf{U}_\mathrm{M} = \iint_{r=a} \mathbf{\sigma}^\mathrm{E} \cdot \frac{\mathbf{r}}{r}\, \mathrm{d}S + \varepsilon \iiint_{b>r>a} \overline{\mathbf{v}}^\mathrm{T} \cdot \mathbf{D}(\nabla \cdot \mathbf{D})\, \mathrm{d}V, \qquad (3.16a)$$

$$8\pi\eta a^3 f_\mathrm{R} \mathbf{\Omega}_\mathrm{M} = \iint_{r=a} \mathbf{r} \times (\mathbf{\sigma}^\mathrm{E} \cdot \frac{\mathbf{r}}{r})\, \mathrm{d}S + \varepsilon \iiint_{b>r>a} \overline{\mathbf{v}}^\mathrm{R} \cdot \mathbf{D}(\nabla \cdot \mathbf{D})\, \mathrm{d}V, \qquad (3.16b)$$

where

$$\mathbf{\sigma}^\mathrm{E} = \varepsilon(\mathbf{DD} - \frac{1}{2}|\mathbf{D}|^2 \mathbf{I}); \qquad (3.17)$$

$$\overline{\mathbf{v}}^\mathrm{T} = \frac{1}{\Gamma_\mathrm{T}}(a_1 \mathbf{I} + 3a_3 \frac{\mathbf{rr}}{r^2}), \qquad (3.18a)$$

$$\overline{\mathbf{v}}^\mathrm{R} = -\frac{a_4}{\Gamma_\mathrm{R}} \mathbf{\varepsilon} \cdot \mathbf{r}; \qquad (3.18b)$$

$$f_\mathrm{T} = (1 - \lambda^5)(1 - \frac{9}{4}\lambda + \frac{5}{2}\lambda^3 - \frac{9}{4}\lambda^5 + \lambda^6)^{-1}, \qquad (3.19a)$$

$$f_\mathrm{R} = (1 - \lambda^3)^{-1}, \qquad (3.19b)$$

$\mathbf{I}$ is the unit dyadic, and $\mathbf{\varepsilon}$ is the alternating unit triadic. In Eqs. (3.16)-(3.18), the dyadics $\overline{\mathbf{v}}^\mathrm{T}$ (dimensionless) and $\overline{\mathbf{v}}^\mathrm{R}$ (with the dimension of length) represent the

normalized Stokes flow fields around an uncharged sphere translating and rotating, respectively, in a concentric spherical cavity for the generalized reciprocal theorem, and $\boldsymbol{\sigma}^{E}$ is the Maxwell stress tensor.

After the substitution of Eqs. (3.3), (3.10), (3.14), and (3.17)-(3.19) into Eq. (3.16) and some mathematical manipulations, we obtain

$$\mathbf{U}_{M} = \frac{\varepsilon}{\eta}[(\mathrm{M}_{pp}\zeta_{p} + \mathrm{M}_{wp}\zeta_{w})\mathbf{U}_{p} + (\mathrm{M}_{pw}\zeta_{p} + \mathrm{M}_{ww}\zeta_{w})\mathbf{U}_{w}] \times \mathbf{B}_{\infty}, \tag{3.20a}$$

$$\boldsymbol{\Omega}_{M} = \frac{\varepsilon}{\eta}[(\mathrm{N}_{pp}\zeta_{p} + \mathrm{N}_{wp}\zeta_{w})\boldsymbol{\Omega}_{p} + (\mathrm{N}_{pw}\zeta_{p} + \mathrm{N}_{ww}\zeta_{w})\boldsymbol{\Omega}_{w}] \times \mathbf{B}_{\infty}. \tag{3.20b}$$

where

$$\mathrm{M}_{pp} = \frac{2}{3f_{T}}[1 + t\lambda \coth t(1-\lambda) - \int_{\lambda}^{1} \frac{t^{2}a_{1}(a_{1}+2a_{3})\tau \sinh t(1-\tau) + b_{1}}{\Gamma_{T}^{2} \sinh t(1-\lambda)} d\tau], \tag{3.21a}$$

$$\mathrm{M}_{wp} = -\frac{2}{3f_{T}}[t \operatorname{csch} t(1-\lambda) + \int_{\lambda}^{1} \frac{t^{2}a_{1}(a_{1}+2a_{3}) \sinh t(\tau-\lambda) + b_{2}}{\lambda\Gamma_{T}^{2} \sinh t(1-\lambda)} d\tau], \tag{3.21b}$$

$$\mathrm{M}_{pw} = -\frac{2}{3f_{T}} \int_{\lambda}^{1} \frac{t^{2}[a_{1}(a_{2}-a_{3})+a_{2}a_{3}]\tau \sinh t(1-\tau) - b_{1}}{\Gamma_{T}^{2} \sinh t(1-\lambda)} d\tau, \tag{3.21c}$$

$$\mathrm{M}_{ww} = -\frac{2}{3f_{T}} \int_{\lambda}^{1} \frac{t^{2}[a_{1}(a_{2}-a_{3})+a_{2}a_{3}]\tau \sinh t(\tau-\lambda) - b_{2}}{\lambda\Gamma_{T}^{2} \sinh t(1-\lambda)} d\tau, \tag{3.21d}$$

$$\mathrm{N}_{pp} = \frac{1}{6f_{R}}[1 + t\lambda \coth t(1-\lambda) - \int_{\lambda}^{1} \frac{t^{2}a_{4}^{2}\tau^{3} \sinh t(1-\tau)}{\lambda^{2}\Gamma_{R}^{2} \sinh t(1-\lambda)} d\tau], \tag{3.21e}$$

$$\mathrm{N}_{wp} = -\frac{1}{6f_{R}}[t \operatorname{csch} t(1-\lambda) + \int_{\lambda}^{1} \frac{t^{2}a_{4}^{2}\tau^{3} \sinh t(\tau-\lambda)}{\lambda^{3}\Gamma_{R}^{2} \sinh t(1-\lambda)} d\tau], \tag{3.21f}$$

$$\mathrm{N}_{pw} = -\frac{1}{6f_{R}} \int_{\lambda}^{1} \frac{t^{2}a_{4}a_{5}\tau^{3} \sinh t(1-\tau)}{\lambda^{2}\Gamma_{R}^{2} \sinh t(1-\lambda)} d\tau, \tag{3.21g}$$

$$\mathrm{N}_{ww} = -\frac{1}{6f_{R}} \int_{\lambda}^{1} \frac{t^{2}a_{4}a_{5}\tau^{3} \sinh t(\tau-\lambda)}{\lambda^{3}\Gamma_{R}^{2} \sinh t(1-\lambda)} d\tau; \tag{3.21h}$$

$$b_1 = \frac{\tau}{\lambda}(a_1 + 3a_3)[5\tau^3(\lambda^2 - 1) - 2(\lambda^5 - 1)][t\tau \cosh t(1 - \tau) + \sinh t(1 - \tau)], \quad (3.22a)$$

$$b_2 = \frac{\tau}{\lambda}(a_1 + 3a_3)[5\tau^3(\lambda^2 - 1) - 2(\lambda^5 - 1)][-t\tau \cosh t(\tau - \lambda) + \sinh t(\tau - \lambda)], \quad (3.22b)$$

and $\tau = r/b = \gamma\lambda$. Equation (3.20a) shows that the induced translational velocity of the confined particle depends on the prescribed translational velocities of the particle and cavity, and it is in the direction perpendicular to both the relevant prescribed velocities and the imposed magnetic field. Equation (3.20b) indicates that the induced angular velocity of the particle depends on the prescribed angular velocities of the particle and cavity, and it is also in the direction normal to both the relevant prescribed angular velocities and the applied magnetic field.

3.4 Results and discussion

We first consider the expressions for the dimensionless mobility parameters M_{pp}, M_{wp}, M_{pw}, M_{ww}, N_{pp}, N_{wp}, N_{pw}, and N_{ww} in Eq. (3.21) for the limiting cases of the electrokinetic parameter κa and separation parameter $\lambda = a/b$. Results of the general case for the boundary effect on the MHD motion of the particle will then be discussed.

3.4.1 Limiting cases

In the limiting case of $\kappa a \to \infty$ (very thin electric double layers), Eq. (3.21) reduces to

$$M_{pp} = -3M_{pw} = -\frac{3}{2} + \frac{5(1 - \lambda^3)}{2(1 - \lambda^5)}, \quad (3.23a)$$

$$M_{wp} = N_{wp} = 0, \quad (3.23b)$$

$$M_{ww} = -\frac{2}{3} + \frac{5(1 - \lambda^2)}{3(1 - \lambda^5)}, \quad (3.23c)$$

$$N_{pp} = \frac{2}{3} + \frac{1}{3}\lambda^3 , \tag{3.23d}$$

$$N_{pw} = N_{ww} = -\frac{1}{2} . \tag{3.23e}$$

When $\lambda \to 0$ (the cavity wall is at an infinite distance from the particle), the above formulas can be further simplified and Eq. (3.20) becomes

$$\mathbf{U}_M = \frac{\varepsilon}{3\eta}[3\zeta_p\mathbf{U}_p - (\zeta_p - 3\zeta_w)\mathbf{U}_w] \times \mathbf{B}_\infty , \tag{3.24a}$$

$$\boldsymbol{\Omega}_M = \frac{\varepsilon}{6\eta}[4\zeta_p\boldsymbol{\Omega}_p - 3(\zeta_p + \zeta_w)\boldsymbol{\Omega}_w)] \times \mathbf{B}_\infty . \tag{3.24b}$$

In the limiting case of $\kappa a \to 0$ (very thick electric double layers), Eq. (3.21) reduces to

$$M_{pp} = -M_{wp} = \frac{44 + 48\lambda - 75\lambda^2 - 150\lambda^3 - 15\lambda^4 + 96\lambda^5 + 52\lambda^6}{24(4 + 11\lambda + 15\lambda^2 + 15\lambda^3 + 15\lambda^4 + 11\lambda^5 + 4\lambda^6)} , \tag{3.25a}$$

$$M_{pw} = -M_{ww} = \frac{(1-\lambda)^2(20 + 68\lambda + 83\lambda^2 + 33\lambda^3 - 12\lambda^4 - 12\lambda^5)}{24(1 - \lambda^5)(4 + 7\lambda + 4\lambda^2)} , \tag{3.25b}$$

$$N_{pp} = -N_{wp} = \frac{1}{6}(1 + \lambda + \lambda^2) , \tag{3.25c}$$

$$N_{pw} = N_{ww} = 0 . \tag{3.25d}$$

When $\lambda \to 0$, Eqs. (3.20) and (3.25) lead to

$$\mathbf{U}_M = \frac{\varepsilon}{24\eta}(\zeta_p - \zeta_w)(11\mathbf{U}_p + 5\mathbf{U}_w) \times \mathbf{B}_\infty , \tag{3.26a}$$

$$\boldsymbol{\Omega}_M = \frac{\varepsilon}{6\eta}(\zeta_p - \zeta_w)\boldsymbol{\Omega}_p \times \mathbf{B}_\infty . \tag{3.26b}$$

Both of the translational and angular velocities of the particle resulting from the MHD effect are proportional to the zeta potential difference between the particle surface and the cavity wall in this limiting case.

In the limit of $\lambda \to 1$ (the particle fills the cavity up completely), Eq. (3.21) results in

$M_{pp} = M_{wp} = M_{pw} = M_{ww} = N_{pw} = N_{ww} = 0$ and $N_{pp} = -N_{wp} = 1/2$, and thus Eq. (3.20)

reduces to

$$\mathbf{U}_M = \mathbf{0},$$ (3.27a)

$$\mathbf{\Omega}_M = \frac{\varepsilon}{2\eta}(\zeta_p - \zeta_w)\mathbf{\Omega}_p \times \mathbf{B}_\infty.$$ (3.27b)

As expected, the translational velocity of the particle caused by the MHD effect vanishes in

this limiting case.

Equations (3.24) and (3.26) with $\zeta_w = 0$ are consistent with Eq. (2.14). Note that the

translational and angular velocities of the charged particle induced by the MHD effect as

expressed by Eqs. (3.24) and (3.26) are independent of the particle size, analogous to the

electrophoretic velocity of the particle in the limiting cases of $\kappa a \rightarrow \infty$ and $\kappa a \rightarrow 0$.

3.4.2 General case

The numerical values of the dimensionless mobility parameters M_{pp}, M_{wp}, M_{pw},

M_{ww}, N_{pp}, N_{wp}, N_{pw}, and N_{ww}, as defined by Eq. (3.20) and calculated from formulas

in Eq. (3.21), are plotted versus the parameter $\lambda = a/b$ for various values of the parameter

κa in Figs. 3.2-3.5.

Figure 3.2 shows the results of the mobility parameters M_{pp} and M_{wp} corresponding

to the translational velocity $\mathbf{U}_p$ of the particle. In general, M_{pp} is a positive value which

decreases with an increase in λ (indicating that the proximity of the cavity wall reduces the

MHD migration of the particle) and with a decrease in κa and M_{wp} is a negative value

which is not a monotonic function of λ and κa, but there are exceptions when λ is large

(say, greater than 0.6).

Figure 3.3 illustrates the results of the mobility parameters M_{pw} and M_{ww} concerning the translational velocity $\mathbf{U}_w$ of the cavity wall. In general, both M_{pw} and M_{ww} are not monotonic functions of λ and κa. M_{pw} is a positive value when κa is small (less than unity) and can be negative otherwise (depending on the value of λ). On the contrary, M_{ww} is a positive value when κa is large (say, greater than 10) and can be negative otherwise (also depending on the value of λ).

The results of the mobility parameters N_{pp} and N_{wp} about the angular velocity $\mathbf{\Omega}_p$ of the particle are plotted in Figure 3.4. It can be seen that N_{wp} is a negative value whose magnitude increases with an increase in λ or with a decrease in κa and disappears as $\lambda \to 0$ or $\kappa a \to \infty$, whereas N_{pp} is positive and increases with an increase in κa for a given value of λ. In general, N_{pp} increases with an increase in λ (illustrating that the approach of the cavity wall enhances the MHD rotation of the particle), but there are exceptions when both λ and κa are large.

Figure 3.5 shows the results of the mobility parameters N_{pw} and N_{ww} regarding the angular velocity $\mathbf{\Omega}_w$ of the cavity wall. Both N_{pw} and N_{ww} are negative values with their magnitudes decreasing monotonically with an increase in λ or with a decrease in κa and vanishing as $\lambda \to 1$ or $\kappa a \to 0$. Namely, the approach of the cavity wall diminishes the MHD rotation of the particle caused by $\mathbf{\Omega}_w$.

It is interesting to examine the special case that both the spherical particle and the cavity wall move with the same translational and angular velocities (which occurs if the particle is freely suspended in the fluid inside the moving cavity without externally applied force and

torque) in the presence of the magnetic field. Substituting $\mathbf{U}_w = \mathbf{U}_p = \mathbf{U}$ and $\mathbf{\Omega}_w = \mathbf{\Omega}_p = \mathbf{\Omega}$ into Eq. (20), we obtain

$$\mathbf{U}_M = \frac{\varepsilon}{\eta}(M_p\zeta_p + M_w\zeta_w)\mathbf{U} \times \mathbf{B}_\infty,$$ (3.28a)

$$\mathbf{\Omega}_M = \frac{\varepsilon}{\eta}(N_p\zeta_p + N_w\zeta_w)\mathbf{\Omega} \times \mathbf{B}_\infty,$$ (3.28b)

where

$$M_p = M_{pp} + M_{pw}, \qquad M_w = M_{wp} + M_{ww},$$ (3.29a,b)

$$N_p = N_{pp} + N_{pw}, \qquad N_w = N_{wp} + N_{ww}.$$ (3.29c,d)

Figure 3.6 illustrates the results of the mobility parameters M_p and M_w about the translation of the particle and cavity. For any given value of κa, M_p is positive and decreases monotonically with an increase in λ from 2/3 at $\lambda = 0$ to zero at $\lambda = 1$. Namely, the proximity of the cavity wall reduces the MHD migration of the particle. M_w is a positive value when κa is large and can be negative if κa is small. For any specified value of λ, both M_p and M_w are monotonically increasing functions of κa.

The results of the mobility parameters N_p and N_w relating to the rotation of the particle and cavity are plotted in Figure 3.7. For any value of κa, N_p is positive and increases monotonically with an increase in λ from 1/6 at $\lambda = 0$ to 1/2 at $\lambda = 1$. Namely, the approach of the cavity wall enhances the MHD rotation of the particle. N_w is always negative and, for a finite value of κa, it first increases with an increase in λ from -1/2 at $\lambda = 0$, reaches a maximum at some value of λ, and then decreases with a further increase in λ to -1/2 again at $\lambda = 1$. For any fixed value of λ, both N_p and N_w are

31

monotonically decreasing functions of κa.

Finally, we consider the relative importance of the MHD effect on the particle movement. As an example, for a particle with $\zeta_p = 100$ mV suspended in an aqueous solution at 20℃ with prescribed magnetic flux density $|\mathbf{B}_\infty| = 1$T, Eq. (3.28a) with $\mathbf{U}_p = \mathbf{U}_w = \mathbf{U}$, $\zeta_w = 0$ and $\lambda = 0$ predicts that $|\mathbf{U}_M|/|\mathbf{U}| \cong 10^{-7}$, which is also the typical value of the small perturbation parameter α. The fact that the MHD effect on the particle movement is relatively weak is understandable knowing that the electric field induced by the interaction between the magnetic field and the fluid motion given by the term $\mathbf{v} \times \mathbf{B}_\infty$ in Eq. (3.5a) is much less than the typical external electric field applied in electrophoresis of charged particles.
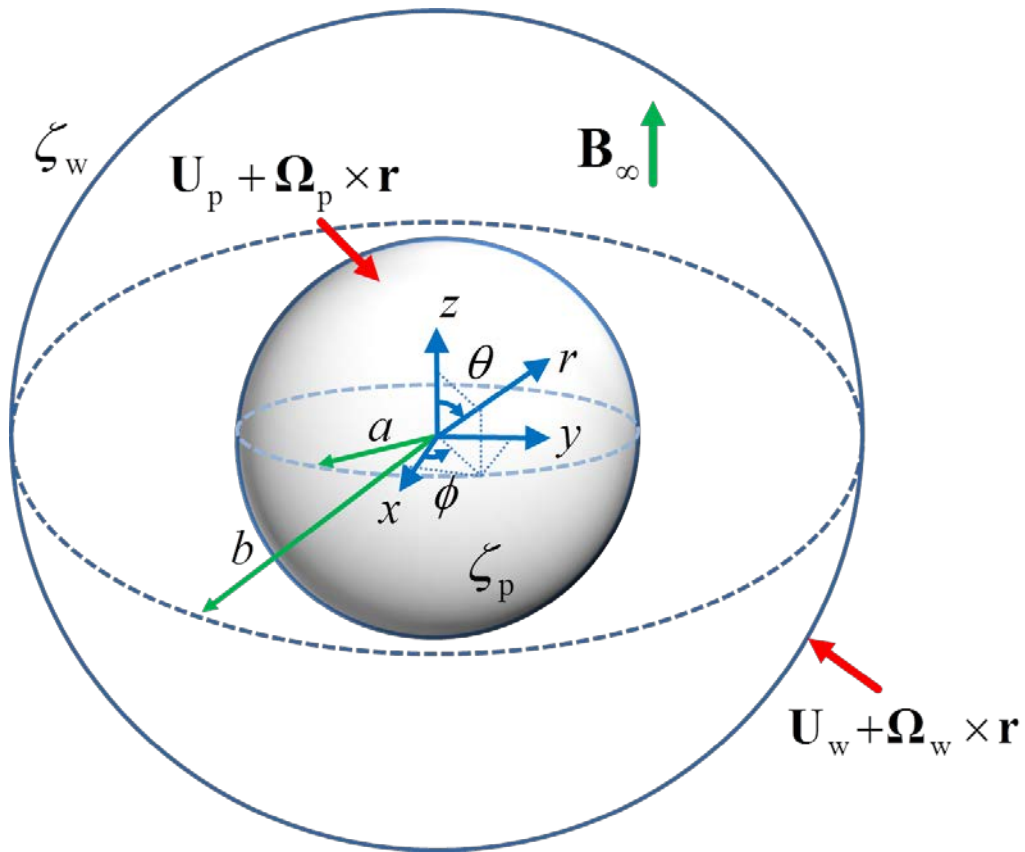
Figure 3.1   Geometric sketch for the MHD effect on the motion of a charged spherical particle in an concentric spherical cavity under applied Stokes flow and magnetic induction field.
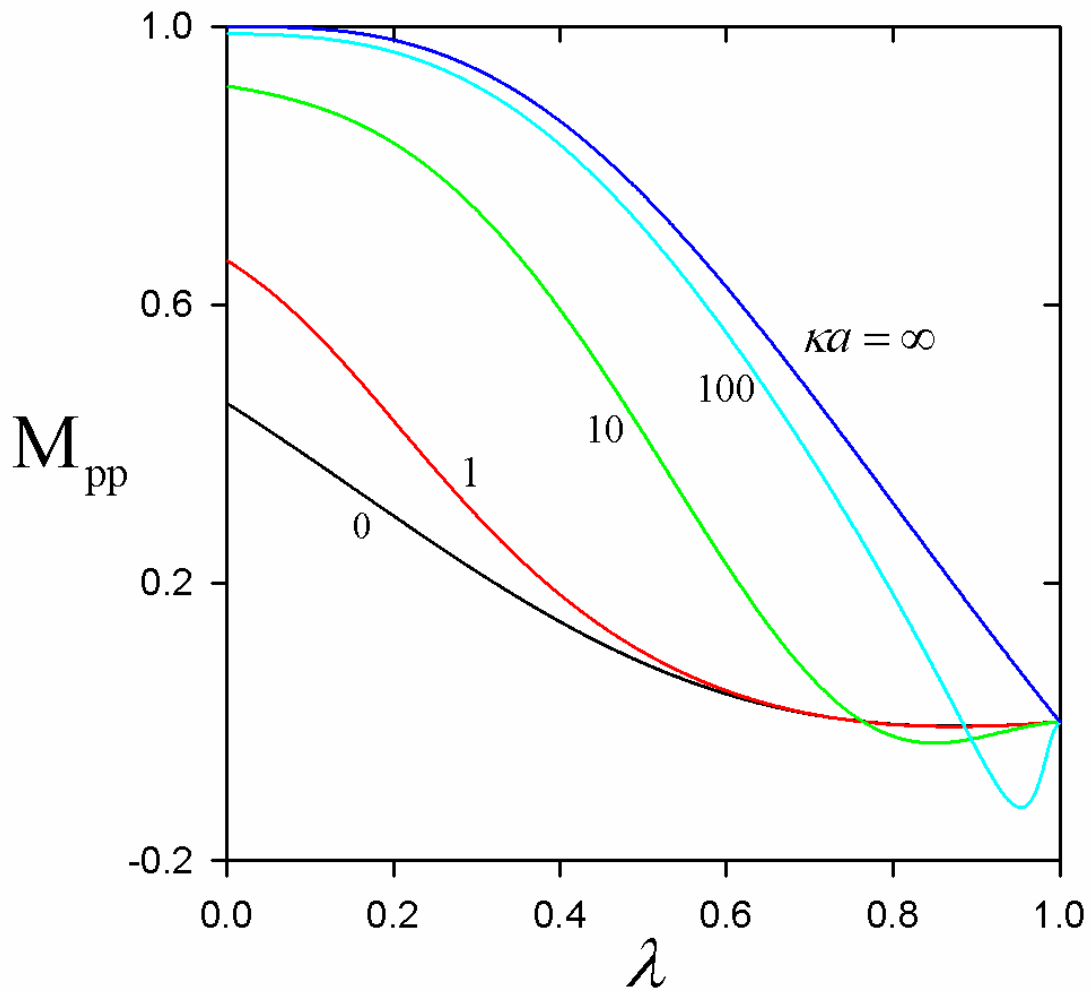
Figure 3.2a   Plots of the dimensionless mobility parameter M_{pp} as defined by Eq. (3.20a) and calculated from Eq. (3.21a) versus the parameter λ for various values of the parameter κa.
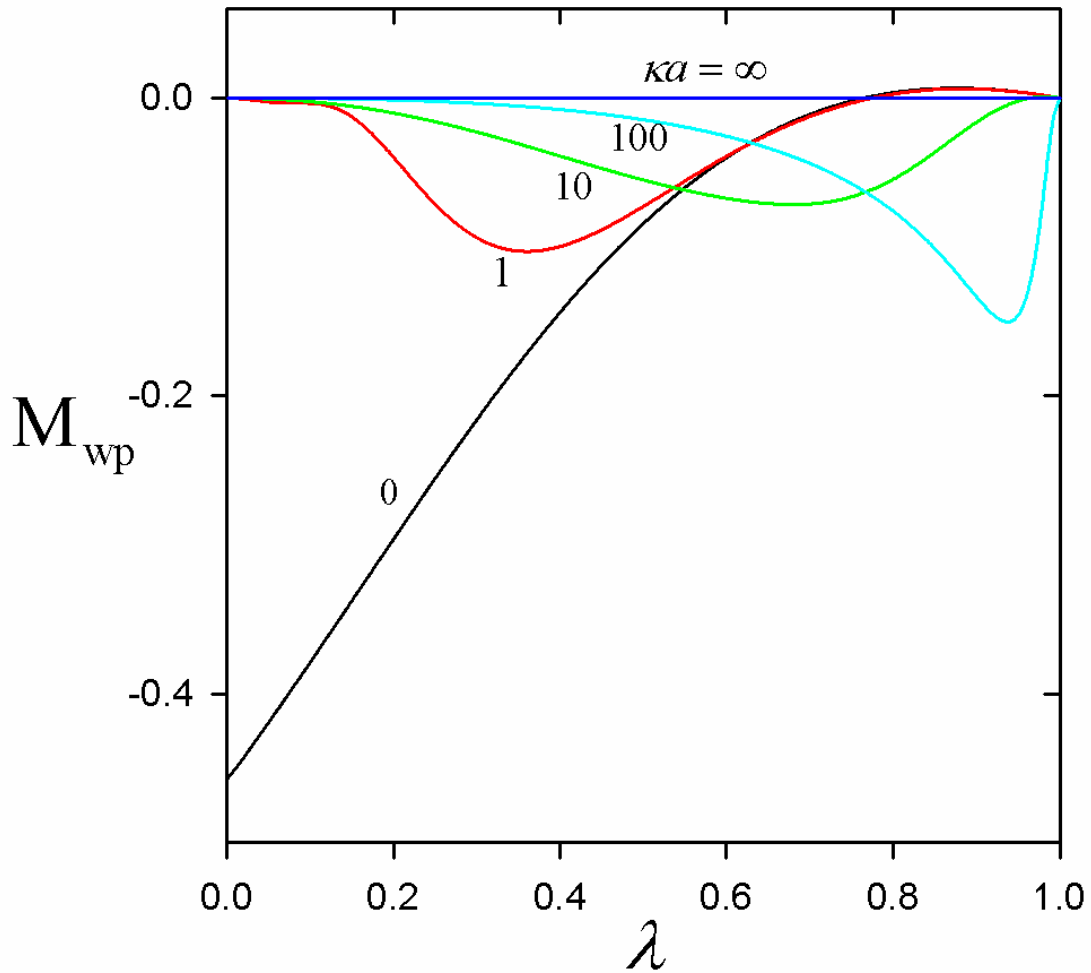
Figure 3.2b   Plots of the dimensionless mobility parameter M_{wp} as defined by Eq. (3.20a)

and calculated from Eq. (3.21b) versus the parameter λ for various values of the parameter

κa.
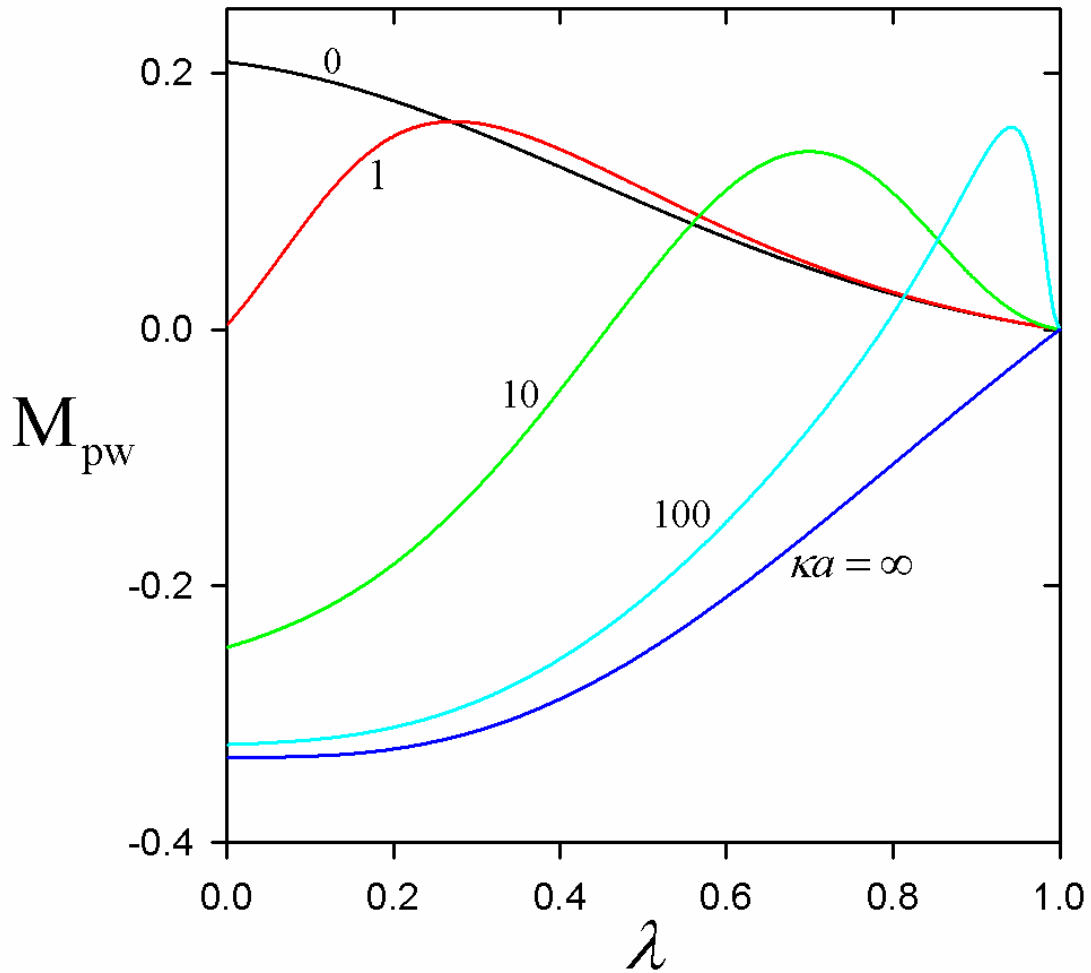
Figure 3.3a   Plots of the dimensionless mobility parameter M_{pw} as defined by Eq. (3.20a) and calculated from Eq. (3.21c) versus the parameter λ for various values of the parameter κa.
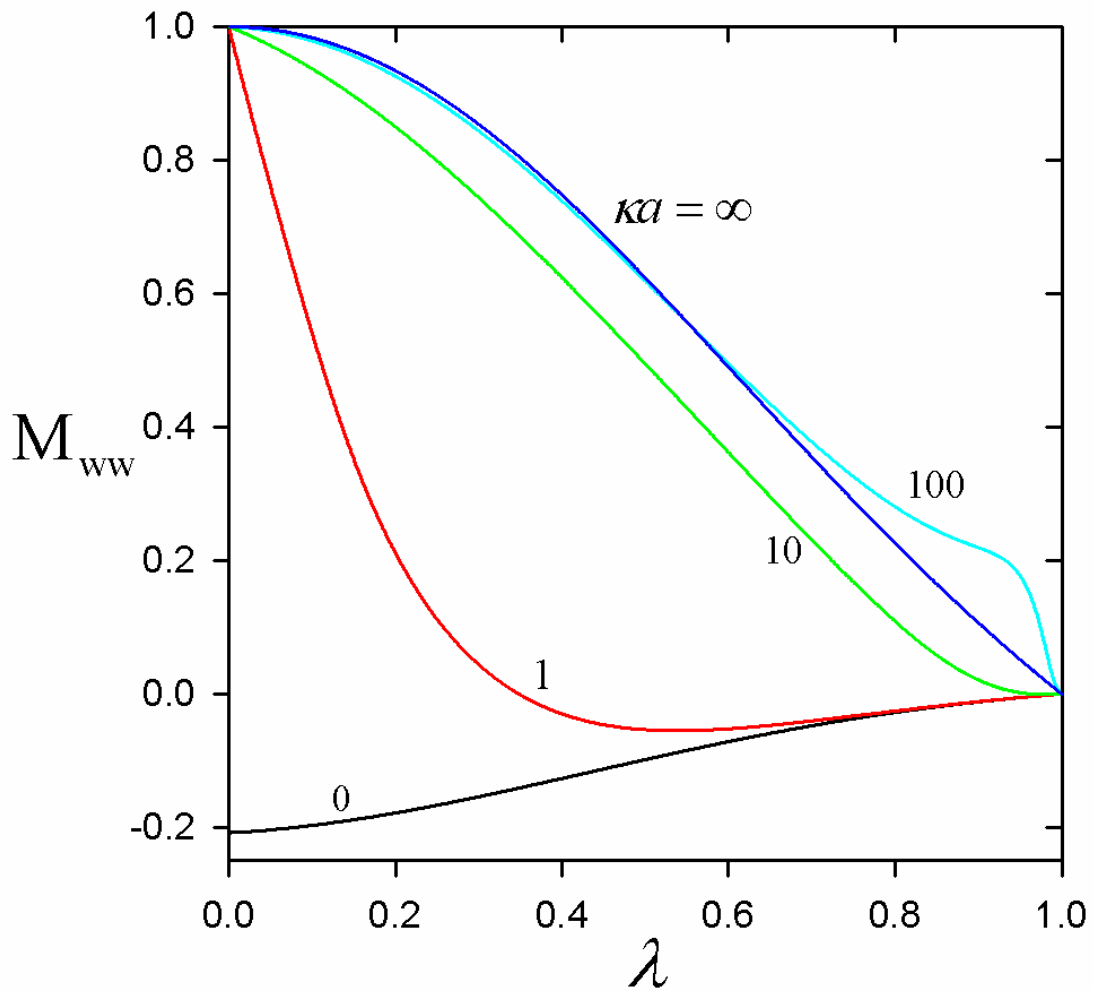
Figure 3.3b   Plots of the dimensionless mobility parameter M_{ww} as defined by Eq. (3.20a) and calculated from Eq. (3.21d) versus the parameter λ for various values of the parameter κa.
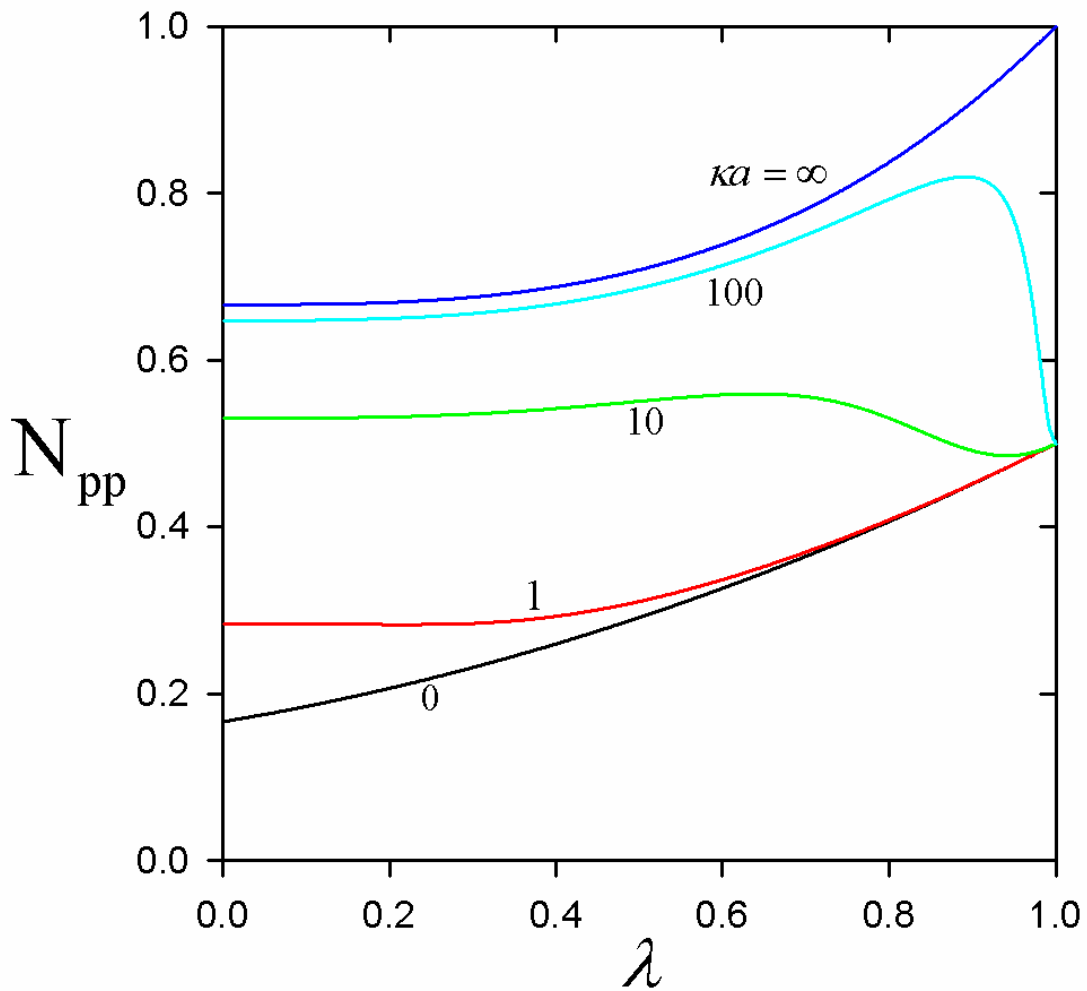
Figure 3.4a   Plots of the dimensionless mobility parameter N_{pp} as defined by Eq. (3.20b)

and calculated from Eq. (3.21e) versus the parameter λ for various values of the parameter

κa.
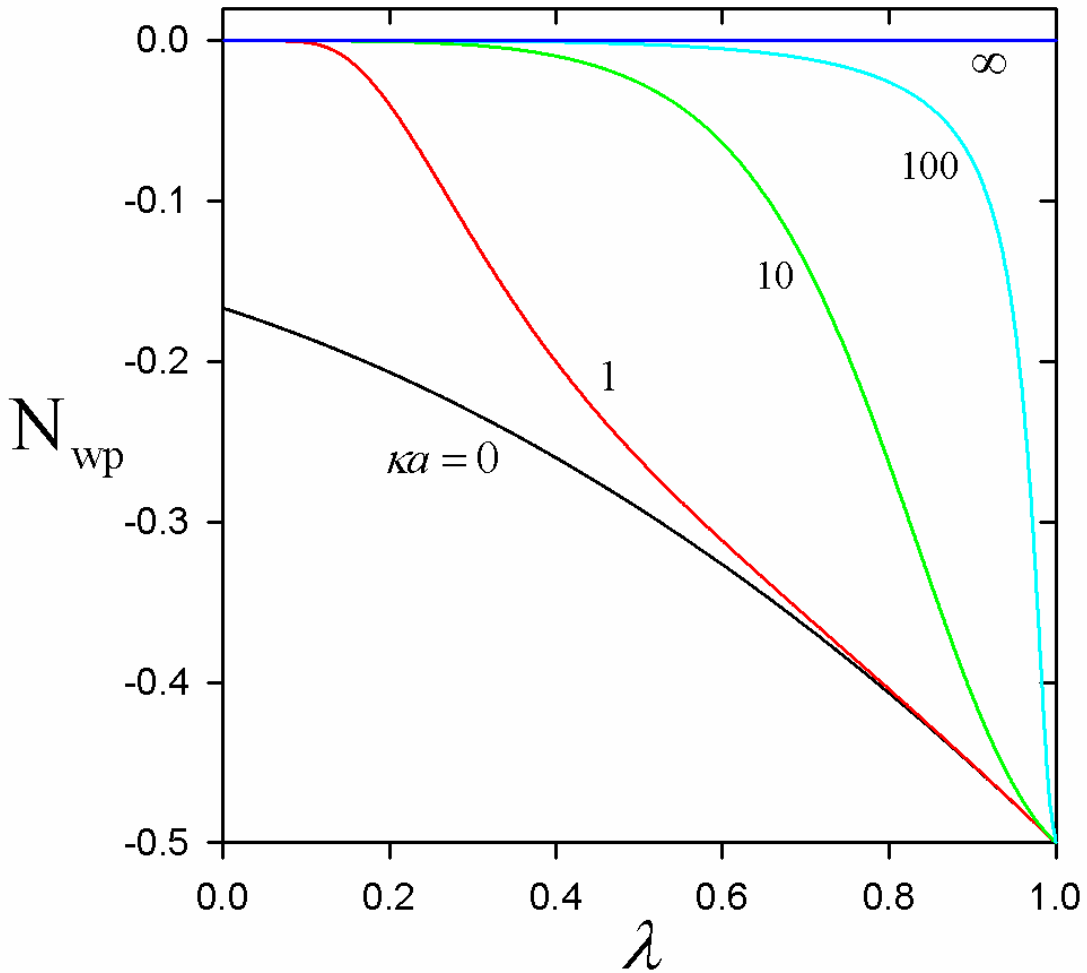
Figure 3.4b   Plots of the dimensionless mobility parameter N_{wp} as defined by Eq. (3.20b) and calculated from Eq. (3.21f) versus the parameter λ for various values of the parameter κa.
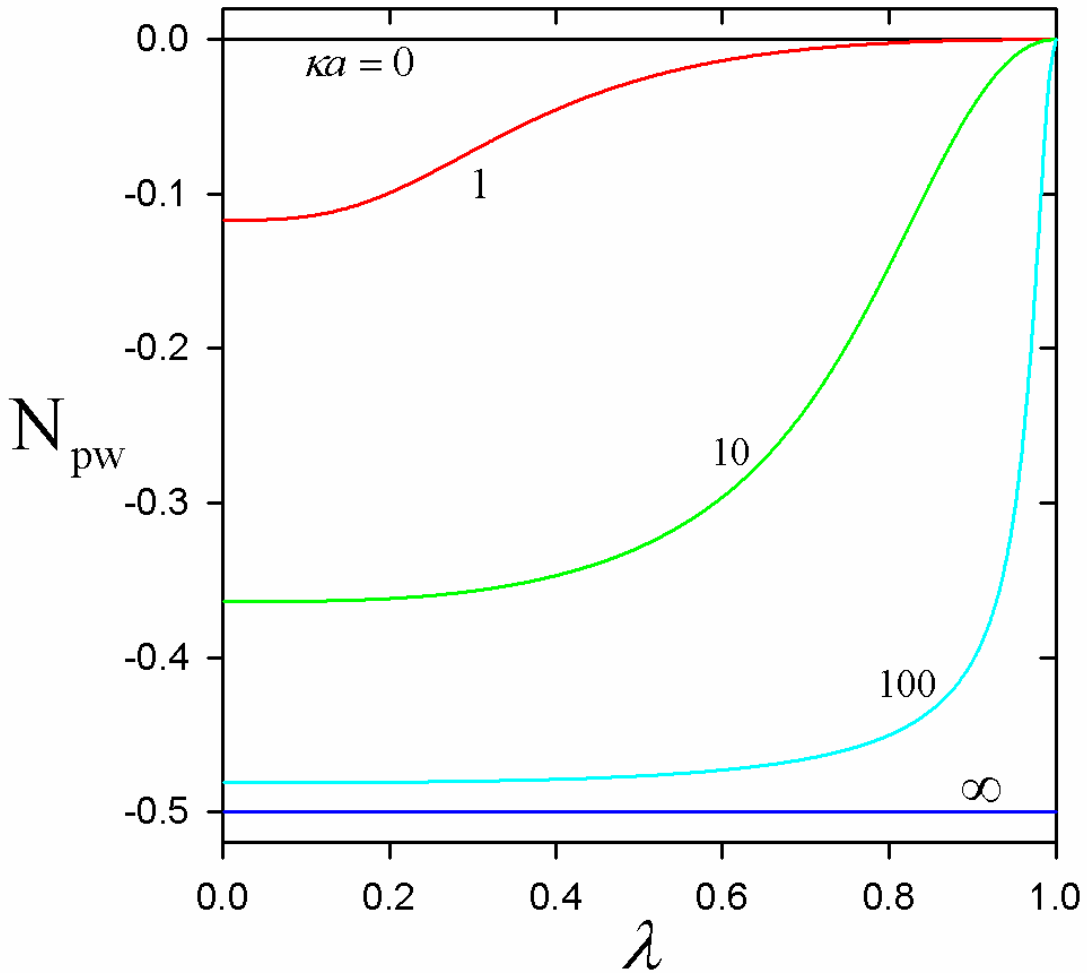
Figure 3.5a   Plots of the dimensionless mobility parameter N_{pw} as defined by Eq. (3.20b)

and calculated from Eq. (3.21g) versus the parameter λ for various values of the parameter

κa .
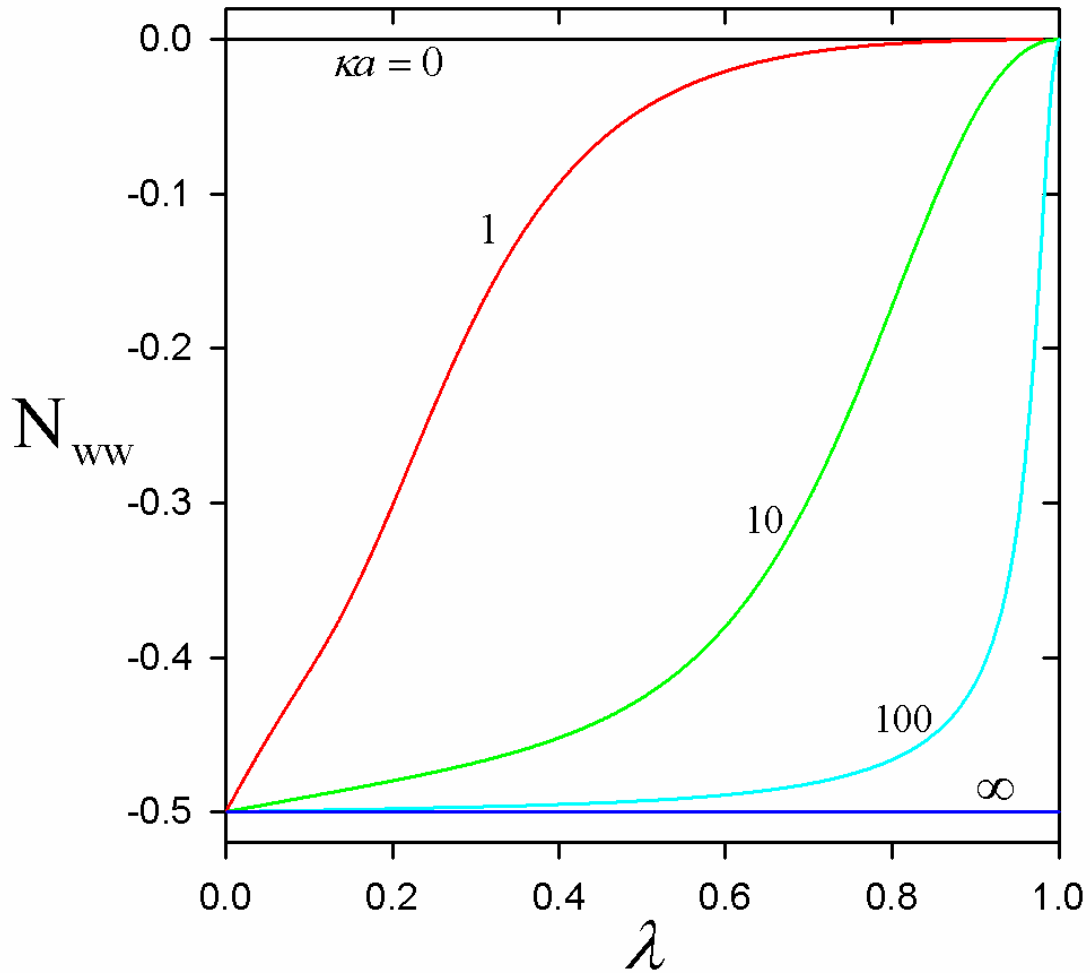
Figure 3.5b   Plots of the dimensionless mobility parameter N_{ww} as defined by Eq. (3.20b) and calculated from Eq. (3.21h) versus the parameter λ for various values of the parameter κa .
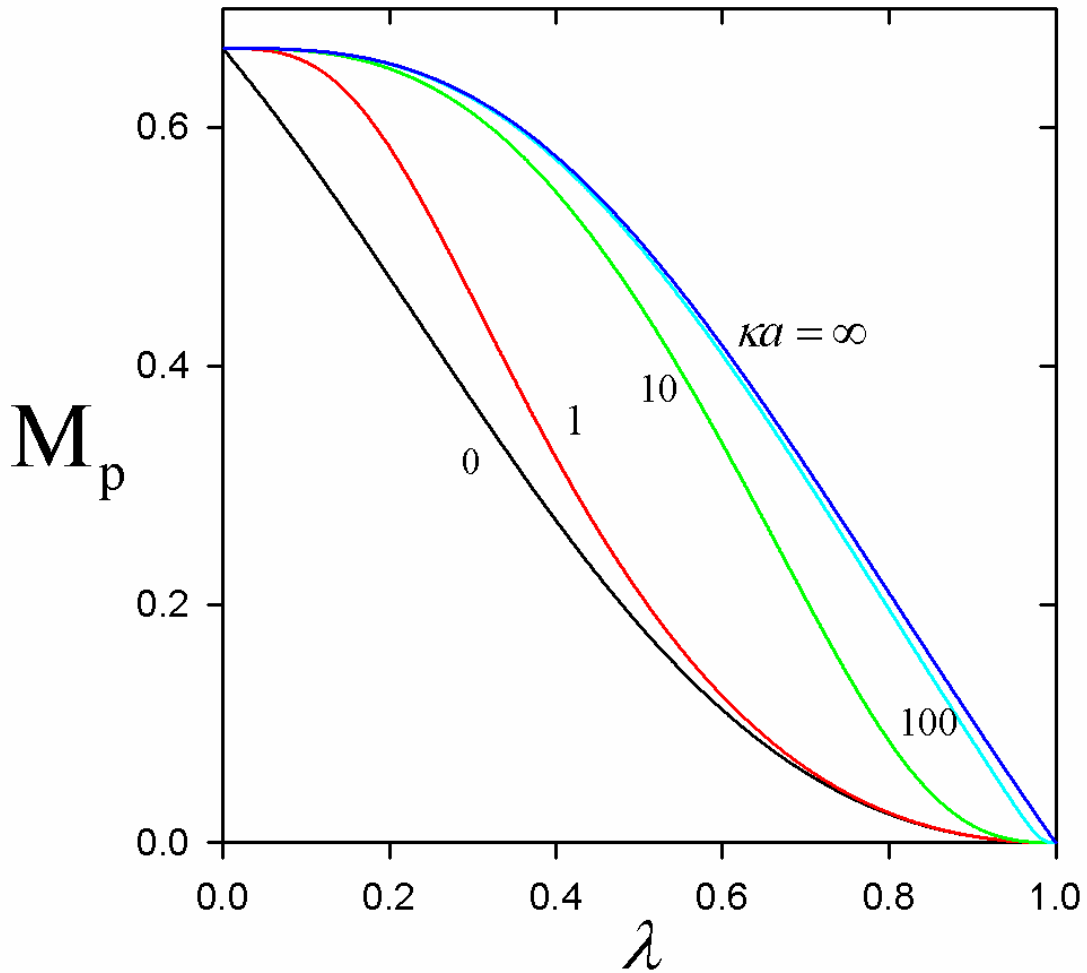
Figure 3.6a   Plots of the dimensionless mobility parameter M_p as defined by Eq. (3.28a)

versus the parameter λ for various values of the parameter κa.

42
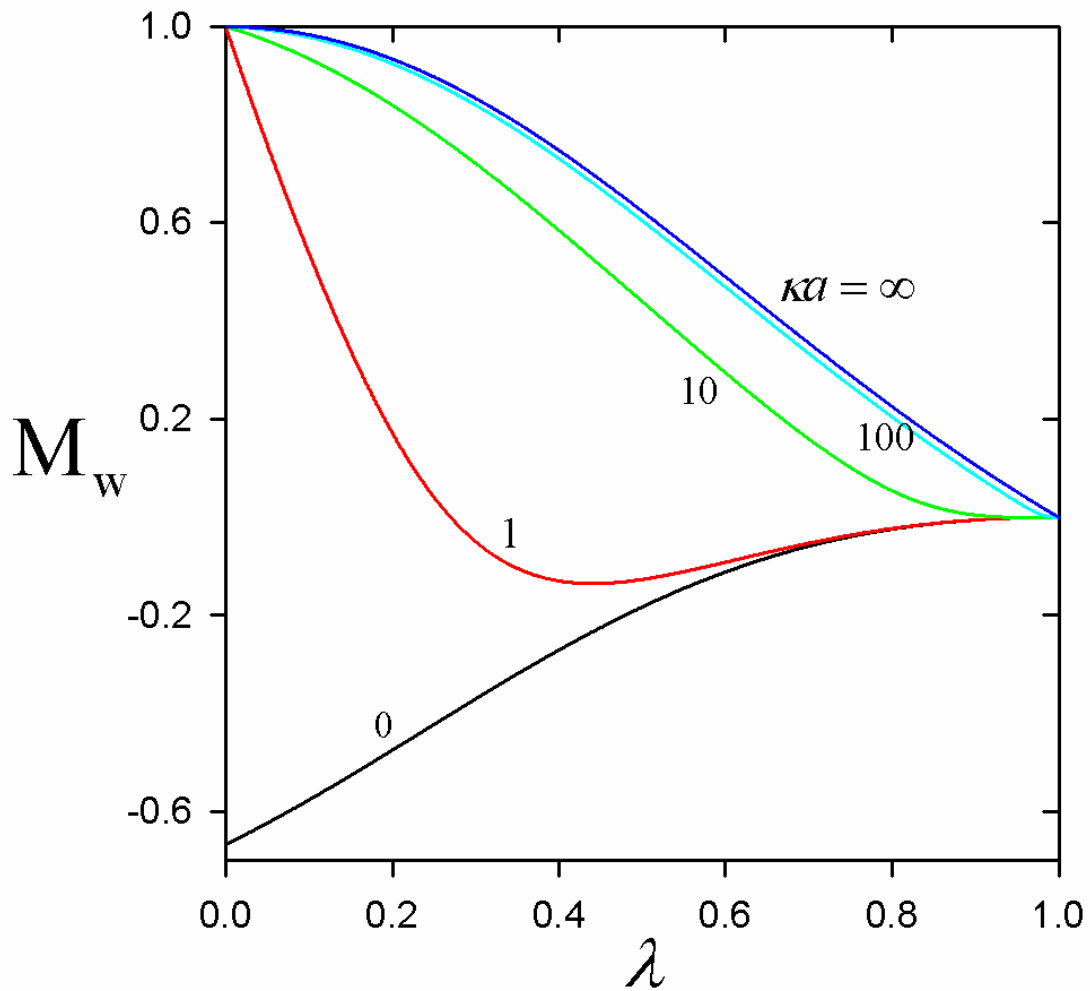
Figure 3.6b   Plots of the dimensionless mobility parameters M_w as defined by Eq. (3.28a)

versus the parameter λ for various values of the parameter κa .
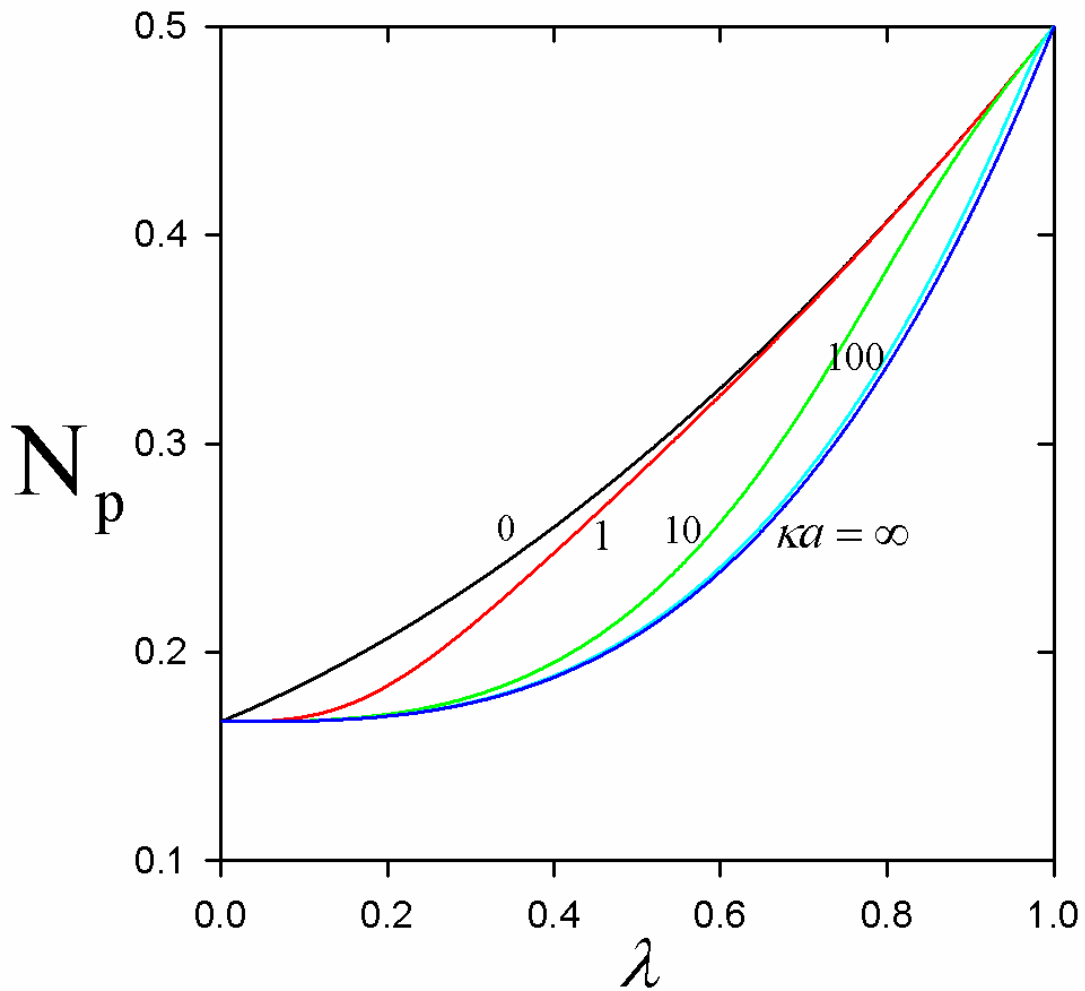
Figure 3.7a   Plots of the dimensionless mobility parameters N_p as defined by Eq. (3.28b)

versus the parameter λ for various values of the parameter κa.

44
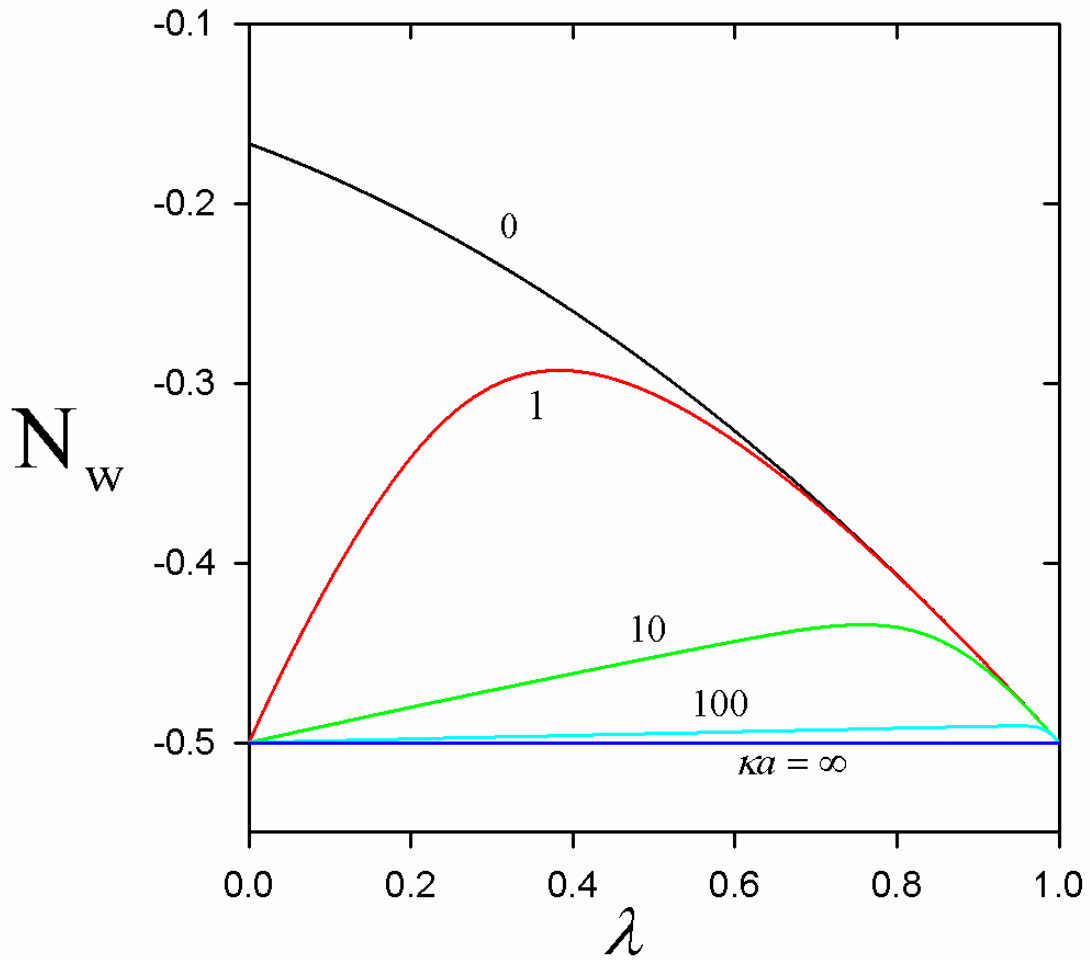
Figure 3.7b   Plots of the dimensionless mobility parameters N_w as defined by Eq. (3.28b)

versus the parameter λ for various values of the parameter κa.

Chapter 4

Electromagnetophoresis of a spherical particle in a spherical cavity

In this chapter, we consider the EMP migration of a spherical colloidal particle of radius a situated at the center of a spherical cavity of radius b filled with a conducting fluid of viscosity η subject to an applied electric current field $\mathbf{J}_\infty = J_\infty \mathbf{e}_y$ and a perpendicularly applied magnetic induction field $\mathbf{B}_\infty = B_\infty \mathbf{e}_z$ at the quasi-steady state and low Reynolds number, as shown in Figure 4.1, where $\mathbf{e}_y$ and $\mathbf{e}_z$ are two principal unit vectors in the rectangular coordinates (x, y, z), and both the electric current density J_∞ and magnetic flux density B_∞ are constant. The particle surface and cavity wall are allowed to bear electric charges and the conducting fluid may be an electrolyte solution, but the electric double layers adjacent to the particle and cavity surfaces are assumed to be thin relative to the particle radius and the gap width between the solid surfaces ($b - a$) such that the entire fluid phase is electrically neutral with a uniformity in the ionic composition. Electrokinetic (electrophoretic/electro-osmotic) and gravitational effects, which have been considered separately (Happel and Brenner 1983; Keh and Hsieh 2007; Keh and Cheng 2011) and can be added directly due to the linearity of the problem, are ignored here. The objective is to determine the boundary effect of the enclosing cavity on the EMP velocity of the particle.

4.1 Electric current density distributions

The electric conductivities σ_p of the particle and σ of the fluid are taken as constants. Thus, the electric potential distributions are governed by the Laplace equations

$$\nabla^2 \psi_p = 0 \quad (0 \le r \le a) \tag{4.1a}$$

for the particle and

$$\nabla^2 \psi = 0 \quad (a \le r \le b) \tag{4.1b}$$

for the fluid, where (r, θ, ϕ) are spherical coordinates.

The boundary conditions for the potential distributions ψ_p and ψ at the particle surface and cavity wall are

$$r = a: \qquad \mathbf{e}_r \cdot (\mathbf{J} - \mathbf{J}_p) = 0, \tag{4.2a}$$

$$\mathbf{e}_r \times (\frac{\mathbf{J}}{\sigma} - \frac{\mathbf{J}_p}{\sigma_p}) = \mathbf{0}; \tag{4.2b}$$

$$r = b: \qquad \mathbf{e}_r \cdot (\mathbf{J} - \mathbf{J}_\infty) = 0, \tag{4.3}$$

where the electric current density distributions in the particle and fluid phases are

$$\mathbf{J}_p = -\sigma_p \nabla \psi_p \qquad \text{and} \qquad \mathbf{J} = -\sigma \nabla \psi, \tag{4a,b}$$

respectively, and $\mathbf{e}_r$ is the unit vector in the r direction. Equations (4.2a) and (4.2b) stand for the continuity of the normal component of the current density and the tangential component of the electric field at the particle surface, and Eq. (4.3) gives the uniformly applied current density $\mathbf{J}_\infty = J_\infty \mathbf{e}_y$ in the fluid phase in the absence of the particle. The additional electric current induced by the fluid motion under the applied magnetic field is negligible relative to the applied electric current (the typical value of their ratio $a^2 B_\infty^2 \sigma / \eta$ will be discussed in Subsection 5.4.3).

The solution to the above equations is

48

$$\psi_\text{p} = -3\frac{J_\infty}{\sigma} S_1(\sigma^*) rY \,, \tag{4.5a}$$

$$\psi = -\frac{J_\infty}{\sigma} S_1(\sigma^*)[\sigma^* + 2 - (\sigma^* - 1)\gamma^{-3}] rY \,, \tag{4.5b}$$

where

$$S_1(x) = [x + 2 + 2\lambda^3(x-1)]^{-1} \,, \tag{4.6}$$

$Y = \sin\theta\sin\phi$ is a surface harmonic, $\gamma = r/a$, $\sigma^* = \sigma_\text{p}/\sigma$, and $\lambda = a/b$. The constant

terms in Eq. (4.5) are trivial and have been omitted.

4.2 Magnetic flux density distributions

The magnetic permeabilities μ_p of the particle and μ of the fluid are also taken to be

constants, and the magnetic flux density distributions are governed by (Jackson 1976)

$$\nabla\cdot\mathbf{B}_\text{p} = 0 \,, \qquad \nabla\times\mathbf{B}_\text{p} = \mu_\text{p}\mathbf{J}_\text{p} \quad (0 \le r \le a) \tag{4.7a,b}$$

for the particle and

$$\nabla\cdot\mathbf{B} = 0 \,, \qquad \nabla\times\mathbf{B} = \mu\mathbf{J} \qquad (a \le r \le b) \tag{4.7c,d}$$

for the fluid.

The boundary conditions for the magnetic field at the particle surface and cavity wall are

$$r = a: \qquad \mathbf{e}_r\cdot(\mathbf{B} - \mathbf{B}_\text{p}) = 0, \tag{4.8a}$$

$$\mathbf{e}_r\times(\frac{\mathbf{B}}{\mu} - \frac{\mathbf{B}_\text{p}}{\mu_\text{p}}) = \mathbf{0} \,; \tag{4.8b}$$

$$r = b: \qquad \mathbf{e}_r\cdot(\mathbf{B} - \mathbf{B}_\infty) = 0. \tag{4.9}$$

Equations (4.8a) and (4.8b) denote that both the normal component of the magnetic flux

density and the tangential component of the magnetic field are continuous at the particle

surface, whereas Eq. (4.9) leads to the imposed magnetic flux density $\mathbf{B}_\infty$ everywhere in the

fluid in the absence of the particle.

The solution to Eqs. (4.7)-(4.9) with the substitution of Eqs. (4.4) and (4.5) can be expressed as

$$\mathbf{B}_p = -\frac{3}{2}\mu_p J_\infty \sigma^* S_1(\sigma^*) r^2 \mathbf{e}_r \times \nabla Y - \mu_p \nabla \Phi_p, \tag{4.10a}$$

$$\mathbf{B} = -\mu J_\infty S_1(\sigma^*)[\frac{\sigma^*+2}{2} + (\sigma^*-1)\gamma^{-3}]r^2 \mathbf{e}_r \times \nabla Y - \mu \nabla \Phi, \tag{4.10b}$$

where the magnetic scalar potential distributions due to the applied magnetic field $\mathbf{B}_\infty = B_\infty \mathbf{e}_z$ are

$$\Phi_p = -3\frac{B_\infty}{\mu}S_1(\mu^*)r\cos\theta, \tag{4.11a}$$

$$\Phi = -\frac{B_\infty}{\mu}S_1(\mu^*)[\mu^*+2-(\mu^*-1)\gamma^{-3}]r\cos\theta, \tag{4.11b}$$

and $\mu^* = \mu_p/\mu$. The constant terms in Eq. (4.11) are trivial and have been neglected.

The first terms on the right-hand side of Eq. (4.10) are induced by the applied electric current density (Ampere's law), whereas the second terms whose curls vanish result from the applied magnetic field. The magnitude of either ratio of the first-to-second terms has the order $\mu a J_\infty / B_\infty$, which is usually small (will be discussed in Subsection 5.4.3).

4.3 Electromagnetophoretic force and velocity

The creeping motion of the fluid in the presence of the applied magnetic flux density and electric current density is governed by the Stokes equations with a Lorentz force density term,

$$\eta\nabla^2\mathbf{v} = \nabla p - \mathbf{J}\times\mathbf{B}, \tag{4.12a}$$

$$\nabla\cdot\mathbf{v} = 0, \tag{4.12b}$$

where $\mathbf{v}$ and p are the fluid velocity and dynamic pressure distributions, respectively. Note that, different from the constant force density in a gravitational field, the Lorentz force density $\mathbf{J}\times\mathbf{B}$ is a function of position in the particle and fluid phases.

The boundary conditions for the fluid velocity at the no-slip particle surface and cavity wall are given by

$$r = a: \qquad \mathbf{v} = \mathbf{U}, \tag{4.13}$$

$$r = b: \qquad \mathbf{v} = \mathbf{0}, \tag{4.14}$$

where $\mathbf{U}$ is the EMP migration velocity of the particle to be determined. There is no rotation of the particle due to the axial symmetry of the fluid flow.

Following Teubner's approach to obtain the particle velocity (without solving for the fluid velocity field) with a generalized reciprocal theorem (Teubner 1982; Yoon 1991; Keh and Hsieh 2008; Miloh 2011), we can express the EMP force exerted on the confined particle as

$$6\pi\eta a f_{\mathrm{T}} \mathbf{U} = \mathbf{F}(\sigma^*, \mu^*) - \mathbf{F}(1,1), \tag{4.15}$$

where the total applied force acting on the particle is composed of relevant surface and volume integrals,

$$\mathbf{F}(\sigma^*, \mu^*) = \iiint_{0<r<a} \mathbf{J}_{\mathrm{p}} \times \mathbf{B}_{\mathrm{p}} \mathrm{d}V + \iiint_{a<r<b} \overline{\mathbf{v}}^{\mathrm{T}} \cdot (\mathbf{J} \times \mathbf{B}) \mathrm{d}V + \iint_{r=a} \boldsymbol{\sigma}^{\mathrm{M}} \cdot \mathbf{e}_r \mathrm{d}S. \tag{4.16}$$

Here, f_{T} is the hydrodynamic resistance coefficient for the migration of the sphere driven by a body force field in the concentric spherical cavity given by Eq. (3.19a), $\boldsymbol{\sigma}^{\mathrm{M}}$ is the magnetic Maxwell stress tensor,

$$\boldsymbol{\sigma}^{\mathrm{M}} = \frac{1}{\mu}(\mathbf{B}\mathbf{B} - \frac{1}{2}|\mathbf{B}|^2 \mathbf{I}), \tag{4.17}$$

and $\overline{\mathbf{v}}^{\mathrm{T}}$ is given by Eq. (3.18a).

In Eq. (4.16), the first term on the right-hand side is the Lorentz body force exerted directly on the particle, known as the electromagnetic weight, the second term is a force contribution from the fluid flow due to the Lorentz force density in Eq. (4.12a), and the third term represents the contribution from the Maxwell stress at the particle surface. $\mathbf{F}(1,1)$

equals $(4/3)\pi a^3 \mathbf{J}_\infty \times \mathbf{B}_\infty$, which is the applied Lorentz force acting on the fluid volume occupied by the particle, known as the electromagnetic buoyancy.

Substituting Eqs. (4.4) and (4.5) for the electric current density distributions and Eqs. (4.10) and (4.11) for the magnetic flux density distributions into Eqs. (4.15) and (4.16), we obtain the ensuing migration velocity of the particle

$$\mathbf{U} = U^* \frac{a^2}{\eta} \mathbf{J}_\infty \times \mathbf{B}_\infty, \tag{4.18}$$

where the dimensionless EMP mobility of the particle

$$U^* = \frac{1}{3f_T}\{S_1(\sigma^*)S_1(\mu^*)[3\sigma^*(3\mu^*+1) - c_1(\sigma^* + \mu^*) - c_2(\sigma^*\mu^*+1)] - \frac{2}{3}\}, \tag{4.19}$$

and the coefficients c_1 and c_2 are functions of the particle-to-cavity radius ratio λ,

$$c_1 = (1 + \lambda + \lambda^2)(5 + 6\lambda + 3\lambda^2 + \lambda^3)(4 + 7\lambda + 4\lambda^2)^{-1}, \tag{4.20a}$$

$$c_2 = (1 - \lambda)(7 + 17\lambda + 15\lambda^2 + 5\lambda^3 + \lambda^4)(4 + 7\lambda + 4\lambda^2)^{-1}. \tag{4.20b}$$

Evidently, U^* is a function of the particle-to-fluid electric conductivity ratio σ^* and magnetic permeability ratio μ^* as well as λ only. For the special case of $\sigma^* = \mu^* = 1$ (the particle and suspending fluid have the same electric conductivity and magnetic permeability), the electromagnetic weight (and the total applied force acting on the particle) equals the electromagnetic buoyancy and there is no particle motion. If only the first term on the right-hand side of Eq. (4.16) is taken approximately to be the total applied force in Eq. (4.15), then Eq. (4.19) becomes

$$U^* = \frac{2}{9f_T}[9\sigma^* S_1(\sigma^*)\mu^* S_1(\mu^*) - 1]. \tag{4.21}$$

Note that Eq. (4.18) predicts $\mathbf{U}$ to be bilinear in the product $\mathbf{J}_\infty \times \mathbf{B}_\infty$, indicating that the integral terms of the second orders J_∞^2 and B_∞^2 in the Maxwell stress $\boldsymbol{\sigma}^M$ and Lorentz force densities $\mathbf{J} \times \mathbf{B}$ and $\mathbf{J}_p \times \mathbf{B}_p$ in Eq. (4.16) vanish and make no contribution to the

particle velocity. Nonetheless, the contribution from the induced magnetic flux density caused by the applied electric current density [the first term in Eq. (4.10b)] is included in Eq. (4.19) via the term containing $\boldsymbol{\sigma}^{\mathrm{M}}$ in Eq. (4.16). For a particle with $a = 1\,\mu\mathrm{m}$ in aqueous solutions with the applied electric current density $J_\infty = 10^4\,\mathrm{A/m^2}$ and magnetic flux density $B_\infty = 1\,\mathrm{T}$, the characteristic particle velocity $a^2 J_\infty B_\infty / \eta$ in Eq. (4.18) is about $10^{-5}\,\mathrm{m/s}$ typically.

In the limit $\lambda \to 0$ (the cavity wall is at an infinite distance from the particle), Eq. (4.19) reduces to

$$U_0^* = \frac{79\sigma^*\mu^* + 5\sigma^* - 31\mu^* - 53}{36(\sigma^* + 2)(\mu^* + 2)} . \tag{4.22}$$

If the term of integration of the Maxwell stress $\boldsymbol{\sigma}^{\mathrm{M}}$ over the particle surface in Eq. (4.16) is not included, Eq. (4.22) becomes

$$U_0^* = \frac{17\sigma^*\mu^* - 5\sigma^* - 5\mu^* - 7}{12(\sigma^* + 2)(\mu^* + 2)} . \tag{4.23}$$

This approximate result agrees with the EMP mobility calculated using the formula obtained earlier by Leenov and Kolin (Leenov and Kolin 1954) for the EMP force acting on a spherical particle in an unbounded fluid with $\mu^* = 1$, in which the effect of the Maxwell stress was not considered. Note that the EMP mobility at $\mu^* = 1$ predicted by Eq. (4.23) is much smaller than that resulting from Eq. (4.22) by a factor of 3/7, and thus the contribution from the Maxwell stress (only due to its part bilinear in J_∞ and B_∞) to the EMP migration of a particle is significant.

In the limit $\lambda \to 1$ (the particle fills the cavity up completely), Eq. (4.19) results in $U^* = 0$, as expected.
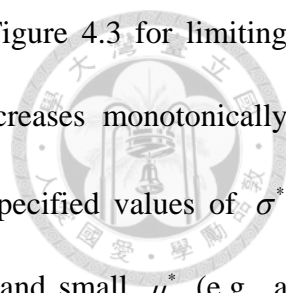
4.4 Results and discussion

Equation (4.18) for the EMP migration of a spherical particle positioned at the center of a spherical cavity indicates that the velocity of the particle is bilinear in the applied electric current and magnetic flux density fields (and proportional to a^2/η). The results of the dimensionless EMP mobility obtained in Eqs. (4.19) and (4.22) for the confined particle and an isolated particle, respectively, as well as the asymptotic behavior of the boundary effect on EMP will be discussed in this section.

4.4.1 Electromagnetophoretic mobility parameter

We first plot the EMP mobility parameter U_0^* of an unconfined spherical particle ($\lambda = 0$) as calculated from Eq. (4.22) in Figure 4.2 for various values of the particle-to-fluid electric conductivity ratio σ^* and magnetic permeability ratio μ^*. As can be derived from Eq. (4.22), U_0^* is always positive if $\sigma^* > 53/5$ and negative if $\sigma^* < 31/79$, regardless of the value of μ^*. In the intermediate range of $31/79 < \sigma^* < 53/5$, U_0^* is positive (negative) if the value of μ^* is sufficiently large (small). For a constant value of μ^*, the value of U_0^* increases monotonically with an increase in σ^* from a negative constant at $\sigma^* = 0$ to a positive one as $\sigma^* \to \infty$. For a specified value of σ^* greater than $1/17$, the value of U_0^* increases monotonically with an increase in μ^*, whereas for a given value of σ^* less than $1/17$, U_0^* is negative and decreases monotonically with an increase in μ^*. When $\sigma^* = 1/17$, $U_0^* = -16/45$, independent of μ^*. Equation (4.22) gives $U_0^* = -31/72$, $-53/144$, $5/72$, and $79/36$ in the limits of (μ^*, σ^*) approaching $(\infty, 0)$, $(0, 0)$, $(0, \infty)$, and (∞, ∞), respectively.

The normalized EMP mobility U^*/U_0^* of a confined particle calculated from Eq. (20)

as a function of the particle-to-cavity radius ratio λ is plotted in Figure 4.3 for limiting conditions of the parameters σ^* and μ^*. In general, U^*/U_0^* decreases monotonically with an increase in λ from unity at $\lambda = 0$ to zero at $\lambda = 1$ for specified values of σ^* and μ^*. However, for the case of large σ^* (thus, U_0^* is positive) and small μ^* (e.g., a superconducting particle), U^*/U_0^* first decreases with an increase in λ from unity at $\lambda = 0$, reaches a minimum of negative value (implying a reversal in the direction of particle migration), then increases with further increase in λ to zero at $\lambda = 1$. In this case, the second term on the right-hand side of Eq. (4.16) dominates the force exerted on the particle and results in the non-monotonic dependence of U^* on λ. For a constant value of λ, U^*/U_0^* decreases (or the boundary effect becomes stronger) with an increase in σ^* and increase (or the boundary effect gets weaker) with an increase in μ^*, keeping the other parameter unchanged. The boundary effect of the cavity on the EMP mobility of the particle is equivalent to that caused by gravitational fields (Happel and Brenner 1983) (in the particular case of $\sigma^* = 1/3$ and $\mu^* = 1$, $U^*/U_0^* = 1/f_T$ for an arbitrary value of λ and the boundary effect on EMP migration is exactly the same as that on sedimentation), but is much stronger than that in electrophoresis (Keh and Hsieh 2007).

4.4.2 Asymptotic behaviors

Yariv and Miloh (Yariv and Miloh 2009) analyzed the EMP motions of an insulating spherical particle suspended in a conducting fluid of matching magnetic permeability (i.e., with $\sigma^* = 0$ and $\mu^* = 1$) in the vicinity of a dielectric plane wall, where an electric current is imposed parallel to the wall and a perpendicular magnetic field is applied either parallel or normal to the wall. Through the use of a method of reflections for the situation of wide

separation ($\lambda \to 0$), they obtained formulas for the hydrodynamic force on the particle and the migration velocity of the particle in asymptotic expansions of λ, the ratio of the particle radius to the distance of the particle center from the wall. The leading-order wall-induced corrections to the EMP force and migration velocity appear to be $O(\lambda^3)$ and $O(\lambda)$, respectively, as opposed to the $O(\lambda)$ variation for both the resistance and the mobility of a sphere undergoing sedimentation near a plane wall.

The Taylor expansions for the EMP force and migration velocity of a spherical particle with $\mu^* = 1$ within a concentric spherical cavity in λ resulting from Eqs. (4.15) and (4.18) together with (3.19a), (4.19), and (4.20) are

$$\mathbf{F}(\sigma^*,1) - \mathbf{F}(1,1) = \frac{14\pi(\sigma^* - 1)}{3(\sigma^* + 2)}[1 - \frac{6(3\sigma^* - 1)}{7(\sigma^* + 2)}\lambda^3 + O(\lambda^4)]a^3\mathbf{J}_\infty \times \mathbf{B}_\infty, \tag{4.24a}$$

$$\mathbf{U} = \frac{7(\sigma^* - 1)}{9(\sigma^* + 2)}[1 - \frac{9}{4}\lambda - \frac{\sigma^* - 82}{14(\sigma^* + 2)}\lambda^3 + O(\lambda^4)]\frac{a^2}{\eta}\mathbf{J}_\infty \times \mathbf{B}_\infty. \tag{4.24b}$$

Here, the leading-order corrections to the EMP force and migration velocity also appear at $O(\lambda^3)$ and $O(\lambda)$, respectively, in contrast to the $O(\lambda)$ correction given by Eq. (3.19a) for both the resistance and the mobility of a sphere settling at the center of a spherical cavity. The $O(\lambda)$ wall effect in Eq. (4.24b) is to hinder the EMP migration velocity of the particle, whereas Eq. (4.24a) indicates that the boundary tends to augment (reduce) the hydrodynamic force exerted on the particle if, under the situation of $\mu^* = 1$, the value of σ^* is smaller (greater) than 1/3. As expected, the boundary effect of the enclosing cavity wall on the EMP migration is much stronger than that of a neighboring plane wall predicted by Yariv and Miloh (Yariv and Miloh 2009), in which, same as in the analysis by Leenov and Kolin (Leenov and Kolin 1954), the contribution from the Maxwell stress in Eq. (4.16) was not included.

It is also interesting to examine the asymptotic behavior of the boundary effect on EMP migration for the situation of near contact ($\lambda \to 1$) between the particle and the concentric

cavity wall. The Taylor expansions for the EMP force and migration velocity of the confined particle with $\mu^* = 1$ in $1 - \lambda$ resulting from Eqs. (4.15) and (4.18) are

$$\mathbf{F}(\sigma^*,1) - \mathbf{F}(1,1) = \frac{2\pi(\sigma^* - 1)}{3\sigma^*}[1 + \frac{2(3\sigma^* - 1)}{\sigma^*}(1 - \lambda)$$

$$+ \frac{2(3\sigma^* - 1)(\sigma^* - 2)}{\sigma^{*2}}(1 - \lambda)^2 + O(1 - \lambda)^3]a^3\mathbf{J}_\infty \times \mathbf{B}_\infty, \quad (4.25a)$$

$$\mathbf{U} = [\frac{\sigma^* - 1}{12\sigma^*}(1 - \lambda)^3 + O(1 - \lambda)^4]\frac{a^2}{\eta}\mathbf{J}_\infty \times \mathbf{B}_\infty. \quad (4.25b)$$

Equation (4.25b) illustrates that the migration velocity of the EMP particle decays with an increase in λ as the order $(1 - \lambda)^3$, same as that resulting from Eq. (3.19a) for a sphere migrating under gravity at the center of a spherical cavity. However, Eq. (4.25a) indicates that the EMP force on the particle is finite (as long as $\sigma^* \neq 0$) at $\lambda = 1$ [with the leading-order correction at $O(1 - \lambda)$ in the direction depending also on the sign of $\sigma^* - 1/3$ (at $\mu^* = 1$)], as opposed to the divergent asymptotic behavior with the order $(1 - \lambda)^{-3}$ for the hydrodynamic force on a settling sphere in a concentric spherical cavity. Note that the wall-corrected EMP force and migration velocity of the particle with $\mu^* = 1$ are proportional to $(\sigma^* - 1)/(\sigma^* + 2)$ as $\lambda \to 0$ and to $(\sigma^* - 1)/\sigma^*$ as $\lambda \to 1$; when $\sigma^* = 1$ (the particle and suspending fluid have the same electric conductivity), there is no EMP motion.
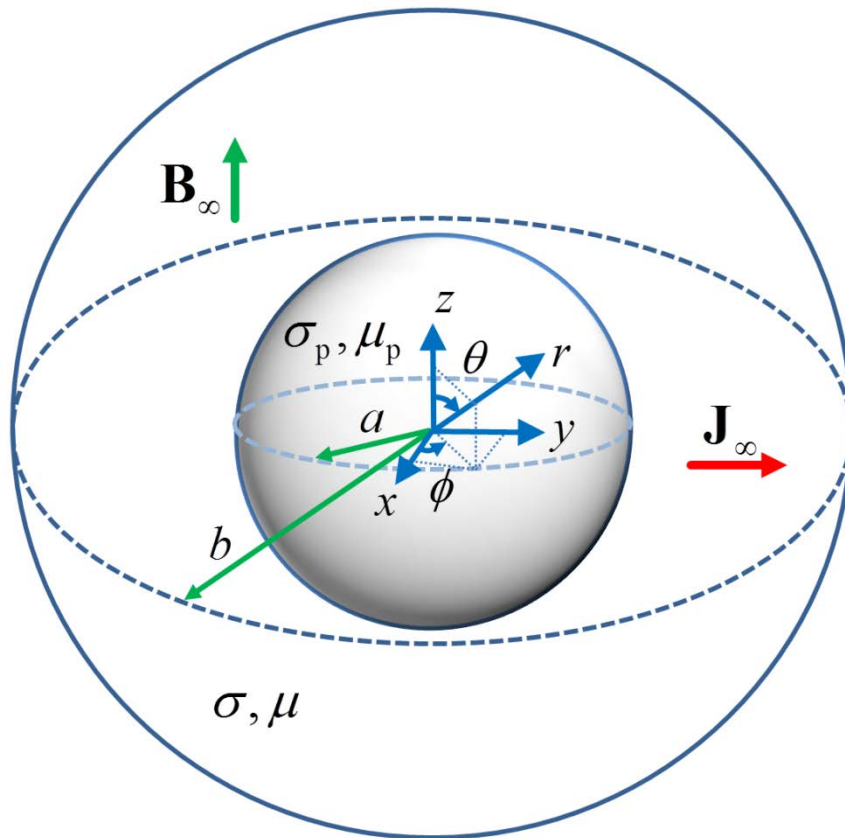
Figure 4.1 Geometric sketch for the EMP motion of a spherical particle in a concentric spherical cavity under applied electric current density $\mathbf{J}_\infty$ and magnetic flux density $\mathbf{B}_\infty$.
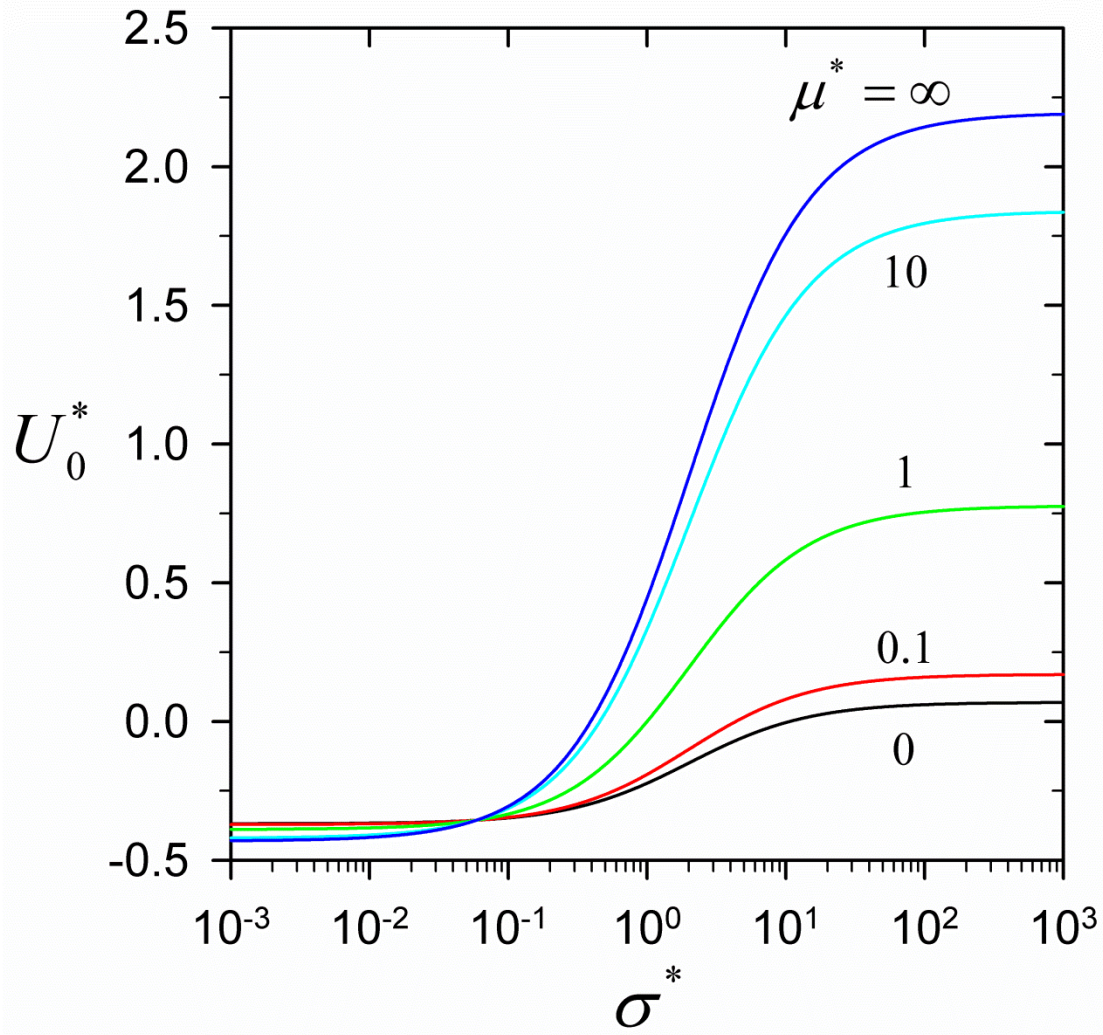
Figure 4.2a   Plots of the dimensionless EMP mobility U_0^* of an unconfined spherical

particle calculated from Eq. (4.22) for various values of the particle-to-fluid electric

conductivity ratio σ^* and magnetic permeability ratio μ^*.
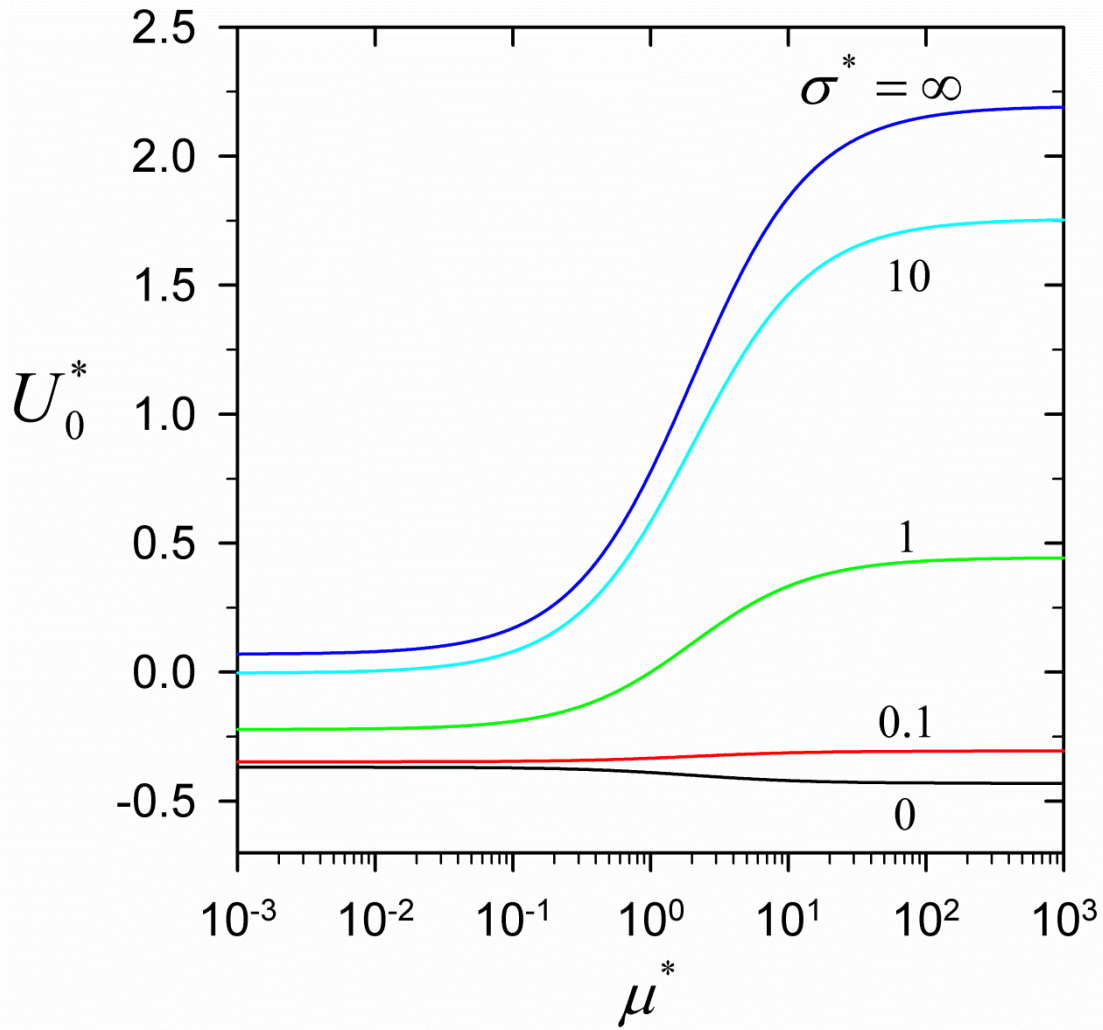
Figure 4.2b   Plots of the dimensionless EMP mobility U_0^* of an unconfined spherical particle calculated from Eq. (4.22) for various values of the particle-to-fluid electric conductivity ratio σ^* and magnetic permeability ratio μ^*.
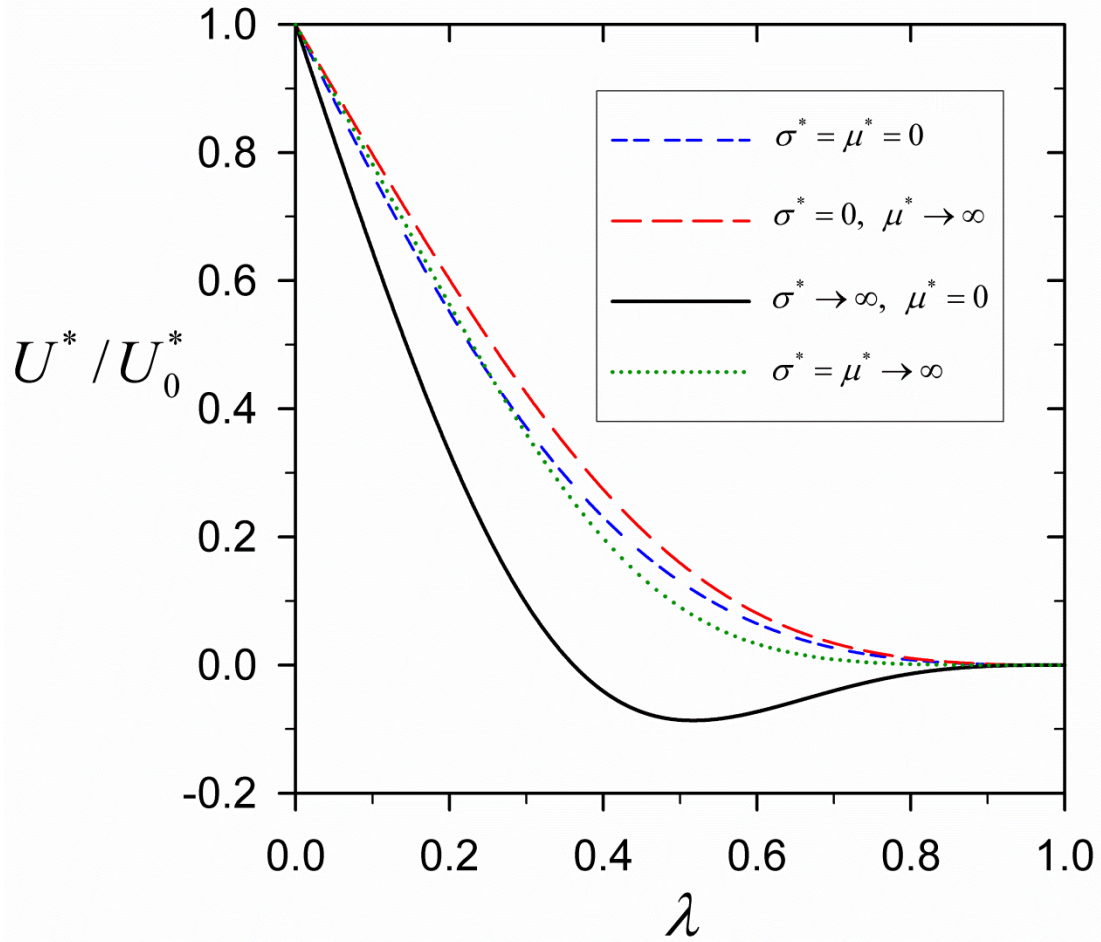
Figure 4.3   Plots of the normalized EMP mobility U^*/U_0^* of a spherical particle calculated from Eqs. (4.20) and (4.22) versus the particle-to-cavity radius ratio λ for various values of the particle-to-fluid electric conductivity ratio σ^* and magnetic permeability ratio μ^*.

Chapter 5

Magnetohydrodynamic motion of a spherical particle with self-electrochemical surface reactions in a spherical cavity

In this chapter, we consider the quasi-steady motion of a colloidal sphere of radius a undergoing self-electrochemical reactions on its surface in a concentric spherical cavity of radius b filled with an electrolyte solution of viscosity η induced by an applied magnetic field $\mathbf{B}_\infty = B_\infty \mathbf{e}_z$, as shown in Figure 5.1, where (r, θ, ϕ) are spherical coordinates, $\mathbf{e}_z$ is the unit vector in the direction of $\theta = 0$, and B_∞ is a constant magnetic flux density. The thickness of the electric double layers adjoining the particle and cavity surfaces is assumed to be very small relative to the particle radius and the distance between the solid surfaces ($b-a$). Other important effects, such as electrokinetic, auto-phoretic, and gravitational effects, which can be treated separately (Happel and Brenner 1983; Keh and Chang 1998; Paxton et al. 2005; Golestanian et al. 2007; Keh and Hsieh 2007; Moran and Posner 2011; Yariv 2011) and added directly due to the linearity of the problem, are not considered here. The purpose is to evaluate the boundary effect of the cavity on the translational and angular velocities of the particle induced by the MHD effect.

5.1 Electric current density distributions

In the particle and fluid phases, an electric current arises from the electrochemical reactions occurring spontaneously on the particle surface. The fluid outside the thin electric double layers adjacent to the particle surface and cavity wall

is electrically neutral and the electric conductivities σ_p and σ of the particle and fluid, respectively, are constants. Thus, the electric potential distributions are governed by the Laplace equations, same as Eq. (4.1),

$$\nabla^2 \psi_p = 0 \qquad (0 \le r \le a) \tag{5.1a}$$

for the particle and

$$\nabla^2 \psi = 0 \qquad (a \le r \le b) \tag{5.1b}$$

for the fluid. Here, Eq. (5.1b) results from charge conservation in a region of uniform composition (Newman 1973; Yariv 2009; 2011); therefore, one needs the ionic concentrations in the fluid outside the double layers to be sufficiently uniform (the ionic strength to be high or the reaction rate to be low) for its justification.

The boundary conditions for ψ_p and ψ at the electrochemically reacting particle surface and the electrically non-conducting cavity wall are

$$r = a: \qquad \mathbf{e}_r \cdot (\sigma \nabla \psi - \sigma_p \nabla \psi_p) = 0, \tag{5.2a}$$

$$\psi - \psi_p = -\zeta = -\overline{\zeta} + V_s; \tag{5.2b}$$

$$r = b: \qquad \mathbf{e}_r \cdot \nabla \psi = 0, \tag{5.3}$$

where $\mathbf{e}_r$ is the unit vector in the r direction. Equations (5.2a) and (5.3) follow from that the normal component of the electric current density is continuous at the particle surface and no current can be conducted into the thin double layer adjoining the insulating cavity wall (which may have surface charges, but does not have surface reactions) (Keh and Anderson 1985; Kalsin et al. 2006), respectively. $\zeta(\theta, \phi)$ in Eq. (5.2b) is the zeta (Nernst) potential non-uniformly distributed over the particle surface (Keh and Li 1994; Hsieh and Keh 2007; Yariv 2011), which is expressed as the sum of its average $\overline{\zeta}$ and deviation distribution $-V_s(\theta, \phi)$ from the average subject to the constraint

$$\int_0^{2\pi}\int_0^{\pi} V_s \sin\theta \, \mathrm{d}\theta \, \mathrm{d}\phi = 0 . \tag{5.4}$$

Here, a linear anodic/cathodic kinetics, which is the simplified Butler-Volmer kinetic expression with a small surface overpotential, for a completely reversible interfacial electrochemical reaction [namely, the reaction rate or current density at the particle surface equal to $(i_0 nF/RT)(\psi_p - \psi - \zeta)$ with $ai_0 nF/\sigma RT \gg 1$, where i_0 and n are the exchange current density and number of charge transfer, respectively, in the reaction, F is the Faraday constant, R is the gas constant, and T is the absolute temperature] (Keh and Li 1994; Li and Keh 1997; Rock et al. 2013) is assumed to distribute over the particle surface. The current conservation constraint requiring that the net current into the particle be zero (Moran and Posner 2011; Yariv 2011; Sabass and Seifert 2012) is satisfied by Eqs. (5.2)-(5.4). The electric field induced by the fluid motion under the applied magnetic field is negligible relative to that developed from the electrochemical reaction on the particle surface (the typical value of the ratio $a^2 B_\infty^2 \sigma/\eta$ will be discussed in Subsection 5.4.3) .

The general solution of ψ_p and ψ, satisfying the requirement of finite potential inside the particle, can be expressed as (Jackson 1976)

$$\psi_p = \psi_0 + \sum_{l=0}^{\infty} \sum_{m=-l}^{l} C_{lm} \gamma^l Y_{lm} , \tag{5.5a}$$

$$\psi = \psi_0 - \overline{\zeta} + \sum_{l=0}^{\infty} \sum_{m=-l}^{l} [A_{lm} \gamma^l + D_{lm} \gamma^{-(l+1)}] Y_{lm} , \tag{5.5b}$$

where $\gamma = r/a$, ψ_0 is the electric potential at the particle center,

$$Y_{lm}(\theta,\phi) = \sqrt{\frac{2l+1}{4\pi} \frac{(l-m)!}{(l+m)!}} P_l^m(\cos\theta) e^{im\phi} \tag{5.6}$$

are spherical harmonics (the operations of their vector spherical harmonics are presented in Appendix B), P_l^m is the associated Legendre function of order l and

degree m, and C_{lm}, A_{lm}, and D_{lm} are the unknown constants to be determined from the boundary conditions.

Applying Eqs. (5.2) and (5.3) to Eq. (5.5), we obtain

$$C_{lm} = -(l+1)(1-\lambda^{2l+1})S_l(\sigma^*)E_{lm}, \qquad (5.7a)$$

$$A_{lm} = (l+1)\lambda^{2l+1}\sigma^*S_l(\sigma^*)E_{lm}, \qquad (5.7b)$$

$$D_{lm} = l\sigma^*S_l(\sigma^*)E_{lm}, \qquad (5.7c)$$

where

$$S_l(x) = [1+l(x+1)+(l+1)\lambda^{2l+1}(x-1)]^{-1}, \qquad (5.8a)$$

$$E_{lm} = \int_0^{2\pi}\int_0^\pi V_s Y_{lm}^* \sin\theta\, \mathrm{d}\theta\, \mathrm{d}\phi, \qquad (5.8b)$$

$\lambda = a/b$, $\sigma^* = \sigma_p/\sigma$, and $Y_{lm}^*(\theta,\phi)$ is the orthonormal conjugate of $Y_{lm}(\theta,\phi)$ (Jackson 1976).

With the knowledge of ψ_p and ψ, the electric current density distributions in the particle and fluid phases due to the interfacial electrochemical reactions can be obtained as

$$\mathbf{J}_p = -\sigma_p\nabla\psi_p \qquad \text{and} \qquad \mathbf{J} = -\sigma\nabla\psi, \qquad (5.9a,b)$$

respectively, same as Eq. (4.4), which increase with the characteristic magnitude of V_s but are independent of the constant potentials $\bar{\zeta}$ and ψ_0.

5.2 Magnetic flux density distributions

The magnetic flux density distributions are governed by

$$\nabla\cdot\mathbf{B}_p = 0, \qquad \nabla\times\mathbf{B}_p = \mu_p\mathbf{J}_p, \ (0\le r\le a) \qquad (5.10a,b)$$

for the particle and

$$\nabla \cdot \mathbf{B} = 0, \qquad \nabla \times \mathbf{B} = \mu \mathbf{J}, \, (a \leq r \leq b) \qquad\qquad (5.10\text{c,d})$$

for the fluid, where the magnetic permeabilities μ_p and μ are constants.

The boundary conditions for the magnetic flux density distributions at the particle surface and cavity wall are

$$r = a: \qquad \mathbf{e}_r \cdot (\mathbf{B} - \mathbf{B}_p) = 0, \qquad\qquad (5.11\text{a})$$

$$\mathbf{e}_r \times (\frac{\mathbf{B}}{\mu} - \frac{\mathbf{B}_p}{\mu_p}) = \mathbf{0} ; \qquad\qquad (5.11\text{b})$$

$$r = b: \qquad \mathbf{e}_r \cdot (\mathbf{B} - \mathbf{B}_\infty) = 0. \qquad\qquad (5.12)$$

Equation (5.10)-(5.12) are the same as Eqs. (4.7)-(4.9).

The solution of Eqs. (5.10)-(5.12) with the substitution of Eqs. (5.5) and (5.9) can be obtained in terms of spherical harmonics and expressed as

$$\mathbf{B}_p = \mu_p \sigma_p \sum_{l=0}^{\infty} \sum_{m=-l}^{l} \frac{C_{lm}}{l+1} \gamma^l r \mathbf{e}_r \times \nabla Y_{lm} - \mu_p \nabla \Phi_p, \qquad\qquad (5.13\text{a})$$

$$\mathbf{B} = \mu \sigma \sum_{l=0}^{\infty} \sum_{m=-l}^{l} [\frac{A_{lm}}{l+1} \gamma^l - \frac{D_{lm}}{l} \gamma^{-(l+1)}] r \mathbf{e}_r \times \nabla Y_{lm} - \mu \nabla \Phi, \qquad\qquad (5.13\text{b})$$

where

$$\Phi_p = -3 \frac{B_\infty}{\mu} S_1(\mu^*) r \cos\theta, \qquad\qquad (5.14\text{a})$$

$$\Phi = -\frac{B_\infty}{\mu} S_1(\mu^*) [\mu^* + 2 - (\mu^* - 1)\gamma^{-3}] r \cos\theta, \qquad\qquad (5.14\text{b})$$

and $\mu^* = \mu_p / \mu$.

The first terms in Eq. (5.13) involving the electric conductivities arise from the self-electrochemical reactions occurring on the particle surface, whereas the second terms whose curls vanish are caused by the applied magnetic flux density. The magnitude of either ratio of the first-to-second terms has the order $\mu \sigma V_s / B_\infty$, which is very small (will be discussed in Subsection 5.4.3).

5.3 Particle velocities

The fluid outside the thin electric double layers adjacent to the moving particle and stationary cavity wall is electrically neutral. Thus, its motion in the presence of the applied magnetic flux density and the electric current density caused by the self-electrochemical reactions on the particle surface is governed by the Stokes equations modified with a Lorentz force density, same as Eq. (4.12),

$$\eta\nabla^2\mathbf{v} = \nabla p - \mathbf{J}\times\mathbf{B} , \tag{5.15a}$$

$$\nabla\cdot\mathbf{v} = 0 , \tag{5.15b}$$

where $\mathbf{v}$ and p are the fluid velocity and dynamic pressure distributions, respectively. Here, the Coulomb body forces in Eq. (5.15a), which are proportional to $\nabla^2\psi\nabla\psi$ (Yariv 2010, 2011), disappear with the validity of Eq. (5.1b).

The boundary conditions for the fluid velocity field at the no-slip particle surface and cavity wall are

$$r = a : \qquad \mathbf{v} = \mathbf{U} + a\mathbf{\Omega}\times\mathbf{e}_r , \tag{5.16}$$

$$r = b : \qquad \mathbf{v} = \mathbf{0} , \tag{5.17}$$

where $\mathbf{U}$ and $\mathbf{\Omega}$ are the to-be-determined translational and angular velocities, respectively, of the particle caused by the MHD effect. As mentioned in the beginning of this section, the slip velocities at the solid surfaces due to electro-osmotic effect are not considered here.

Following Teubner's approach to obtain the particle velocities (without solving for the fluid velocity) with a generalized reciprocal theorem, we can express the force and torque balance equations in terms of surface and volume integrals as

$$6\pi\eta a f_{\mathrm{T}}\mathbf{U} = \mathbf{F}(\sigma^*,\mu^*) , \tag{5.18a}$$

$$8\pi\eta a^3 f_{\mathrm{R}}\mathbf{\Omega} = \mathbf{T}(\sigma^*,\mu^*) , \tag{5.18b}$$

where the total applied force $\mathbf{F}(\sigma^*,\mu^*)$ acting on the particle is the same as Eq. (4.16)

and the total torque acting on the particle is

$$\mathbf{T}(\sigma^*, \mu^*) = \iint_{r=a} r\mathbf{e}_r \times \boldsymbol{\sigma}^{\mathrm{M}} \cdot \mathbf{e}_r \mathrm{d}S + \iiint_{a<r<b} \overset{-\mathrm{R}}{\mathbf{v}} \cdot (\mathbf{J} \times \mathbf{B}) \, \mathrm{d}V$$

$$+ \iiint_{0<r<a} r\mathbf{e}_r \times (\mathbf{J}_\mathrm{p} \times \mathbf{B}_\mathrm{p}) \, \mathrm{d}V \, . \tag{5.19}$$

Note that f_T and f_R are the hydrodynamic resistance coefficients for the translation and rotation, respectively, of the sphere driven by a body force field in the concentric spherical cavity given by Eq. (3.19), $\boldsymbol{\sigma}^{\mathrm{M}}$ is the magnetic Maxwell stress tensor given by Eq. (4.17), and $\overset{-\mathrm{R}}{\mathbf{v}}$ is given by Eq. (3.18b).

Substituting Eqs. (5.5)-(5.9) for the electric current density distributions and Eqs. (5.13) and (5.14) for the magnetic flux density distributions into Eq. (5.18) and performing mathematical operations, we obtain the particle velocities

$$\mathbf{U} = U^* a \frac{\sigma}{\eta} \mathbf{D} \times \mathbf{B}_\infty , \tag{5.20a}$$

$$\boldsymbol{\Omega} = \Omega^* \frac{\sigma}{\eta} \mathbf{Q} \cdot \mathbf{B}_\infty , \tag{5.20b}$$

where $\mathbf{D}$ and $\mathbf{Q}$ are the dipole and quadrupole moments, respectively, of the zeta potential distribution on the particle surface defined by

$$\mathbf{D} = \frac{1}{4\pi} \int_0^{2\pi} \int_0^\pi V_s \mathbf{e}_r \sin\theta \, \mathrm{d}\theta \, \mathrm{d}\phi , \tag{5.21a}$$

$$\mathbf{Q} = \frac{1}{4\pi} \int_0^{2\pi} \int_0^\pi V_s (3\mathbf{e}_r\mathbf{e}_r - \mathbf{I}) \sin\theta \, \mathrm{d}\theta \, \mathrm{d}\phi , \tag{5.21b}$$

the dimensionless translational and rotational mobility parameters of the particle

$$U^* = \frac{(1-\lambda)^4}{4(1-\lambda^5)} \sigma^* S_1(\sigma^*) S_1(\mu^*)(\mu^* u_1 + u_2) , \tag{5.22a}$$

$$\Omega^* = \frac{(1-\lambda)^2}{4} \sigma^* S_2(\sigma^*) S_1(\mu^*)(\mu^* \omega_1 + \omega_2) , \tag{5.22b}$$

and

69

$$u_1 = 3(7 + 13\lambda + 10\lambda^2 - 2\lambda^3 - 8\lambda^4 - 5\lambda^5) \,, \tag{5.23a}$$

$$u_2 = (1 - \lambda)(7 + 17\lambda + 15\lambda^2 + 5\lambda^3 + \lambda^4) \,, \tag{5.23b}$$

$$\omega_1 = 10 + 20\lambda + 30\lambda^2 + 29\lambda^3 + 28\lambda^4 + 12\lambda^5 + 6\lambda^6 \,, \tag{5.23c}$$

$$\omega_2 = 2(1 - \lambda)(1 + 3\lambda + 6\lambda^2 + 5\lambda^3) \,. \tag{5.23d}$$

Note that the particle velocities depend on the distribution and rate of the interfacial electrochemical reaction via the dipole and quadrupole moments of V_{s}.

Clearly, both U^* and Ω^* are positive functions of the particle-to-fluid electric conductivity ratio σ^* and magnetic permeability ratio μ^* as well as the particle-to-cavity radius ratio λ only, and the particle velocities are proportional to the fluid conductivity σ or particle conductivity $\sigma_{\mathrm{p}} = \sigma\sigma^*$. For the case that either the particle or the fluid is nonconductive ($\sigma_{\mathrm{p}} = 0$ or $\sigma = 0$), the electric current disappears and there is no particle motion. Note that Eq. (5.20) predicts $\mathbf{U}$ and $\mathbf{\Omega}$ to be bilinear in the products $\mathbf{D} \times \mathbf{B}_\infty$ and $\mathbf{Q} \cdot \mathbf{B}_\infty$, respectively, indicating that the integral terms of the second orders V_s^2 and B_∞^2 in the Maxwell stress $\boldsymbol{\sigma}^{\mathrm{M}}$ and Lorentz force densities $\mathbf{J} \times \mathbf{B}$ and $\mathbf{J}_{\mathrm{p}} \times \mathbf{B}_{\mathrm{p}}$ in Eq. (5.18) vanish and make no contribution to the particle velocities.

In the limit $\lambda \to 0$ (the cavity wall is at an infinite distance from the particle), Eq. (5.22) reduces to

$$U_0^* = \frac{7\sigma^*(3\mu^* + 1)}{4(\sigma^* + 2)(\mu^* + 2)} \,, \tag{5.24a}$$

$$\Omega_0^* = \frac{\sigma^*(5\mu^* + 1)}{2(2\sigma^* + 3)(\mu^* + 2)} \,. \tag{5.24b}$$

In the limit $\lambda \to 1$ (the particle fills the cavity up completely), Eq. (5.22) results in $U^* = \Omega^* = 0$. As expected, the translational and rotational velocities of

the particle vanish in this limiting case.

5.4 Results and discussion

Equation (5.20) for the motion of a spherical particle in a concentric spherical cavity induced by the interaction between the self-electrochemical reactions on the particle surface and an applied magnetic field indicates that the translational and angular velocities of the particle are proportional to the dipole and quadrupole moments, respectively, of the potential distribution $V_s(\theta, \phi)$ over the particle surface. The results of the particle mobilities obtained in Eqs. (5.22)-(5.24) and the dipole and quadrupole moments of some typical examples of V_s calculated from Eq. (5.21) will be discussed and compared with those of the electromagnetophoretic mobility of the particle in this section.

5.4.1 Models of the zeta potential distribution

As an example, we consider a sphere composed of two orthotropically symmetric caps of the constant zeta potentials with $V_s = V_1$ and $V_s = V_3$, respectively, each spanning a solid angle 2α (where $0 \leq 2\alpha \leq \pi$), connected by a middle section of the constant potential $V_s = V_2$, as shown in Figure 5.2. Without loss in generality, we take $V_1 \geq 0$. The axis of revolving symmetry of this three-slice spherical particle is defined by the unit vector $\mathbf{e}$ (outward to the cap surface of the potential V_1), which is allowed to orient arbitrarily with respect to the applied magnetic field $\mathbf{B}_\infty$. From the normalization requirement on the potential distribution V_s given by Eq. (5.4), we have

$$V_2 = -\frac{1 - \cos\alpha}{2\cos\alpha}(V_1 + V_3).$$

(5.25)

71

Three special cases of this three-slice particle may be of interest.

The first special case is a sphere with an odd distribution of the potential V_s, and Eq. (5.25) is replaced by

$$V_3 = -V_1 \quad \text{and} \quad V_2 = 0. \tag{5.26}$$

For an odd distribution of V_s over the particle surface, its quadrupole moment vanishes ($\mathbf{Q} = \mathbf{0}$), and Eqs. (5.13a) and (5.26) lead to the dipole moment as

$$\mathbf{D} = \frac{1}{2}\sin^2\alpha V_1\mathbf{e}. \tag{5.27}$$

Thus, the particle will translate without rotation perpendicular to both the applied magnetic field $\mathbf{B}_\infty$ and the particle orientation $\mathbf{e}$, as long as they are not collinear. For a given finite potential strength V_1 and non-collinear orientation $\mathbf{e}$ relative to $\mathbf{B}_\infty$, the velocity of the particle (or the dipole moment) increases monotonically with the solid angle 2α from zero as $\alpha = 0$ to the maximum as $\alpha = \pi/2$.

The second special case, in contrast to the previous one, in Figure 5.2 is a sphere with an even distribution of the potential V_s, and Eq. (5.25) reduces to

$$V_3 = V_1 \quad \text{and} \quad V_2 = -\frac{1-\cos\alpha}{\cos\alpha}V_1. \tag{5.28}$$

For an even distribution of V_s over the particle surface, its dipole moment disappears ($\mathbf{D} = \mathbf{0}$), and Eqs. (5.21b) and (5.28) result in the quadrupole moment as

$$\mathbf{Q} = \frac{1}{2}\sin^2\alpha V_1(3\mathbf{ee} - \mathbf{I}). \tag{5.29}$$

Thus, the particle will rotate without translation for any arbitrary particle orientation $\mathbf{e}$ relative to the applied magnetic field $\mathbf{B}_\infty$. For such a particle with specified finite values of the solid angle 2α and the potential strength V_1, its angular velocity has a minimum magnitude in the direction of $-\mathbf{B}_\infty$ when the axis of revolving

symmetry is normal to the applied magnetic field and has a maximum magnitude (doubling the minimum) in the direction of $\mathbf{B}_\infty$ when they are collinear; the dependences of the magnitude and direction of the angular velocity on the orientation $\mathbf{e}$ relative to $\mathbf{B}_\infty$ are monotonic in between these two limits. For a given finite potential strength V_1 and orientation $\mathbf{e}$ relative to $\mathbf{B}_\infty$, the angular velocity of the particle (or the quadrupole moment) increases monotonically with the solid angle 2α from $\alpha = 0$ to $\alpha = \pi/2$. For the singular situation of $\alpha = 0$, Eqs. (5.28) and (5.29) result in $V_1 \to \infty$ (on two point sources at the poles) and $\mathbf{Q} = -V_2(3\mathbf{ee} - \mathbf{I})$ for a finite value of V_2. For the other singular situation of $\alpha = \pi/2$, Eqs. (5.28) and (5.29) lead to $V_2 \to -\infty$ (on a circle sink at the equator) and $\mathbf{Q} = (V_1/2)(3\mathbf{ee} - \mathbf{I})$ for a finite value of V_1.

The third special case in Figure 5.2 is a sphere composed of two supplementary caps of potentials V_1 and V_2, respectively, and Eq. (5.25) becomes
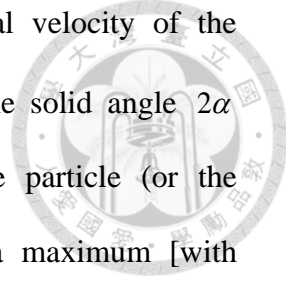
$$V_3 = V_2 = -\frac{1 - \cos\alpha}{1 + \cos\alpha} V_1. \tag{5.30}$$

For this case, the potential distribution V_s over the particle surface is neither odd nor even, and the dipole and quadrupole moments of V_s can be calculated using Eqs. (5.21) and (5.30), with the result

$$\mathbf{D} = \sin^2\frac{\alpha}{2} V_1 \mathbf{e}, \tag{5.31a}$$

$$\mathbf{Q} = \cos\alpha \sin^2\frac{\alpha}{2} V_1 (3\mathbf{ee} - \mathbf{I}). \tag{5.31b}$$

Equations (5.20) and (5.31) predict that the particle will translate perpendicular to both the applied magnetic field $\mathbf{B}_\infty$ and the particle orientation $\mathbf{e}$, if they are not collinear, and rotate for any arbitrary $\mathbf{e}$ relative to $\mathbf{B}_\infty$. For a given finite potential

strength V_1 and orientation $\mathbf{e}$ relative to $\mathbf{B}_\infty$, the translational velocity of the particle (or the dipole moment) increases monotonically with the solid angle 2α from $\alpha = 0$ to $\alpha = \pi/2$, whereas the angular velocity of the particle (or the quadrupole moment) first increases with 2α from $\alpha = 0$ to a maximum [with $\mathbf{Q} = (V_1/8)(3\mathbf{ee} - \mathbf{I})$] at $\alpha = \pi/3$, and then decreases with 2α to zero at $\alpha = \pi/2$. Since the dipole moments given by Eqs. (5.31a) and (5.27) and the quadrupole moments given by Eqs. (5.31b) and (5.29) for the current and previous cases have identical directions, respectively, their dependences of the magnitudes and directions of the translational and angular velocities of the particle on the orientation $\mathbf{e}$ relative to $\mathbf{B}_\infty$ have the same behaviors. For the singular situation of $\alpha = 0$, Eqs. (5.30) and (5.31) lead to $V_1 \to \infty$ (on a point source at one pole), $\mathbf{D} = -V_2\mathbf{e}$, and $\mathbf{Q} = -V_2(3\mathbf{ee} - \mathbf{I})$ for a finite value of V_2.

When the two caps of the particle are hemispherical in the first or third special case discussed above (with $\alpha = \pi/2$ and $V_3 = -V_1$) to form a Janus sphere, both Eq. (5.27) and Eq. (31) reduce to $\mathbf{D} = (V_1/2)\mathbf{e}$ and $\mathbf{Q} = \mathbf{0}$. For this particular case of an odd distribution of V_s, the dipole moment reaches its maximum for a given V_1 and the particle translates at the greatest speed for a specified orientation $\mathbf{e}$ relative to the applied magnetic field $\mathbf{B}_\infty$ without rotation. If the orientation $\mathbf{e}$ is randomly distributed for an ensemble of identical particles with the zeta potential distribution in any of the above three cases, the average of Eq. (5.20) with Eq. (27), (29), or (31) over all $\mathbf{e}$ leads to zero mean translational and angular velocities of the ensemble, as expected.

5.4.2 Particle mobility parameters

We plot the translational and rotational mobility parameters U_0^* and Ω_0^* of an
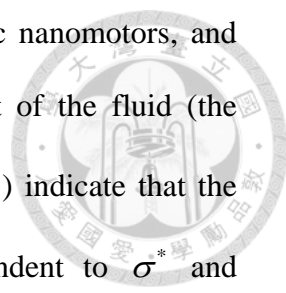
unconfined spherical particle ($\lambda = 0$) with interfacial self-electrochemical reactions in an applied magnetic field as calculated from Eq. (5.24) in Figure 5.3 and Figure 5.4, respectively, for various values of the particle-to-fluid electric conductivity ratio σ^* and magnetic permeability ratio μ^*. For a constant value of μ^*, both U_0^* and Ω_0^* increase monotonically with an increase in σ^* from zero at $\sigma^* = 0$; for a given value of σ^*, U_0^* and Ω_0^* increase monotonically with an increase in μ^* from finite constants at $\mu^* = 0$. Equation (5.24) gives $U_0^* = 7/8$ and $\Omega_0^* = 1/8$ in the limit of $\mu^* = 0$ and $\sigma^* \to \infty$, $U_0^* = 21/4$ and $\Omega_0^* = 5/4$ in the limit of $\mu^* \to \infty$ and $\sigma^* \to \infty$, as well as $U_0^* = 7/9$ and $\Omega_0^* = 1/5$ for the special case of $\sigma^* = \mu^* = 1$ (the particle and suspending fluid have the same electric conductivity and magnetic permeability). In general, U_0^* is greater than Ω_0^* by a factor about 4.

The normalized mobility parameters U^*/U_0^* and Ω^*/Ω_0^* of a confined particle with self-electrochemical surface reactions in an imposed magnetic field calculated from Eqs. (5.22) and (5.24) as functions of the particle-to-cavity radius ratio λ are plotted in Figure 5.5 and Figure 5.6, respectively, for various values of the parameters σ^* and μ^*. For specified values of σ^* and μ^*, both U^*/U_0^* and Ω^*/Ω_0^* decrease monotonically with an increase in λ from unity at $\lambda = 0$ to zero at $\lambda = 1$. The boundary effect of the cavity on the translational velocity of the particle induced by the MHD force (which is stronger than the effect on the rotational velocity) is equivalent to (in the particular case of $\sigma^* = 1/3$ and $\mu^* = 1$, $U^*/U_0^* = 1/f_T$ for an arbitrary value of λ and the effect is exactly the same as that on sedimentation) that caused by gravitational fields (Happel and Brenner 1983; Keh

and Chang 1998), but is much stronger than that in electrophoresis, diffusiophoresis, and thermophoresis (Keh and Chang 1998; Keh and Hsieh 2007). For a constant value of λ, U^*/U_0^* and Ω^*/Ω_0^* decrease (or the boundary effect becomes stronger) with an increase in σ^* and increase (or the boundary effect gets weaker) with an increase in μ^*, keeping the other parameter unchanged. The dependence of U^*/U_0^* on the parameters σ^* and μ^* is much less sensitive than that of Ω^*/Ω_0^*. Note that the curves with $\sigma^* = 0$ in Figure 5.5 and Figure 5.6 are drawn only to illustrate the upper bounds of the normalized mobilities for specified values of μ^* and λ knowing that $U^* = \Omega^* = 0$ in this limit.

5.4.3 Typical dimensionless numbers and particle velocities

For the formulas of the translational and angular velocities of the particle obtained in Eqs. (5.20)-(5.23), which are exact for any distribution of the zeta potential distribution at the particle surface, to be valid, it is necessary to assume that the dimensionless numbers $\mu\sigma V_s/B_\infty$ and $a^2 B_\infty^2 \sigma/\eta$ (the square root of the latter is known as the Hartmann number) (Moffatt and Sellier 2002; Yariv and Miloh 2009) are much less than unity so that the magnetic flux density induced by the electric current density $\mathbf{J}$ is small compared with the applied magnetic field $\mathbf{B}_\infty$ and the Lorentz field $\mathbf{v} \times \mathbf{B}$ induced by the fluid motion is weak relative to the electric field $-\nabla\psi$ generated by the interfacial electrochemical reactions. For a particle with $a = 1\,\mu\mathrm{m}$ and V_s of the order 100 mV in aqueous solutions of $\sigma = 10$ S/m with a prescribed magnetic flux density $B_\infty = 1\mathrm{T}$, the typical values of $\mu\sigma V_s/B_\infty$ and $a^2 B_\infty^2 \sigma/\eta$ are 10^{-6} and 10^{-8}, respectively. Thus, the result in Eqs. (5.20)-(5.23) is sufficiently accurate in practical applications.

The typical autonomously propelled swimmers are bimetallic nanomotors, and the electric conductivity of the particle is much larger than that of the fluid (the conductivity ratio $\sigma^* \gg 1$). For this case, Eqs. (5.20) and (5.21) indicate that the translational and angular velocities of the particle are independent to σ^* and proportional to the fluid conductivity σ. Thus, the MHD effect of the self-electrochemical reactions occurring on the particle surface is significant in fluids of high conductivity. Note that the typical magnitudes of the translational velocity $\mathbf{U}$ and angular velocity $\mathbf{\Omega}$ of a particle (with $a = 1\,\mu$m and V_s of the order 100 mV in aqueous solutions of $\sigma = 10$ S/m with an applied magnetic flux density $B_0 =$ 1T) predicted by Eq. (5.20) could be 10^{-3} m/s and 10^3 s^{-1}, respectively, which are unexpectedly significant. With these particle velocities, the typical value of the Reynolds number is 10^{-3}.

5.4.4 Comparisons with electromagnetophoresis and auto-phoresis

The MHD velocity obtained in Eq. (5.20a) for a spherical particle with interfacial self-electrochemical reactions is different from the electromagnetophoretic velocity given by Eq. (4.18) which does not equal zero as $\sigma^* = 0$ and can reverse its direction if the value of σ^* or μ^* varies. Also, the particle velocity in Eq. (5.20a) is proportional to both the fluid conductivity σ and the particle radius a (evidently, the quantity $\sigma \mathbf{D}/a$ stands for the effective electric current density induced by the interfacial reactions to follow a boundary-corrected Stokes law), whereas the electromagnetophoretic velocity is independent of the fluid conductivity alone (only depends on the conductivity ratio σ^*) and proportional to a^2.

On the other hand, the migration velocity of electrocatalytic micro/nanomotors in the absence of applied magnetic field can decrease with the fluid conductivity (Paxton

et al. 2006; Golestanian et al. 2007) and swimmer size (Wheat et al. 2010; Ebbens et al. 2012) because these swimmers undergo the self-electrophoresis and/or self-diffusiophoresis with thin interfacial diffuse layers relative to the particle size (force-free phoretic motion with an apparent slip velocity at the particle surface) (Golestanian et al. 2007; Keh and Hsieh 2007; Moran and Posner 2011; Yariv 2011), instead of the MHD motion induced by the Lorentz force. These opposite dependences on solution conductivity and particle size between MHD and auto-phoretic effects suggest a good magnetically-guided efficiency for a large electrocatalytic micro/nanomotor swimming in a highly conductive fluid.
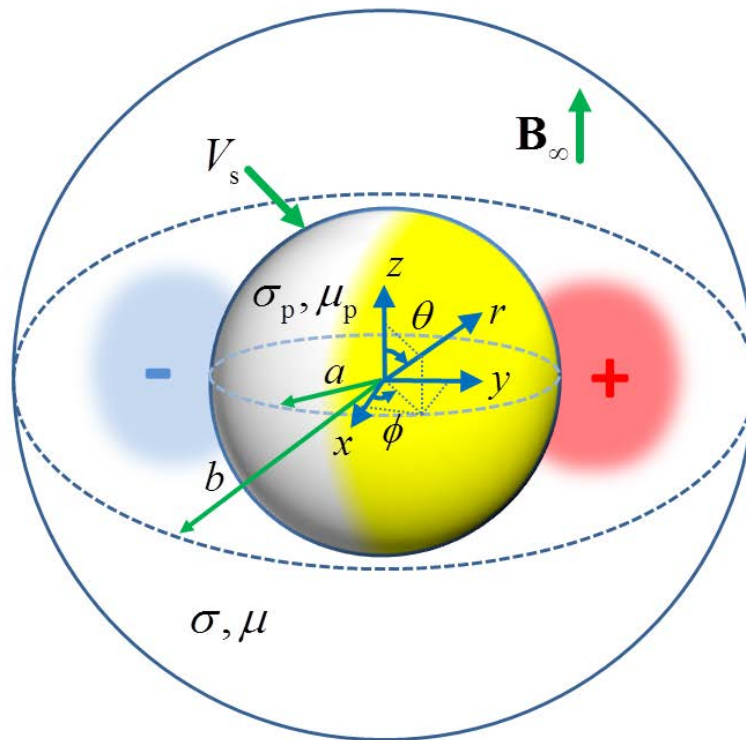
Figure 5.1　Geometric sketch for the motion of a spherical particle undergoing interfacial electrochemical reactions in an applied magnetic field in a concentric spherical cavity.
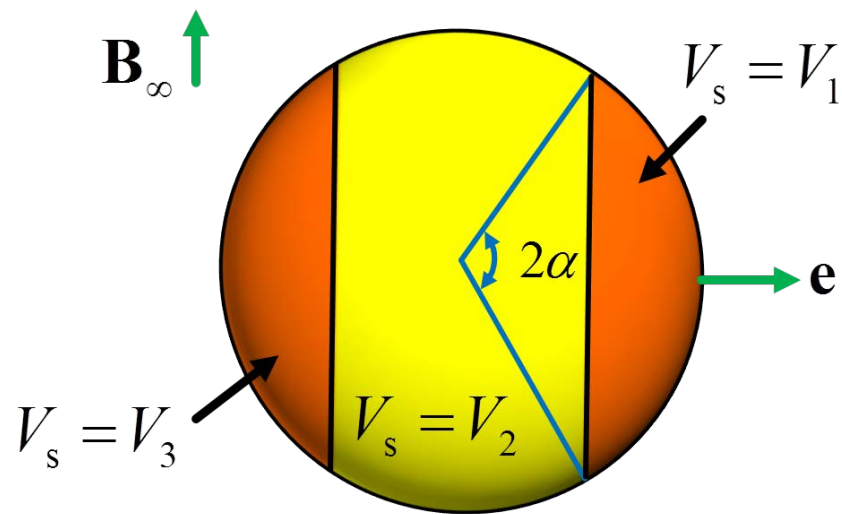
Figure 5.2　　Sketch for a three-slice spherical particle composed of two orthotropically symmetric caps of the constant surface potentials V_1 and V_3, respectively, each spanning a solid angle 2α, connected by a middle section of the constant surface potential V_2.
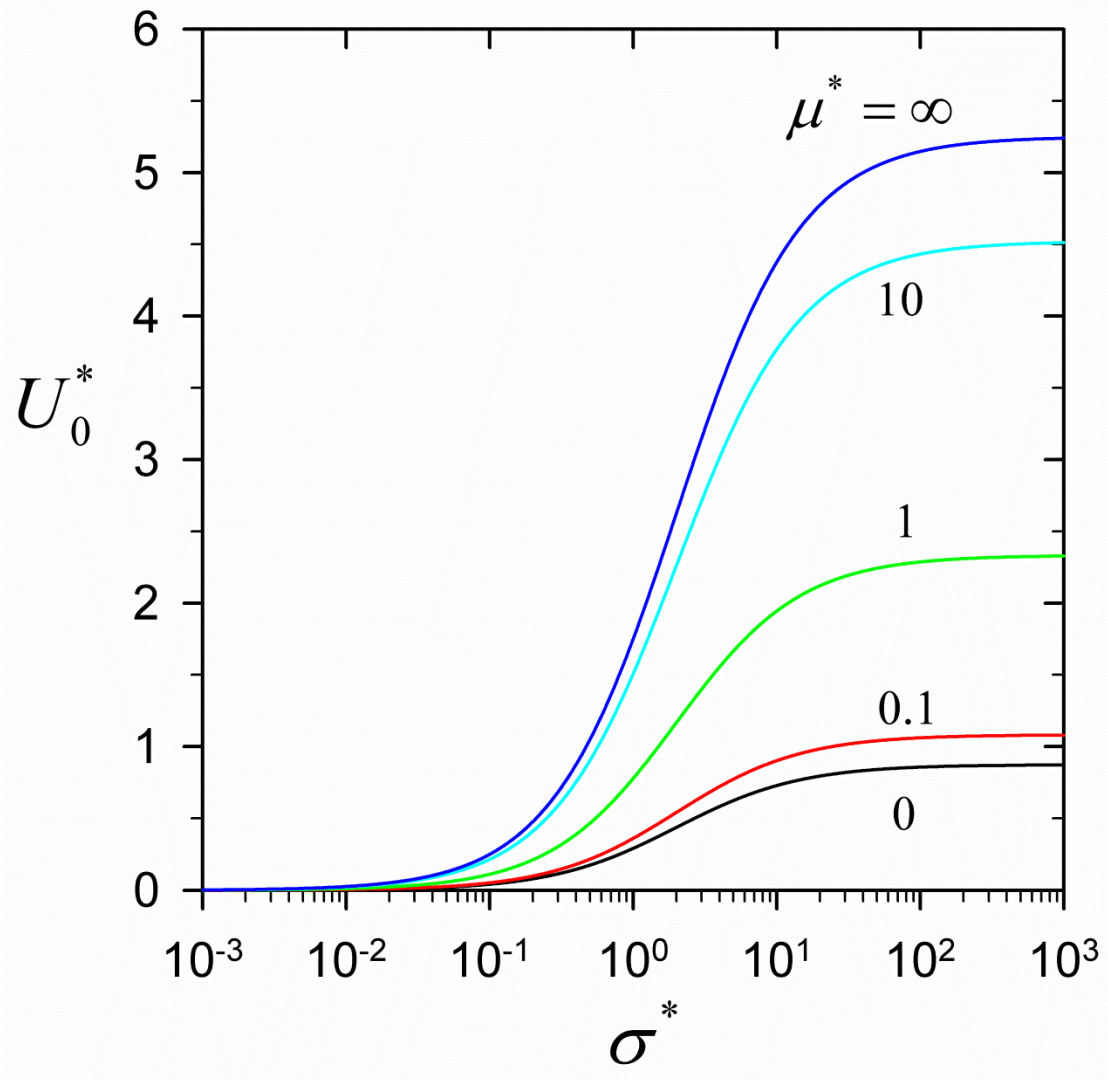
Figure 5.3a   Plots of the translational mobility parameter U_0^* calculated from Eq.

(5.24a) for various values of the electric conductivity ratio σ^* and magnetic

permeability ratio μ^*.
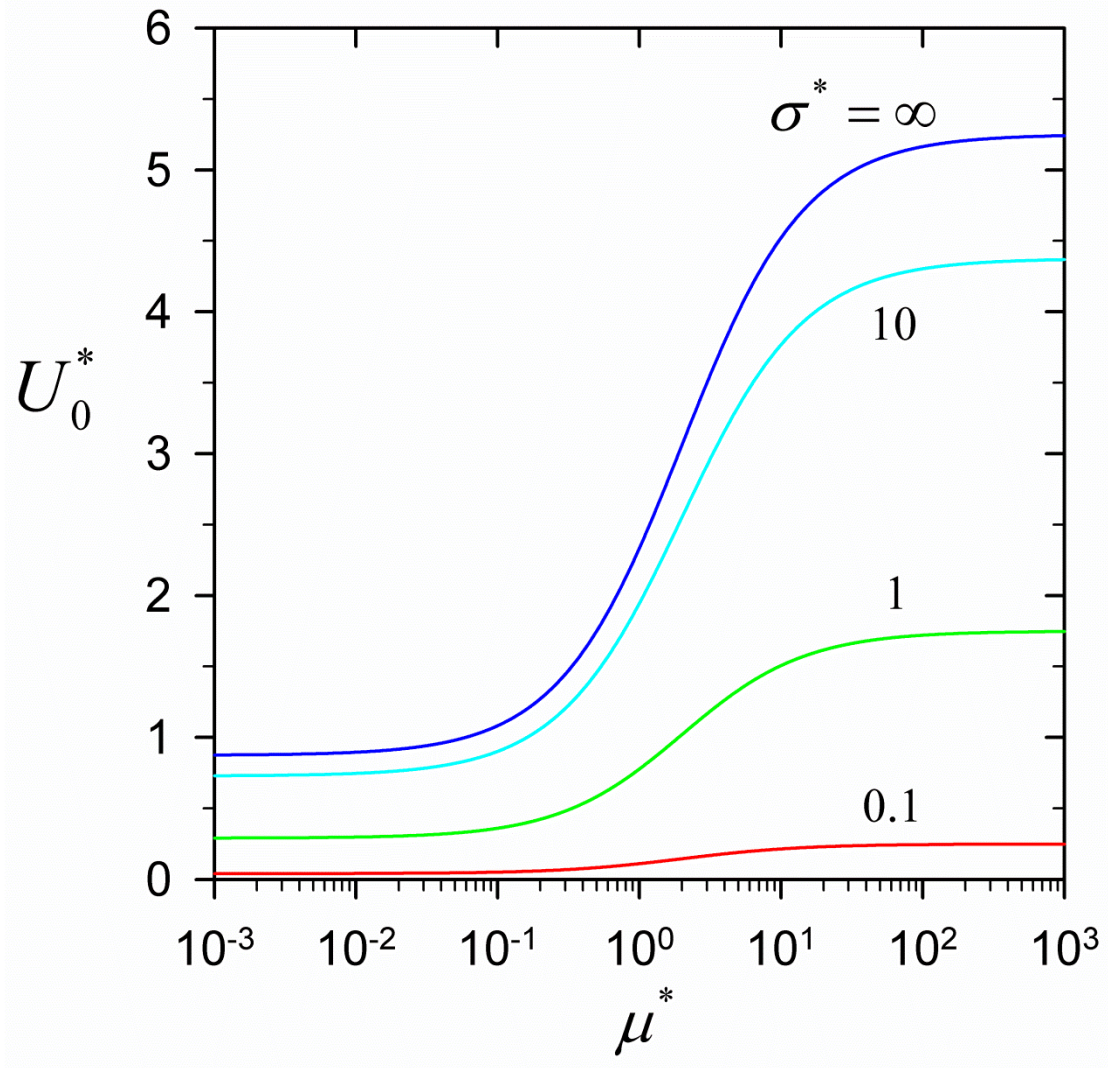
Figure 5.3b   Plots of the translational mobility parameter U_0^* calculated from Eq.

(5.24a) for various values of the electric conductivity ratio σ^* and magnetic

permeability ratio μ^*.
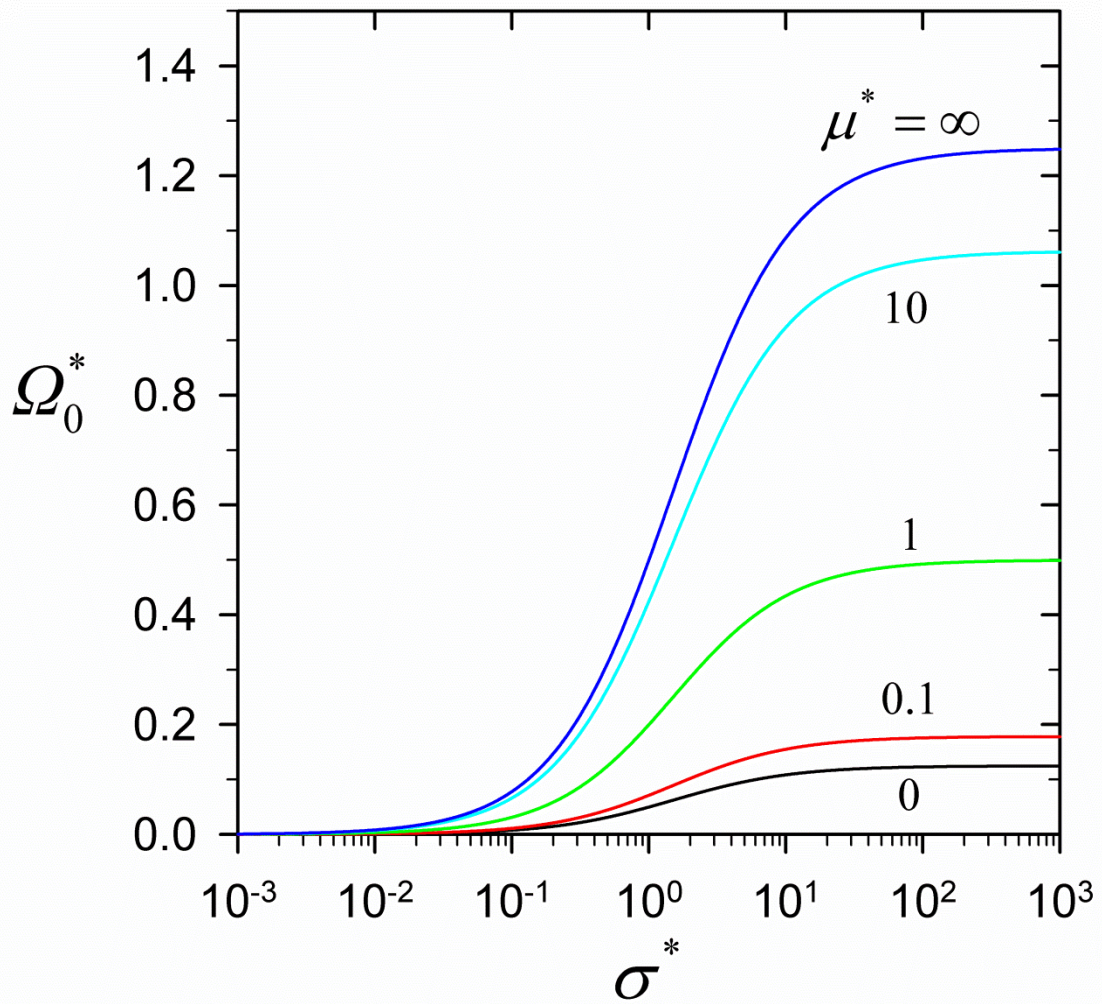
Figure 5.4a   Plots of the rotational mobility parameter Ω_0^* calculated from Eq.

(5.24b) for various values of the electric conductivity ratio σ^* and magnetic

permeability ratio μ^*.
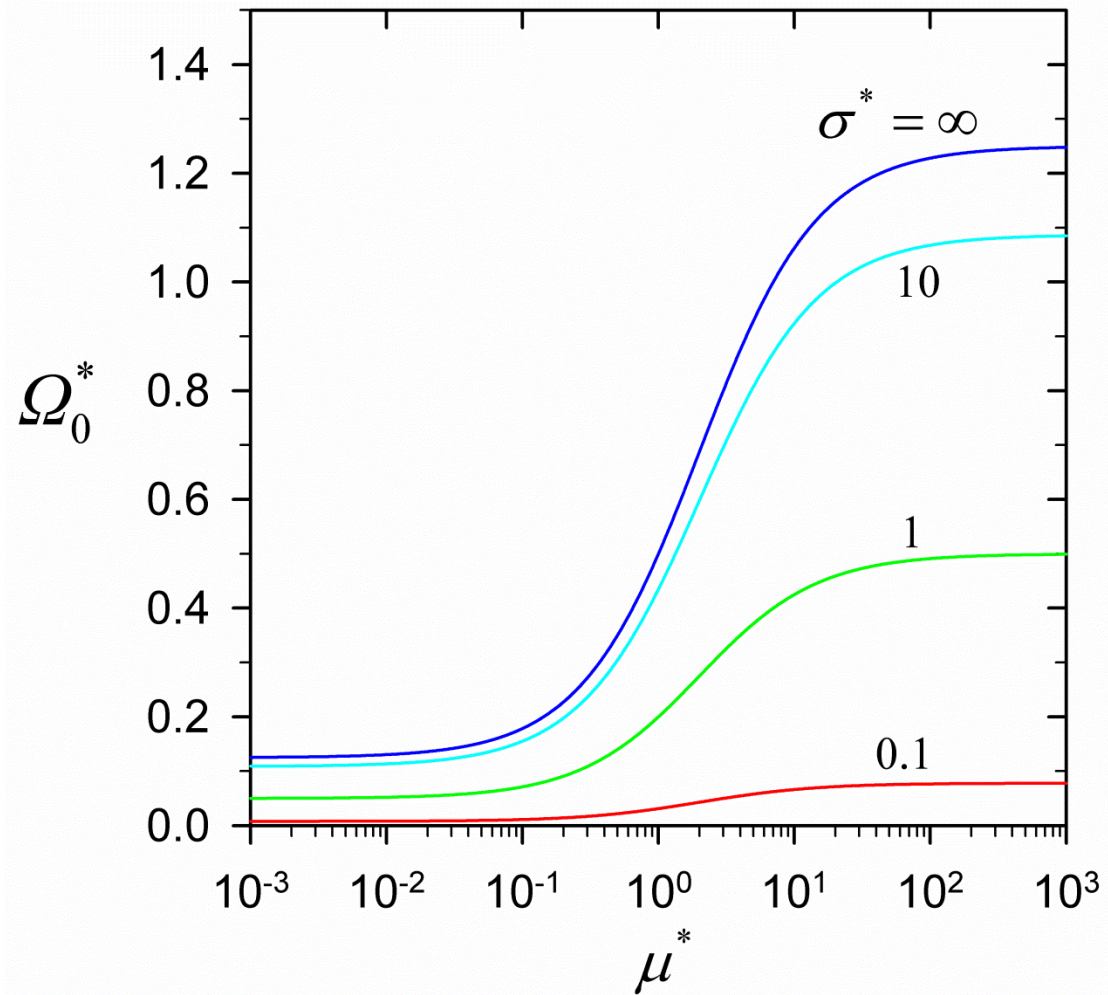
Figure 5.4b   Plots of the rotational mobility parameter Ω_0^* calculated from Eq.

(5.24b) for various values of the electric conductivity ratio σ^* and magnetic

permeability ratio μ^*.
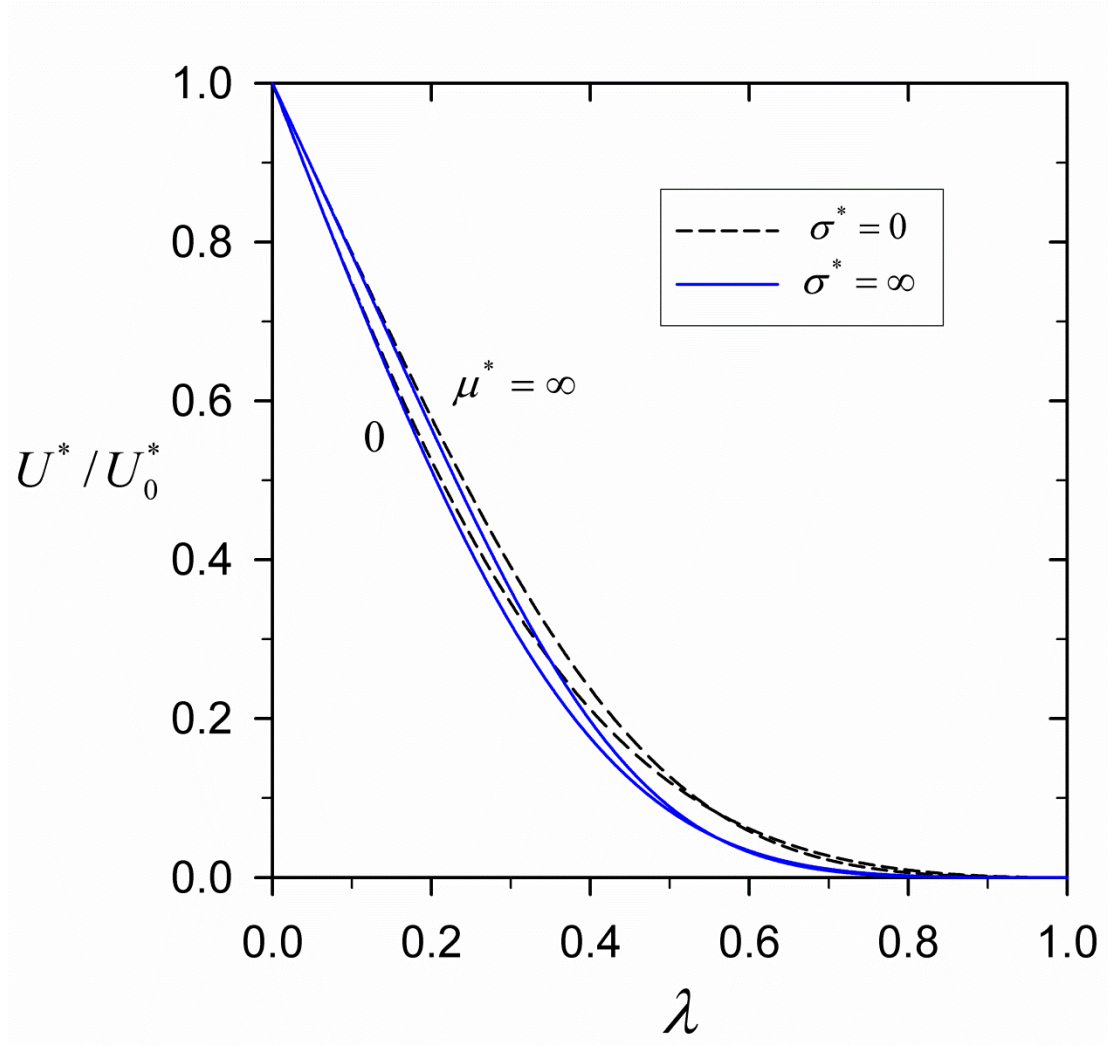
Figure 5.5   Plots of the normalized translational mobility U^*/U_0^* calculated from

Eqs. (5.22a) and (5.24a) versus the particle-to-cavity radius ratio λ for various

values of the electric conductivity ratio σ^* and magnetic permeability ratio μ^*.
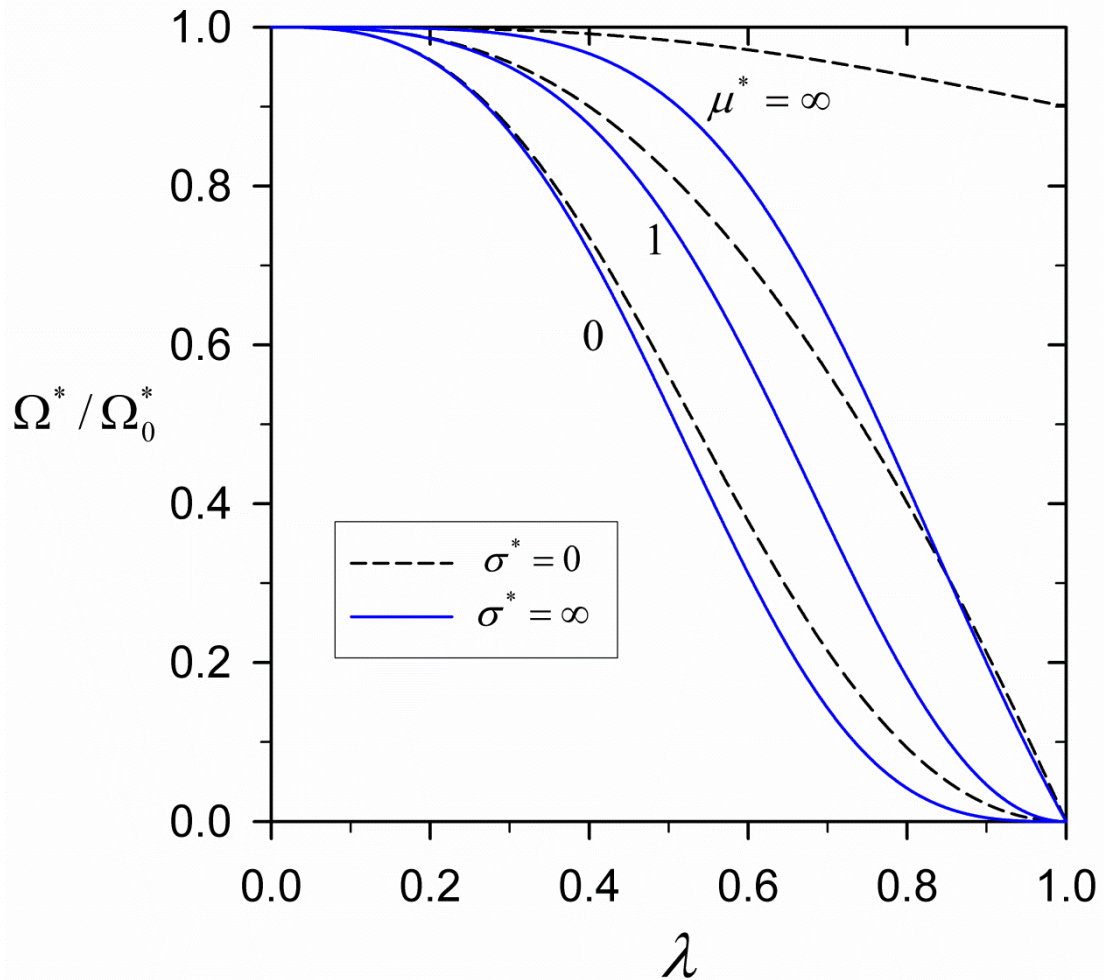
Figure 5.6　　Plots of the normalized rotational mobility Ω^*/Ω_0^* calculated from Eqs. (5.22b) and (5.24b) versus the particle-to-cavity radius ratio λ for various values of the electric conductivity ratio σ^* and magnetic permeability ratio μ^*.

Chapter 6

Conclusions

The quasi-steady motions of a spherical colloidal particle inside a concentric spherical cavity filled with a conducting fluid induced by the MHD effect are analyzed at low Reynolds number. Through the use of a generalized reciprocal theorem to the Stokes equations modified with the Lorentz force density resulting from the interaction of an applied magnetic field with the existing electric current and the consideration of the Maxwell stress to the force exerted on the particle, the translational and angular velocities of the particle are obtained in closed forms valid for an arbitrary value of the particle-to-cavity radius ratio.

In Chapter 2, the MHD effects on a translating and rotating colloidal sphere in an arbitrary electrolyte solution prescribed with a general flow field and a constant magnetic field are analyzed. The thickness of the electric double layer adjacent to the particle surface can be arbitrary relative to the particle radius. The equilibrium double-layer potential distribution is determined through the use of the Debye-Huckel approximation. The modified Stokes equations governing the fluid velocity field are dealt with using a simple perturbation method and a generalized reciprocal theorem, and explicit formulas for the translational and angular velocities of the particle induced by the MHD effects are obtained in Eq. (2.14), with the relevant mobility parameters (dimensionless functions of κa) given by Eq. (2.15) and Figs. 2.2 and 2.3. The MHD effects on the particle movement associated with the translation and rotation of the particle and the ambient fluid flow are found to be monotonically increasing functions of κa, and the interaction between the magnetic field and a pure

rotational or straining Stokes flow produces no direct MHD effect on the particle when its electric double layer is very thick. The MHD effect caused by the pure straining flow of the electrolyte solution is able to drive the particle to rotate, but makes no contribution to the translation of the particle.

In Chapter 3, the MHD effects on the translation and rotation of a charged colloidal sphere in a concentric spherical cavity filled with an arbitrary electrolyte solution subject to a uniformly applied magnetic field are analyzed. The thickness of the electric double layers adjacent to the solid surfaces can be arbitrary relative to the particle and cavity radii. The equilibrium double-layer potential distribution in the fluid phase is determined through the use of the Debye-Huckel approximation. The modified Stokes equations governing the fluid velocity field are dealt by using a simple perturbation method and a generalized reciprocal theorem, and closed-form formulas for the translational and angular velocities of the confined particle resulting from the MHD effects are obtained in Eqs. (3.20) and (3.28), with the relevant mobility parameters given by Eqs. (3.21) and (3.29) and Figs. 3.2-3.7. These mobility parameters are qualitatively and quantitatively sensible functions of the separation parameter λ and electrokinetic parameter κa. In general, the proximity of the cavity wall diminishes the MHD migration but enhances the MHD rotation of the particle.

In Chapter 4, the EMP migration of a spherical particle situated at the center of a spherical cavity filled with a conducting fluid subjected to uniformly applied electric and magnetic fields is analyzed. After solving the electric current and magnetic flux density distributions in the particle and fluid phases of arbitrary electric conductivities and magnetic permeabilities, the Stokes equations modified with the resulted Lorentz force density for the fluid motion are treated by a generalized reciprocal theorem, and the EMP migration velocity of the particle is obtained explicitly in Eqs. (4.19)-(4.21).

The effect of the Maxwell stress, which was neglected in previous studies, on the EMP force and velocity of the particle is found to be significant. The migration velocity of the particle in general decreases monotonically with an increase in the particle-to-cavity radius ratio λ, with an exception for the case that the electric conductivity ratio σ^* is large and the magnetic permeability ratio μ^* is small, where the particle may reverse its direction of migration with the variation in λ. At the touching limit $\lambda = 1$, the particle velocity vanishes, but the EMP force acting on the particle is finite. The boundary effect on the EMP migration of the particle, which increases with an increase in σ^* and decreases with an increase in μ^*, is equivalent to that on its sedimentation, but is much stronger than that on its electrophoretic motion.

In Chapter 5, the MHD motion of a spherical particle with interfacial self-electrochemical reactions in a concentric spherical cavity filled with an ionic fluid subject to an applied magnetic field is analyzed. The thickness of the electric double layers adjacent to the particle and cavity surfaces is assumed to be small relative to the particle radius and the distance between the solid surfaces, but the zeta potential at the particle surface may have an arbitrary distribution. After solving the electric current and magnetic flux density distributions in the particle and fluid phases of arbitrary electric conductivities and magnetic permeabilities, the Stokes equations modified with the Lorentz force density for the fluid motion are treated by a generalized reciprocal theorem, and the translational and angular velocities of the particle induced by the MHD effect are obtained explicitly in Eqs. (5.20)-(5.23). These translational and angular velocities, which depend on the dipole and quadrupole moments, respectively, of the zeta potential distribution over the particle surface, decrease monotonically with an increase in the particle-to-cavity radius ratio λ and

vanishes in the limit. The induced velocities of the particle are unexpectedly significant, and their dependence on the characteristics of the particle-fluid system is physically different from that for EMP particles or phoretic swimmers. The boundary effect on the movement of the particle with self-electrochemical surface reactions induced by the MHD force increases with an increase in the particle-to-fluid electric conductivity ratio σ^* and decreases with an increase in the magnetic permeability ratio μ^*. This boundary effect is equivalent to that caused by the gravity, but is much stronger than that in general phoretic motions.
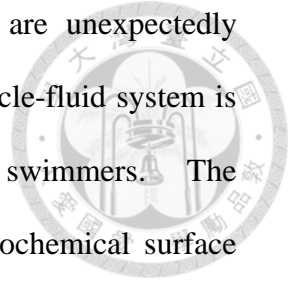
List of symbols

a	radius of spherical particle, m
$a_1 \sim a_5$	function of λ and γ defined by Eqs. (3.11)
b	radius of concentric spherical cavity, m
$\mathbf{B}$	magnetic flux density, $V \cdot s \cdot m^{-2}$ (T)
$\mathbf{B}_\infty$	uniform applied magnetic flux density, $V \cdot s \cdot m^{-2}$ (T)
c_1, c_2	function of λ in Eqs. (4.20)
C_{lm}, D_{lm}, E_{lm}	coefficient of spherical harmonic
$\mathbf{D}$	dipole moment of deviation distribution of zeta potential, V
$\mathbf{e}$	unit vector outward to the cap surface of the potential V_1
$\mathbf{e}_r, \mathbf{e}_z$	unit vector in r and z direction
$\mathbf{E}_\infty$	constant rate-of-strain dyadic, s^{-1}
$f_\mathrm{T}, f_\mathrm{R}$	hydrodynamic resistance coefficients for the translation and rotation.
F	Faraday constant, C/mol
$\mathbf{F}$	Force acting on the particle, N
$\mathbf{I}$	unit dyadic
$\mathbf{J}, \mathbf{J}_\mathrm{p}$	electric current density of the fluid and particle, A/m^2
$\mathbf{J}_\infty$	uniform applied electric current density, A/m^2
M, M_0, M_∞	dimensionless translational mobility parameter
N, N_0, N_∞	dimensionless rotational mobility parameter
p	pressure distribution, N/m^2
p_M	MHD effect induced fluid pressure, $N \cdot m^{-2}$
$\mathbf{Q}$	quadrupole moment of deviation distribution of zeta potential, V

r, θ, ϕ	spherical coordinates
r	position vector from the particle center, m
R	gas constant, J$\cdot$ K^{-1} $\cdot$mol^{-1}
T	absolute temperature, K
T	Torque acting on the particle, N$\cdot$ m
u_1, u_2	function of λ in Eqs. (5.23a,b)
U^*	dimenstionless translational mobility parameter
U	translational velocity of the particle, m$\cdot$s^{-1}
U$_\text{M}$	MHD induced translational velocity of the particle, m$\cdot$s^{-1}
V_s	deviation distribution of zeta potential, V
v	fluid velocity field distribution, m$\cdot$s^{-1}
v$_0$	zeroth-order flow field, m$\cdot$s^{-1}
v$_\text{M}$	MHD effect induced fluid velocity, m$\cdot$s^{-1}
$\overline{\textbf{v}}^{\text{T}}, \overline{\textbf{v}}^{\text{R}}$	normalized Stokes flow field of translation and rotation, -, m
$\overline{\textbf{v}}_0^{\text{T}}, \overline{\textbf{v}}_0^{\text{R}}$	normalized Stokes flow field of translation and rotation in an unbounded fluid, -, m
x, y, z	rectangular coordinates, m
Y_{lm}	spherical harmonics of order l and degree m

Greek symbols

α	perturbation expansion parameter, equal to $\varepsilon \zeta_\text{p} |\textbf{B}_\infty| / \eta$
ε	permittivity of fluid, C^2 $\cdot$ J^{-1} $\cdot$ m^{-1}
Φ, Φ_p	magnetic scalar potential of the fluid and particle, A
η	fluid viscosity, kg $\cdot$ m^{-1} $\cdot$ s^{-1}

γ	equal to r/a
$\Gamma_\mathrm{T}, \Gamma_\mathrm{R}$	function of λ and γ defined by Eqs. (3.12)
κ	Debye screening length, m^{-1}
λ	equal to a/b
μ, μ_p	permeability of the fluid and particle, H/m (N/A^2)
μ^*	relative permeability
ψ, ψ_p	electric potential distribution of fluid and particle, V
ω_1, ω_2	function of λ in Eqs. (5.23c,d)
$\mathbf{\Omega}$	angular velocity of the particle, s^{-1}
$\mathbf{\Omega}_0$	angular velocity of the particle without boundary, s^{-1}
$\mathbf{\Omega}_\mathrm{M}$	MHD induced rotational velocity of the particle, s^{-1}
Ω^*	dimensionless rotational mobility parameter
ρ	total space charge density, C$\cdot$ m^{-3}
$\sigma, \sigma_\mathrm{p}$	electrical conductivity of the fluid and particle, S$\cdot$m^{-1} (A$\cdot$ V$^{-1}\cdot$ m^{-1})
σ^*	relative conductivity
$\mathbf{\sigma}^\mathrm{E}$	Maxwell stress tensor of electric field contribution, N$\cdot$ m^{-2}
$\mathbf{\sigma}^\mathrm{M}$	Maxwell stress tensor of magnetic field contribution, N$\cdot$ m^{-2}
ζ	zeta potential of particle, V
$\overline{\zeta}$	average zeta potential over the particle surface, V
τ	equal to r/b

Subscripts

p	particle
w	cavity wall

References

Bishop, K. J. M. and Grzybowski, B. A. (2007). ""Nanoions": Fundamental properties and analytical applications of charged nanoparticles". *ChemPhysChem* **8**:2171-2176.

Burdick, J., Laocharoensuk, R., Wheat, P. M., Posner, J. D. and Wang, J. (2008). "Synthetic nanomotors in microchannel networks: Directional microchip motion and controlled manipulation of cargo". *Journal of the American Chemical Society* **130**:8164-8165.

Busch, K. W., Gopalakrishnan, S., Busch, M. A. and Tombácz, E. (1996). "Magnetohydrodynamic aggregation of cholesterol and polystyrene latex suspensions". *Journal of Colloid and Interface Science* **183**:528-538.

Chang, Y. C. and Keh, H. J. (2008). "Diffusiophoresis and electrophoresis of a charged sphere perpendicular to two plane walls". *Journal of Colloid and Interface Science* **322**:634-653.

Chaturvedi, N., Hong, Y., Sen, A. and Velegol, D. (2010). "Magnetic enhancement of phototaxing catalytic motors". *Langmuir* **26**:6308-6313.

Cheng, K.-L., Sheng, Y.-J., Jiang, S. and Tsao, H.-K. (2008). "Electrophoretic size separation of particles in a periodically constricted microchannel". *The Journal of Chemical Physics* **128**:101101-1-4.

Chung, J. and Liang, R.-C. (2009). Electro-magnetophoresis display, in *U.S. Patent* No. 7576904.

Davidson, P. A. (2001). *An Introduction to Magnetohydrodynamics*. Cambridge University Press, Cambridge, England.

De Las Cuevas, G., Faraudo, J. and Camacho, J. (2008). "Low-gradient magnetophoresis through field-induced reversible aggregation". *The Journal of Physical Chemistry C* **112**:945-950.

De Vicente, J., Segovia-Gutierrez, J. P., Andablo-Reyes, E., Vereda, F. and Hidalgo-Alvarez, R. (2009). "Dynamic rheology of sphere- and rod-based magnetorheological fluids". *The Journal of Chemical Physics* **131**:194902-1-10.

Dreyfus, R., Baudry, J., Roper, M. L., Fermigier, M., Stone, H. A. and Bibette, J. (2005). "Microscopic artificial swimmers". *Nature* **437**:862-865.

Ebbens, S., Tu, M.-H., Howse, J. R. and Golestanian, R. (2012). "Size dependence of the propulsion velocity for catalytic Janus-sphere swimmers". *Physical Review E* **85**:020401-1-4.

Gibbs, J. G., Fragnito, N. A. and Zhao, Y. (2010). "Asymmetric Pt/Au coated catalytic micromotors fabricated by dynamic shadowing growth". *Applied Physics Letters* **97**:253107-1-3.

Golestanian, R., Liverpool, T. B. and Ajdari, A. (2007). "Designing phoretic micro- and nano-swimmers". *New Journal of Physics* **9**:126-1-8.

Grant, K. M., Hemmert, J. W. and White, H. S. (2002). "Magnetic field-controlled microfluidic transport". *Journal of the American Chemical Society* **124**:462-467.

Happel, J. and Brenner, H. (1983). *Low Reynolds Number Hydrodynamics*. Martinus Nijhoff, Dordrecht, The Netherlands.

Haverkort, J. W. and Peeters, T. W. J. (2010). "Magnetohydrodynamic effects on insulating bubbles and inclusions in the continuous casting of steel". *Metallurgical and Materials Transactions B* **41**:1240-1246.

Henry, D. C. (1931). "The cataphoresis of suspended particles. Part I. The equation of cataphoresis". *Proceedings of the Royal Society of London. Series A* **133**:106-129.

Hsieh, T. H. and Keh, H. J. (2007). "Boundary effects on electrophoresis of a colloidal cylinder with a nonuniform zeta potential distribution". *Journal of Colloid and Interface Science* **315**:343-354.

Huang, Y. C. and Keh, H. J. (2005). "Transient electrophoresis of spherical particles at low potential and arbitrary double-layer thickness". *Langmuir* **21**:11659-11665.

Hubbard, J. B. and Wolynes, P. G. (1981). "An electrohydrodynamic contribution to the Hall effect in electrolyte solutions". *The Journal of Chemical Physics* **75**:3051-3054.

Iiguni, Y. and Watarai, H. (2003). "Simultaneous measurement of the migration velocity and adsorption force of micro-particles using an electromagnetophoretic

force under a high magnetic field". *Analytical Sciences* **19**:33-37.

Iiguni, Y. and Watarai, H. (2005). "New principle of electromagnetophoretic adsorption–desorption microchromatography". *Journal of Chromatography A* **1073**:93-98.

Iiguni, Y. and Watarai, H. (2010). "Dynamic electromagnetophoretic force analysis of a single binding interaction between lectin and mannan polysaccharide on yeast cell surface". *Analyst* **135**:1426-1432.

Jackson, J. D. (1976). *Classical Electrodynamics*. John Wiley & Sons, New York.

Kalsin, A. M., Fialkowski, M., Paszewski, M., Smoukov, S. K., Bishop, K. J. M. and Grzybowski, B. A. (2006). "Electrostatic self-assembly of binary nanoparticle crystals with a diamond-like lattice". *Science* **312**:420-424.

Keh, H. J. and Anderson, J. L. (1985). "Boundary effects on electrophoretic motion of colloidal spheres". *Journal of Fluid Mechanics* **153**:417-439.

Keh, H. J. and Chang, J. H. (1998). "Boundary effects on the creeping-flow and thermophoretic motions of an aerosol particle in a spherical cavity". *Chemical Engineering Science* **53**:2365-2377.

Keh, H. J. and Chen, S. H. (1996). "The motion of a slip spherical-particle in an arbitrary Stokes-flow". *European Journal of Mechanics - B/Fluids* **15**:791-807.

Keh, H. J. and Cheng, T. F. (2011). "Sedimentation of a charged colloidal sphere in a charged cavity". *The Journal of Chemical Physics* **135**:214706-1-10.

Keh, H. J. and Chiou, J. Y. (1996). "Electrophoresis of a colloidal sphere in a circular cylindrical pore". *AIChE Journal* **42**:1397-1406.

Keh, H. J. and Hsieh, T. H. (2007). "Electrophoresis of a colloidal sphere in a spherical cavity with arbitrary zeta potential distributions". *Langmuir* **23**:7928-7935.

Keh, H. J. and Hsieh, T. H. (2008). "Electrophoresis of a colloidal sphere in a spherical cavity with arbitrary zeta potential distributions and arbitrary double-layer thickness". *Langmuir* **24**:390-398.

Keh, H. J. and Li, W. J. (1994). "Interactions among bipolar spheres in an electrolytic cell". *Journal of The Electrochemical Society* **141**:3103-3114.

Kim, J. Y. and Yoon, B. J. (2002). "Electrophoretic motion of a slightly deformed sphere with a nonuniform zeta potential distribution". *Journal of Colloid and Interface Science* **251**:318-330.

Kim, J. Y. and Yoon, B. J. (2003). "High-order field electrophoresis theory for a nonuniformly charged sphere". *Journal of Colloid and Interface Science* **262**:101-106.

Kline, T. R., Iwata, J., Lammert, P. E., Mallouk, T. E., Sen, A. and Velegol, D. (2006). "Catalytically driven colloidal patterning and transport". *The Journal of Physical Chemistry B* **110**:24513-24521.

Kline, T. R., Paxton, W. F., Mallouk, T. E. and Sen, A. (2005). "Catalytic nanomotors: remote-controlled autonomous movement of striped metallic nanorods". *Angewandte Chemie International Edition* **44**:744-746.

Kolin, A. (1953). "An electromagnetokinetic phenomenon involving migration of neutral particles". *Science* **117**:134-137.

Kolin, A. and Kado, R. T. (1958). "Fractionation of cell suspensions in an electromagnetic force field". *Nature* **182**:510-512.

Laocharoensuk, R., Burdick, J. and Wang, J. (2008). "Carbon-nanotube-induced acceleration of catalytic nanomotors". *ACS Nano* **2**:1069-1075.

Leenov, D. and Kolin, A. (1954). "Theory of electromagnetophoresis. I. Magnetohydrodynamic forces experienced by spherical and symmetrically oriented cylindrical particles". *The Journal of Chemical Physics* **22**:683-688.

Li, W. J. and Keh, H. J. (1997). "Boundary effects on the bipolar behavior of a spherical particle in an electrolytic cell". *Journal of The Electrochemical Society* **144**:3536-3544.

Luca, R. D. (2009). "Lorentz force on sodium and chlorine ions in a salt water solution flow under a transverse magnetic field". *European Journal of Physics* **30**:459-466.

Mills, R. A. (1968). "A microscopic formulation of electromagnetophoresis". *The Bulletin of Mathmetical Biophysics* **30**:309-318.

Miloh, T. (2011). "Dipolophoresis of interacting conducting nano-particles of finite

electric double layer thickness". *Physics of Fluids* **23**:122002-1-14.

Moffatt, H. K. and Sellier, A. (2002). "Migration of an insulating particle under the action of uniform ambient electric and magnetic fields. Part 1. General theory". *Journal of Fluid Mechanics* **464**:279-286.

Moran, J. L. and Posner, J. D. (2011). "Electrokinetic locomotion due to reaction-induced charge auto-electrophoresis". *Journal of Fluid Mechanics* **680**:31-66.

Moran, J. L., Wheat, P. M. and Posner, J. D. (2010). "Locomotion of electrocatalytic nanomotors due to reaction induced charge autoelectrophoresis". *Physical Review E* **81**:065302-1-4.

Newman, J. S. (1973). *Electrochemical Systems*. Prentice-Hall, Englewood Cliffs, NJ.

Nozaki, O., Munese, M. and Kawamoto, H. (2004). "Determination of glycation on diabetic erythrocytes by electromagnetophoresis". *Bunseki Kagaku* **53**:85-90.

O'Brien, R. W. and White, L. R. (1978). "Electrophoretic mobility of a spherical colloidal particle". *Journal of the Chemical Society, Faraday Transactions 2: Molecular and Chemical Physics* **74**:1607-1626.

Ohshima, H., Healy, T. W. and White, L. R. (1983). "Approximate analytic expressions for the electrophoretic mobility of spherical colloidal particles and the conductivity of their dilute suspensions". *Journal of the Chemical Society, Faraday Transactions 2: Molecular and Chemical Physics* **79**:1613-1628.

Ozawa, S., Kurosaka, D., Yamamoto, I. and Takamasu, T. (2011). "DNA electromagnetophoresis under the condition of magnetic fields perpendicular to electric fields". *Japanese Journal of Applied Physics* **50**:070212-1-3.

Paxton, W. F., Baker, P. T., Kline, T. R., Wang, Y., Mallouk, T. E. and Sen, A. (2006). "Catalytically induced electrokinetics for motors and micropumps". *Journal of the American Chemical Society* **128**:14881-14888.

Paxton, W. F., Sen, A. and Mallouk, T. E. (2005). "Motility of catalytic nanoparticles through self-generated forces". *Chemistry – A European Journal* **11**:6462-6470.

Qi, H., Chen, Q., Wang, M., Wen, M. and Xiong, J. (2009). "Study of self-assembly of

octahedral magnetite under an external magnetic field". *The Journal of Physical Chemistry C* **113**:17301-17305.

Qian, S. and Bau, H. H. (2005). "Magnetohydrodynamic flow of RedOx electrolyte". *Physics of Fluids* **17**:067105-1-12.

Qin, M. and Bau, H. H. (2012). "Magnetohydrodynamic flow of a binary electrolyte in a concentric annulus". *Physics of Fluids* **24**:037101-1-20.

Rock, R. M., Sides, P. J. and Prieve, D. C. (2013). "The effect of electrode kinetics on electrophoretic forces". *Journal of Colloid and Interface Science* **393**:306-313.

Sabass, B. and Seifert, U. (2012). "Nonlinear, electrocatalytic swimming in the presence of salt". *The Journal of Chemical Physics* **136**:214507-1-13.

Sekhar, T. V. S., Sivakumar, R. and Kumar, T. V. R. R. (2005). "Magnetohydrodynamic flow around a sphere". *Fluid Dynamics Research* **37**:357-373.

Sellier, A. (2003). "Migration of an insulating particle under the action of uniform ambient electric and magnetic fields. Part 2. Boundary formulation and ellipsoidal particles". *Journal of Fluid Mechanics* **488**:335-353.

Sellier, A. (2005). Migration of a solid conducting sphere immersed in a liquid metal near a plane boundary under the action of uniform ambient electric and magnetic fields, in *The 15th Riga and 6th PAMIRConference on Fundamental and Applied MHD*, Rigas Jurmala, Latvia, 311-314.

Sellier, A. (2006). "Migration of a solid conducting sphere immersed in a liquid metal near a plane conducting solid wall under the action of uniform ambient electric and magnetic fields". *Magnetohydrodynamics* **42**:317-326.

Sellier, A. (2007). "Slow viscous migration of a conducting solid particle under the action of uniform ambient electric and magnetic fields". *Computer Modeling in Engineering and Sciences* **21**:105-132.

Sen, A., Ibele, M., Hong, Y. and Velegol, D. (2009). "Chemo and phototactic nano/microbots". *Faraday Discussions* **143**:15-27.

Shevchenko, E. V., Talapin, D. V., Kotov, N. A., O'Brien, S. and Murray, C. B. (2006).

"Structural diversity in binary nanoparticle superlattices". *Nature* **439**:55-59.

Stuyven, B., Chen, Q., Moortel, W. V. d., Lipkens, H., Caerts, B., Aerts, A., Giebeler, L., Eerdenbrugh, B. V., Augustijns, P., Mooter, G. V. d., Humbeeck, J. V., Vanacken, J., Moshchalkov, V. V., Vermant, J. and Martens, J. A. (2009). "Magnetic field assisted nanoparticle dispersion". *Chemical Communications* **45**:47-49.

Tai, C. T. (1964). "A study of electrodynamics of moving media". *Proceedings of the IEEE* **52**:685-689.

Teubner, M. (1982). "The motion of charged colloidal particles in electric fields". *The Journal of Chemical Physics* **76**:5564-5573.

Tombácz, E., Ma, C., Busch, K. W. and Busch, M. A. (1991). "Effect of a weak magnetic field on hematite sol in stationary and flowing systems". *Colloid and Polymer Science* **269**:278-289.

Tretiakov, K. V., Bishop, K. J. M. and Grzybowski, B. A. (2009). "Additivity of the excess energy dissipation rate in a dynamically self-assembled system". *The Journal of Physical Chemistry B* **113**:7574-7578.

Watarai, H., Suwa, M. and Iiguni, Y. (2004). "Magnetophoresis and electromagnetophoresis of microparticles in liquids". *Analytical and Bioanalytical Chemistry* **378**:1693-1699.

Wei, H.-H. and Jan, J.-S. (2010). "Self-propulsion and dispersion of reactive colloids due to entropic anisotropy". *Journal of Fluid Mechanics* **657**:64-88.

Wheat, P. M., Marine, N. A., Moran, J. L. and Posner, J. D. (2010). "Rapid fabrication of bimetallic spherical motors". *Langmuir* **26**:13052-13055.

Xu, Z., Li, T. and Zhou, Y. (2007). "Continuous removal of nonmetallic inclusions from aluminum melts by means of stationary electromagnetic field and DC current". *Metallurgical and Materials Transactions A* **38**:1104-1110.

Yang, Y., Grant, K. M., White, H. S. and Chen, S. (2003). "Magnetoelectrochemistry of nitrothiophenolate-functionalized gold nanoparticles". *Langmuir* **19**:9446-9449.

Yariv, E. (2009). "An asymptotic derivation of the thin-debye-layer limit for electrokinetic phenomena". *Chemical Engineering Communications* **197**:3-17.

Yariv, E. (2011). "Electrokinetic self-propulsion by inhomogeneous surface kinetics". *Proceedings of the Royal Society A: Mathematical, Physical and Engineering Science* **467**:1645-1664.

Yariv, E. and Miloh, T. (2007). "Electro-magneto-phoresis of slender bodies". *Journal of Fluid Mechanics* **577**:331-340.

Yariv, E. and Miloh, T. (2009). "Boundary effects on electro-magneto-phoresis". *Journal of Fluid Mechanics* **622**:195-207.

Yoon, B. J. (1991). "Electrophoretic motion of spherical particles with a nonuniform charge distribution". *Journal of Colloid and Interface Science* **142**:575-581.

Zydney, A. L. (1995). "Boundary effects on the electrophoretic motion of a charged particle in a spherical cavity". *Journal of Colloid and Interface Science* **169**:476-485.
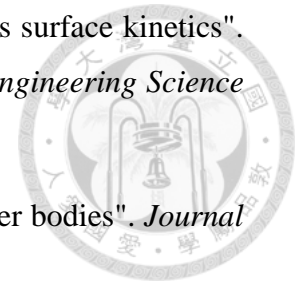
Appendix A

Generalized reciprocal theorem

Let $\mathbf{v}_1$ and $\mathbf{\Pi}_1$ be the fluid velocity and stress fields satisfying the Stokes equations modified with the force density $\mathbf{X}_1$. The governing equations of the fluid velocity field $\mathbf{v}_1$ are

$$\nabla \cdot \mathbf{\Pi}_1 = \mathbf{X}_1 = -\nabla \cdot \mathbf{\Pi}^M, \quad \nabla \cdot \mathbf{v}_1 = 0, \tag{A.1a,b}$$

The force density $\mathbf{X}_1$ is an electromagnetic force density or any other force density. The boundary conditions for the fluid velocity field $\mathbf{v}_1$ can be expressed as

$$\mathbf{v}_1 = \mathbf{U} + \mathbf{\Omega} \times \mathbf{r} \qquad \text{at } r = a, \tag{A.2a}$$

$$\mathbf{v}_1 = \mathbf{0}, \qquad \text{at } r = b \text{ or } r \to \infty. \tag{A.2b}$$

Let $\mathbf{v}_2$ and $\mathbf{\Pi}_2$ be the normalized fluid velocity and stress fields satisfying the homogeneous Stokes equations. The governing equations of the fluid velocity field $\mathbf{v}_2$ are

$$\nabla \cdot \mathbf{\Pi}_2 = \mathbf{0}, \quad \nabla \cdot \mathbf{v}_2 = \mathbf{0}. \tag{A.3a,b}$$

The field $\mathbf{v}_2$ can be expressed as the translation field $\overline{\mathbf{v}}^{\mathrm{T}}$ (dimensionless) or rotation field $\overline{\mathbf{v}}^{\mathrm{R}}$ (with dimension of length) fluid fields. The boundary conditions for the fluid velocity fields $\overline{\mathbf{v}}^{\mathrm{T}}$ and $\overline{\mathbf{v}}^{\mathrm{R}}$ can be expressed as

$$\overline{\mathbf{v}}^{\mathrm{T}} = \mathbf{I}, \ \overline{\mathbf{v}}^{\mathrm{R}} = \mathbf{I} \times \mathbf{r} \qquad \text{at } r = a, \tag{A.4a}$$

$$\overline{\mathbf{v}}^{\mathrm{T}} = \mathbf{0}, \ \overline{\mathbf{v}}^{\mathrm{R}} = \mathbf{0}, \qquad \text{at } r = b, \text{ or } r \to \infty. \tag{A.4b}$$

From the generalized reciprocal theorem we obtain

$$\boldsymbol{\Pi}_1 : \Delta \mathbf{v}_2 = \boldsymbol{\Pi}_2 : \Delta \mathbf{v}_1,$$ (A.5)

where

$$\Delta \mathbf{v}_i = \frac{1}{2}(\nabla \mathbf{v}_i + (\nabla \mathbf{v}_i)^{\mathrm{T}})$$ (A.6)

From the symmetry of the stress tensor, we have

$$\boldsymbol{\Pi}_i : \nabla \mathbf{v}_j = \nabla \cdot (\mathbf{v}_j \cdot \boldsymbol{\Pi}_i) - \mathbf{v}_j \cdot (\nabla \cdot \boldsymbol{\Pi}_i).$$ (A.7)

Integrating the right-hand side of the above equation over the fluid volume V, we apply the divergence theorem to obtain,

$$\int_V \nabla \cdot (\mathbf{v}_2 \cdot \boldsymbol{\Pi}_1) dV - \int_V \mathbf{v}_2 \cdot (\nabla \cdot \boldsymbol{\Pi}_1) dV$$

$$= -\int_{S_a} \mathbf{v}_2 \cdot \boldsymbol{\Pi}_1 \cdot dS - \int_V \mathbf{v}_2 \cdot \mathbf{X}_1 dV = -\int_{S_a} \mathbf{v}_1 \cdot \boldsymbol{\Pi}_2 \cdot dS .$$ (A.8)

The force and torque exerted on the particle surface by the hydrodynamic stress are

$$\mathbf{F}_{\mathrm{H}} = \int_S \boldsymbol{\Pi}^{\mathrm{H}} \cdot d\mathbf{S} = -6\pi\eta a f_{\mathrm{T}} \mathbf{U} - \int_V \overline{\mathbf{v}}^{\mathrm{T}} \cdot \mathbf{X}_1 dV ,$$ (A.9a)

$$\mathbf{T}_{\mathrm{H}} = \int_S \mathbf{r} \times (\boldsymbol{\Pi}^{\mathrm{H}} \cdot d\mathbf{S}) = -8\pi\eta a^3 \boldsymbol{\Omega} - \int_V \overline{\mathbf{v}}^{\mathrm{R}} \cdot \mathbf{X}_1 dV ,$$ (A.9b)

where

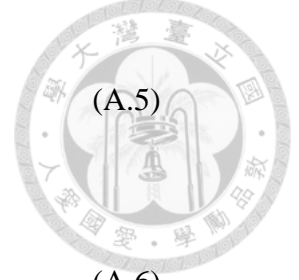$$\boldsymbol{\Pi}^{\mathrm{H}} = -p\mathbf{I} + 2\mu\Delta = -p\mathbf{I} + \mu[\nabla \mathbf{v} + (\nabla \mathbf{v})^+].$$ (A.10)

The force and torque exerted on the particle surface by the electromagnetic stress are

$$\mathbf{F}_{\mathrm{M}} = \int_{S_a} \boldsymbol{\Pi}^{\mathrm{M}} \cdot d\mathbf{S},$$ (A.11a)

$$\mathbf{T}_{\mathrm{M}} = \int_{S_a} \mathbf{r} \times (\boldsymbol{\Pi}^{\mathrm{M}} \cdot d\mathbf{S}),$$ (A.11b)

where

$$\mathbf{\Pi}^{\mathrm{M}} = \varepsilon\left(\mathbf{EE} - \frac{1}{2}|\mathbf{E}|^2\mathbf{I}\right) + \frac{1}{\mu}\left(\mathbf{BB} - \frac{1}{2}|\mathbf{B}|^2\mathbf{I}\right), \tag{A.12}$$

The total force and torque exerted on the particle by the fluid are

$$\mathbf{F}_{\mathrm{H}} + \mathbf{F}_{\mathrm{M}} = -6\pi\eta a f_{\mathrm{T}}\mathbf{U} + \int_{S_a}\mathbf{\Pi}^{\mathrm{M}}\cdot d\mathbf{S} - \int_V \overline{\mathbf{v}}^{\mathrm{T}}\cdot\mathbf{X}_1 dV, \tag{A.13a}$$

$$\mathbf{T}_{\mathrm{H}} + \mathbf{T}_{\mathrm{M}} = -8\pi\eta a^3\mathbf{\Omega} + \int_{S_a}\mathbf{r}\times(\mathbf{\Pi}^{\mathrm{H}}\cdot d\mathbf{S}) - \int_V \overline{\mathbf{v}}^{\mathrm{R}}\cdot\mathbf{X}_1 dV. \tag{A.13b}$$

Appendix B

Vector spherical harmonics

B1. Definition of vector spherical harmonics (VSH)

Y_{lm} are the spherical harmonics, and we define three VSHs

$$\mathbf{Y}_{lm} = Y_{lm}\mathbf{e}_r \qquad\qquad \mathbf{\Psi}_{lm} = r\nabla Y_{lm} \qquad\qquad \mathbf{\Phi}_{lm} = \mathbf{r}\times\nabla Y_{lm}$$

B2. Orthogonality of VSH

$$\mathbf{Y}_{lm}\cdot\mathbf{\Psi}_{lm} = 0 \qquad\qquad \mathbf{Y}_{lm}\cdot\mathbf{\Phi}_{lm} = 0 \qquad\qquad \mathbf{\Psi}_{lm}\cdot\mathbf{\Phi}_{lm} = 0$$

$$\int \mathbf{Y}_{lm}\cdot\mathbf{Y}_{l'm'}^{*}d\Omega = \delta_{ll'}\delta_{mm'} \qquad\qquad \int \mathbf{\Psi}_{lm}\cdot\mathbf{\Psi}_{l'm'}^{*}d\Omega = l(l+1)\delta_{ll'}\delta_{mm'}$$

$$\int \mathbf{\Phi}_{lm}\cdot\mathbf{\Phi}_{l'm'}^{*}d\Omega = l(l+1)\delta_{ll'}\delta_{mm'} \qquad\qquad \int \mathbf{Y}_{lm}\cdot\mathbf{\Psi}_{l'm'}^{*}d\Omega = 0$$

$$\int \mathbf{Y}_{lm}\cdot\mathbf{\Phi}_{l'm'}^{*}d\Omega = 0 \qquad\qquad \int \mathbf{\Psi}_{lm}\cdot\mathbf{\Phi}_{l'm'}^{*}d\Omega = 0$$

B3. Multipole expansion of a vector field

$$\mathbf{E} = \sum_{l=0}^{\infty}\sum_{m=-l}^{l}(E_{lm}^{r}(r)\mathbf{Y}_{lm} + E_{lm}^{(1)}(r)\mathbf{\Psi}_{lm} + E_{lm}^{(2)}(r)\mathbf{\Phi}_{lm})$$

B4. Gradient, divergence and curl of VSH:

The multipole expansion of a scalar field ϕ is

$$\phi = \sum_{l=0}^{\infty}\sum_{m=-l}^{l}\phi_{lm}(r)Y_{lm}$$

We can express its gradient, divergence and curl in VSH form.

$$\nabla \phi = \sum_{l=0}^{\infty} \sum_{m=-l}^{l} \frac{d\phi_{lm}}{dr} \mathbf{Y}_{lm} + \frac{\phi_{lm}}{r} \mathbf{\Psi}_{lm} \; ,$$

$$\nabla \cdot \mathbf{E} = \sum_{l=0}^{\infty} \sum_{m=-l}^{l} (\frac{dE_{lm}^{r}}{dr} + \frac{2}{r} E_{lm}^{r} - \frac{l(l+1)}{r} E_{lm}^{(1)}) Y_{lm} \; ,$$

$$\nabla \times \mathbf{E} = \sum_{l=0}^{\infty} \sum_{m=-l}^{l} (-\frac{l(l+1)}{r} E_{lm}^{(2)} \mathbf{Y}_{lm} - (\frac{dE_{lm}^{(2)}}{dr} + \frac{1}{r} E_{lm}^{(2)}) \mathbf{\Psi}_{lm} +$$

$$+ (-\frac{1}{r} E_{lm}^{r} + \frac{dE_{lm}^{(1)}}{dr} + \frac{1}{r} E_{lm}^{(1)}) \mathbf{\Phi}_{lm}) \; .$$

B5. Solution for the magnetic flux density

The governing equations for the magnetic flux density are

$$\nabla \times \mathbf{B} = \mu \mathbf{J} = -\sigma \mu \nabla \psi \; , \tag{B.1}$$

$$\nabla \cdot \mathbf{B} = 0 \; . \tag{B.2}$$

The solution of electrical potential ψ which satisfies the Laplace equation is

$$\psi = \sum_{l=0}^{\infty} \sum_{m=-l}^{l} \psi_{lm}(r) Y_{lm}(r) = \sum_{l=0}^{\infty} \sum_{m=-l}^{l} [D_{lm}(\frac{a}{r})^{l+1} + E_{lm}(\frac{r}{a})^{l}] Y_{lm} \; , \tag{B.3}$$

The gradient of ψ expressed by VSH is

$$\nabla \psi = \sum_{l=0}^{\infty} \sum_{m=-l}^{l} \frac{d\psi_{lm}}{dr} \mathbf{Y}_{lm} + \frac{\psi_{lm}}{r} \mathbf{\Psi}_{lm} \tag{B.4}$$

The magnetic flux density can be solved by the VSH expansions

$$\mathbf{B} = \sum_{l=0}^{\infty} \sum_{m=-l}^{l} (B_{lm}^{r}(r) \mathbf{Y}_{lm} + B_{lm}^{(1)}(r) \mathbf{\Psi}_{lm} + B_{lm}^{(2)}(r) \mathbf{\Phi}_{lm}) \tag{B.5}$$

From some identities of VSH, the curl and divergence of a magnetic flux density are

$$\nabla \times \mathbf{B} = \sum_{l=0}^{\infty} \sum_{m=-l}^{l} (-\frac{l(l+1)}{r} B_{lm}^{(2)} \mathbf{Y}_{lm} - (\frac{dB_{lm}^{(2)}}{dr} + \frac{1}{r} B_{lm}^{(2)}) \mathbf{\Psi}_{lm} (-\frac{1}{r} B_{lm}^{r} + \frac{dB_{lm}^{(1)}}{dr} + \frac{1}{r} B_{lm}^{(1)}) \mathbf{\Phi}_{lm})$$

$$\tag{B.6}$$

$$\nabla \cdot \mathbf{B} = \sum_{l=0}^{\infty} \sum_{m=-l}^{l} (\frac{\mathrm{d}B_{lm}^r}{\mathrm{d}r} + \frac{2}{r} B_{lm}^r - \frac{l(l+1)}{r} B_{lm}^{(1)}) Y_{lm} \tag{B.7}$$

From the orthogonality of the VSH, we can obtain the unknown functions B_{lm}^r, $B_{lm}^{(1)}$, and $B_{lm}^{(2)}$.

The equation for $B_{lm}^{(2)}$ is

$$-(\frac{\mathrm{d}B_{lm}^{(2)}}{\mathrm{d}r} + \frac{1}{r} B_{lm}^{(2)}) = -\sigma\mu \frac{\psi_{lm}}{r} \tag{B.8}$$

After solving the above equation, we obtain

$$B_{lm}^{(2)} = \mu\sigma[-\frac{1}{l}(\frac{a}{r})^{l+1} D_{lm} + \frac{1}{l+1}(\frac{r}{a})^l E_{lm}] \tag{B.9}$$

The equations for B_{lm}^r and $B_{lm}^{(1)}$ are

$$-\frac{1}{r} B_{lm}^r + \frac{\mathrm{d}B_{lm}^{(1)}}{\mathrm{d}r} + \frac{1}{r} B_{lm}^{(1)} = 0 \tag{B.10}$$

$$\frac{\mathrm{d}B_{lm}^r}{\mathrm{d}r} + \frac{2}{r} B_{lm}^r - \frac{l(l+1)}{r} B_{lm}^{(1)} = 0 \tag{B.11}$$

After solving the above equation, we obtain

$$B_{lm}^r = \frac{\mathrm{d}\chi_{lm}(r)}{\mathrm{d}r} \tag{B.12}$$

$$B_{lm}^{(1)} = \frac{\chi_{lm}(r)}{r} \tag{B.13}$$

where

$$\Phi = \sum_{l=0}^{\infty} \sum_{m=-l}^{l} \chi_{lm}(r) Y_{lm} \tag{B.14}$$

which satisfies the Laplace equation.

Biographical Sketch

Hsieh, Tzu-Hsien was born in Taipei, Taiwan on May 27, 1983. He graduated from Kaohsiung Senior High School in the summer of 2001, and the entered the Department of Chemical Engineering of National Cheng Kung University in the same year. He acquired Book Coupon Award in 2002, 2003, 2004. After earning his Degree of Bachelor in 2005, he continued his advanced study in the Department of Chemical Engineering of National Taiwan University for a Master Degree and graduated in 2007. After 2 years work experience, he studied his doctorate up to the present. He got married to Annie Wen in May 2012 and had a daughter Pin-His in May 2013.